Anton de Kom Universiteit van Suriname

Bibliotheek

Universiteitscomplex, Leysweg 86, Paramaribo, Suriname, Postbus 9212
Telefoon (597)464547, Fax (597)434211, E-mail: adekbib@uvs.edu

APPROVAL

NAAM: Ramkhulawan Sujata S.

verleent aan de AdeKUS kosteloos de niet-exclusieve toestemming om haar/~~zijn~~ afstudeerscriptie via de catalogus full-text beschikbaar te stellen aan gebruikers binnen en buiten de AdeKUS.

Plaats en datum, Adekus, 2 oktober 2019

Handtekening Sujata

ANTON DE KOM UNIVERSITEIT VAN SURINAME
Faculteit der Technologische Wetenschappen

Detecting the changes in the mangrove forest cover using Remote Sensing for Paramaribo and Coronie to support the National Forest Monitoring System in Suriname

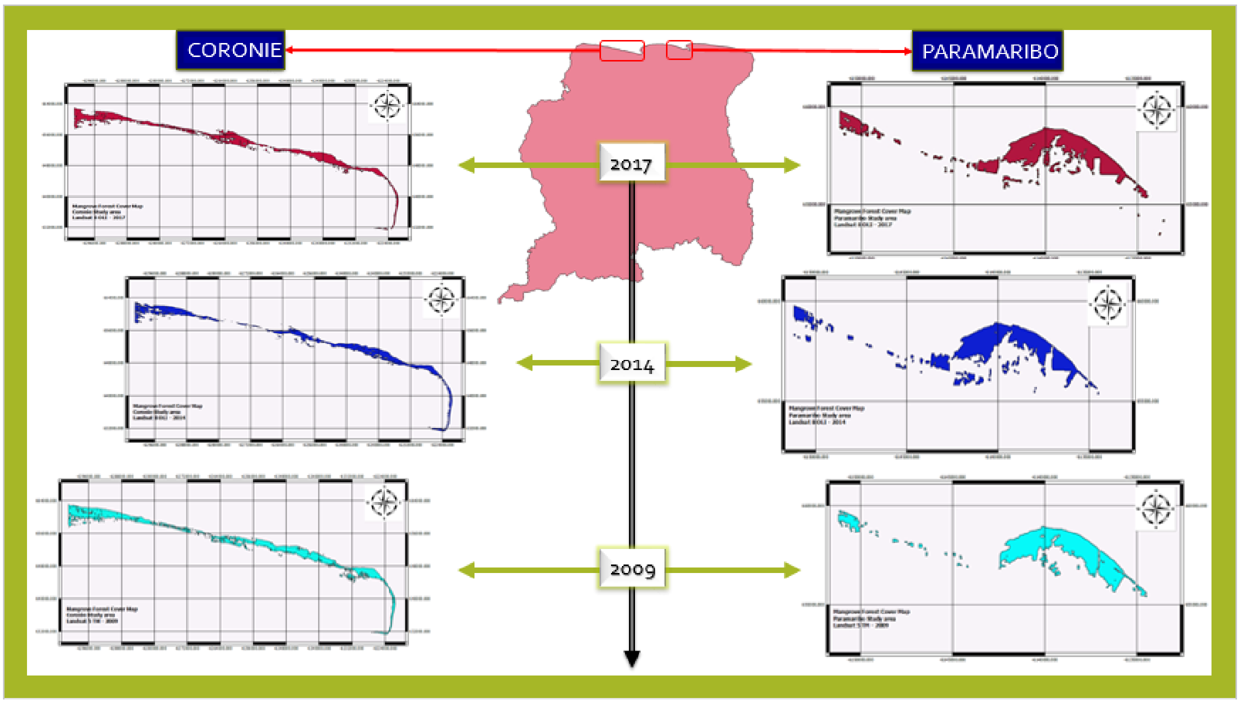

A thesis submitted in completion of the study **Bachelor of Science (BSc)** in ENVIRONMENTAL SCIENCES

By:
Sujata Sheetel Ramkhelawan
November 8, 2019
Paramaribo, Suriname

PREFACE

To graduate for the bachelor’s degree in environmental science at the technological faculty of the Anton de Kom University of Suriname, thesis research was included in the curriculum. The aim was to apply the acquired knowledge in solving problems in the work field. The whole had to be presented and defended.

Because of my interest in "Geographic Information System (GIS)" and "Remote Sensing (RS)", I chose the project: "Detecting changes in the mangrove forest cover using Remote Sensing for Paramaribo and Coronie to support the National Forest Monitoring System in Suriname". The graduation project was carried out at Forest Cover Monitoring Unit (FCMU) located within the Foundation for Forest Management and Production Control (SBB) at Ds. Martin Luther Kingweg 283. This unit was established within the Amazon Cooperation Treaty Organization (ACTO) project "Monitoring the forest cover in the Amazon region ". The research of my project was carried out from October 2017 to January 2018. I expressed my appreciation and gratitude to the staff within SBB/ FCMU for the provision of the necessary facilities and the support, cooperation, and guidance in the realization of this thesis. A special thanks to Ms. Sarah Crabbe M.Sc. as a practical supervisor, Ms. Devika Narain M.Sc. as Faculty Supervisor, Ms. Cindyrella Kasanpawiro M.Sc., Ms. Valentien Moe Soe Let B.Sc., Mr. Joey Zalman M.Sc. as sub-supervisors, Professor Naipal, Smieta Benimadho-Mahabier, Vikaash Benimadho, and Sarvam Puijmbroeck as field supporters.

I found it interesting, in the field of Remote Sensing (RS) and Geographic Information System (GIS), to look for possibilities to be able to detect the changes in the mangrove forest cover. I hope that the results and recommendations of this project could be a contribution to a better classification method for mangrove forest monitoring in Suriname.

Sujata Sheetel Ramkhelawan

EXECUTIVE SUMMARY

The mangrove forest along the dynamic mud coast of Suriname provides the most productive ecosystems and supplies several economically significant products, but also ensure stabilization of the coast. Despite most of the country's mangrove forests are having a protected status as Multiple Use Management Areas (MUMA) and/or as Nature Reserves, still, two-thirds of Suriname's mangroves are facing significant problems caused naturally or by humans. Therefore, monitoring a spatiotemporal distribution of the mangrove forest is crucial for Suriname. The research objectives were to map the extent of the mangrove forest cover in the Paramaribo and Coronie region and to identify the changes in 2009, 2014 and 2017 by using Landsat imagery data. The mangrove classification process included four main steps: pre-processing, core-processing, post-processing and change detection analysis. Accuracy assessment was done by comparing the classification results with reference data, which indicated an overall accuracy between 97 % - 100 % for Paramaribo and 98 % - 100 % for Coronie. In Paramaribo, the change of mangrove to non-mangrove during the period 2009-2017 was 205 ha, 0.18 % of the Suriname mangrove area, and regenerated of about 230 ha, 0.20 %. The changes in Coronie during the same period represented a loss by approximately 3847 ha, 3.35 % of the Suriname mangrove area, but recovered about 2452 ha, 2.13 %. The "Weg naar Zee" and the "Sea Dike" region were the locations that were most affected by heavy coastal erosion, extensive land use for urbanization, agriculture and dike construction. These threats led to a naturally reducing vitality of the mangrove forest cover. This study demonstrated the effectiveness of the method used for change detection in the mangrove forest through historical assessment and the results could provide planners with quantitative data for monitoring the mangrove forest cover.

TABLE OF CONTENT

LIST OF TABLES

LIST OF FIGURES

LIST OF ABBREVIATIONS

ACTO	Amazon Cooperation Treaty Organization
DN	Digital Number
DTC	Decision Tree Classifier
FAO	Food and Agriculture Organization of the United Nations
FCMU	Forest Cover Monitoring Unit
GPS	Global Positioning System
LC08	Landsat 8 – OLI
LT05	Landsat 5 – TM
MTL	Material Template Library format (Metadata file)
MLC	Maximum Likelihood Classifier
MUMA	Multiple Use Management Areas
NASA	National Aeronautics and Space Administration
NFMS	National Forest Monitoring System
NIR	Near Infrared
NNC	Neural Network Classifier
NR	Nature Reserves
OLI	Operational Land Imager
QA	Quality Assessment
QGIS	Quantum Geographic Information System
RGB	Red Green Blue
ROI	Region of Interest
RS	Remote Sensing
S2A	Sentinel 2A
SBB	Foundation for Forest Management and Production Control
SCP	Semi – Automatic Classification Plugin
SLMS	Satellite Land Monitoring System
SR	Surface Reflectance
SVM	Support Vector Machines
SWIR	Short-wave Infrared

TIRS	Thermal Infrared
TM	Thematic Mapper
UNDP	United Nations Development Programme
UNFCCC	the United Nations Framework Convention of Climate Change
USGS	United States Geological Survey
WHSRN	Western Hemisphere Shorebird Reserve Network
WWF	World Wildlife Fund

1. INTRODUCTION

The world area of mangroves was recently mapped at 152,360 km2 with South America as the continent with the second-highest quantity of mangrove forest of 23,882 km2 (Kainuma, et al. 2011). According to global sources and national experts, the total mangrove area of Suriname was about 115,000 ha and was known as the sixth country of South America with a high mangrove forest cover (FAO 2010; Kainuma, et al. 2011; WWF 2018; FCMU 2019).

The mangrove forests along the young coastal plain of Suriname are part of an ongoing belt of coastal wetlands, which extends from the Amazon River in Brazil to the Orinoco Delta in Venezuela (Erftemeijer and Teunissen 2009). The dynamic mud coast of Suriname is 386 km long and varied in the width of about 100 km in the west to 20 km in the east, depending on the local state of land loss and land acquisition caused by the local westward sea current regime (Augustinus 1978; Noordam 2010).

The extensive mudflats along the coast are overgrown with Black mangrove (Avicennia germinans - Parwa), Red mangrove (Rhizophora mangle - Mangro) and White mangrove (Laguncularia racemosa - Akira) (Figure 1). These three main species of mangroves provide the richest and most productive ecosystems and supply several economically significant products, but also ensured stabilization of the coast (Erftemeijer and Teunissen 2009). Most of Suriname's coastline is located within a MUMA, Multiple Use Management Area, while the two areas “Coppename Monding” and “Galibi” were assigned as a Nature Reserve (UNDP 2011). Despite their protected status, two-thirds of Suriname’s mangroves faced significant problems such as loss of the mangrove forest cover, habitat destruction, and conversion, coastal erosion, sea-level rise and various other threats and challenges (Erftemeijer and Teunissen 2009).

Figure 1: An illustration of the three main mangrove species in Suriname (Source: https://swbiodiversity.org/seinet/index.php)

Remote sensing, for example, aerial photography and satellite images, was a useful tool to analyze the changes in mangrove forest covers (Erftemeijer and Teunissen 2009). According to Erftemeijer and Teunissen (2009), this should be happening at regular intervals of 3-5 years in the problem areas and 5-10 years nationwide. The Forest Cover Monitoring Unit (FCMU), which is described in appendix I, would be monitoring the mangrove forest cover in Suriname.

Problem description

The dynamic coastal plain near Paramaribo and Coronie is under the influence of land accretion, land erosion and anthropogenic activities with significant changes in the mangrove forest cover, which is an essential ecosystem in Suriname (Erftemeijer and Teunissen 2009; Augustinus 1978; Noordam 2010). Despite their importance, comprehensive and reliable information on their spatial extent is missing which is crucial for monitoring the changes in the mangrove forest cover.

Research question

Had there been a change in the mangrove forest cover near the coast of Paramaribo and Coronie between the years 2009, 2014 and 2017?

Research sub question

- What was the extent of the mangrove forest cover in 2009 for Paramaribo and Coronie with the use of available Landsat images?
- What was the extent of the mangrove forest cover in 2014 for Paramaribo and Coronie with the use of available Landsat images?
- What was the extent of the mangrove forest cover in 2017 for Paramaribo and Coronie with the use of available Landsat images?
- Were there significant changes in the mangrove forest cover for the periods 2009-2014, 2014-2017 and 2009-2017 for Paramaribo and Coronie?

Research goal

The purpose of this thesis was to detect the changes in the mangrove forest cover of Paramaribo and Coronie for the years 2009, 2014 and 2017, through a remote sensing historical assessment with the use of available Landsat images. The detection was done to provide decision-makers of comprehensive and reliable information on their spatial extent for monitoring the changes.

Relevance

From a global perspective, healthy mangrove forest ecosystems can contribute to the protection of climate change threats. But first, all possible causes of the loss of mangroves in Suriname had to be understood and studied to see which of the impacts were significant. In addition to natural dynamics, anthropogenic activities are one of the impacts that are still a significant cause of the loss of mangrove ecosystems in the world (Ellison et al. 2012). The monitoring of mangrove forests in Suriname would provide estimates on the extent and conditions of mangrove. This data could be used for sustainable management of mangrove ecosystems by maintaining their environment, ecological and socio-economic benefits. In the end, mangrove forest monitoring would be part of the implementation of the Roadmap to a National Forest Monitoring System of Suriname (NFMS) (SBB 2016).

Scope

In this research, a method was created using Landsat satellite images. The mangrove forest cover, along the coast of Paramaribo and Coronie, was being visualized and detected for 2009, 2014 and 2017. The change analysis was done for the period 2009-2014, 2014-2017 and 2009-2017 to monitor the mangrove forest cover of Paramaribo and Coronie.

Structure of report

Chapter one contains introductory information about the research, including problem description, the research question, research sub-questions, research goal, relevance, and scope. The second chapter represents the relevant background information about remote sensing and Landsat imagery for mangrove forest cover detection. The third chapter discusses the material and method of this research. The fourth chapter consists of the results and is represented in the fifth chapter, followed by conclusions and recommendations.

2. MONITORING THE MANGROVE FOREST COVER USING REMOTE SENSING

Remote sensing is the science and technology by which the earth's surface characteristics can be identified, measured and analyzed without direct contact. This could be done by sensing and recording reflected or emitted energy from the earth's features (JARS 1993; Richards and Jia 2006; Natural Resources Canada 2015). The remote sensing systems have several components, which are described in appendix II.

2.1 Remote Sensing for mangrove forest detection

In 1978 the mangrove forest on the ecosystem map of Suriname was produced by Teunissen/ Stinasu with aerial photographs (Central Bureau for Aerial Survey, Paramaribo, 1970-1973) and reconnaissance soil maps (Department of Soil Survey, Paramaribo, 1978*)*. Erftemeijer and Teunissen (2009) also recommended in their research that the modern scientific technologies of remote sensing and digital image processing were a great opportunity to analyze the changes in the mangrove forest cover for Suriname. In 1998 CELOS/ NARENA classified the mangrove forest on the preliminary vegetation map, which was based on field observations and Landsat satellite imagery. Within the FCMU remotely sensed data is used to produce forest and deforestation maps from 2000 onwards, but there was no distinct coverage of the mangrove forest within these maps. Besides, in the regional project "REDD+ for the Guiana Shield", an Alos Palsar (Global Radar Imagery) mosaic for 2010 was made available for Suriname which was used to carry out a preliminary detection of the mangrove forest in 2016 (Moe Soe Let 2016). An overview of all these maps is given in appendix III.

Many scientific types of research by neighboring and foreign countries like Brazil, French Guiana, India, China, Malaysia, Vietnam showed that remote sensing was essential in monitoring and mapping the mangrove forest cover (Bock and Krause 2006; Polidori 2008; Kuenzer, et al. 2011; Kanniah, et al. 2015). In 2006 a research was done on techniques for remote sensing and airborne-based classification for assessment of mangrove forest structures and monitoring of their dynamics within the Mangrove Dynamics and Management Project (MADAM) for North Brazil (Bock and Krause 2006). French Guiana also did remote sensing-based research on monitoring the coastal ecosystem including the mangrove forest (Polidori 2008). The literature studies of Suriname, neighboring and foreign countries showed that remote sensing could be used to analyze changes in the mangrove forest in general and in the selected study area Paramaribo and Coronie in particular (Bock and Krause 2006; Polidori 2008; Erftemeijer and Teunissen 2009; Kuenzer, et al. 2011; Kanniah, et al. 2015).

2.2 Landsat imagery for mangrove detection

Landsat, a set of multispectral earth observation satellites, was built by the National Aeronautics and Space Administration of USA (NASA), since 1970 and has a temporal resolution of 16 days (NASA 2013; USGS 2018). Figure 2 gives an overview of the four decades of the Landsat multispectral satellites, which also indicates the lifetime of each satellite.

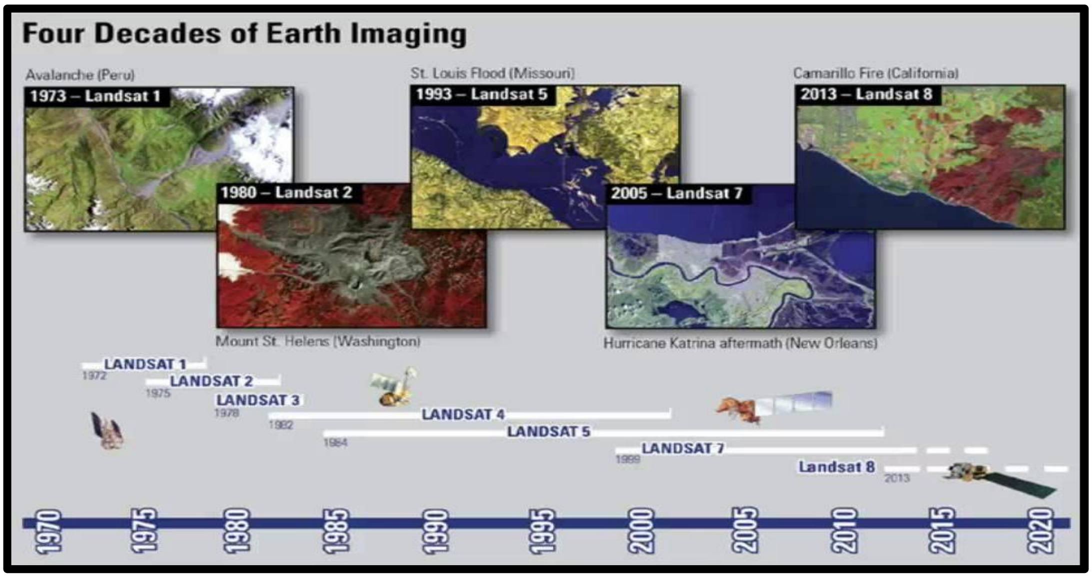

Figure 2: The four decades of the Landsat multispectral satellites with duration of each satellite (Source: USGS)

The sensors of the satellites quantized all measured energy and converted it into digital images, where pixels have a value in units of Digital Number (DN). These images had several kinds of resolutions, depending on the sensor (Richards and Jia 2006; NASA 2013), which are:

- **Spatial resolution**, also known as geometric resolution, represents the features on the earth's surface which can be detected on the image and the obtained information is converted into a pixel or image element.
- **Spectral resolution** is the location and number of the spectral band in the Electromagnetic Spectrum, which is defined by two wavelengths. Each band represents a spectral image.
- **Radiometric resolution** is the range of brightness values with a maximum range of DNs in the image.
- **Temporal resolution** is the time interval of the satellite for revisiting the same location of the earth’s surface.

Each Landsat satellite can measure the electromagnetic radiation at specific ranges in the Electromagnetic Spectrum, which are known as bands (Abadal G., et al. 2014, NASA 2013). The bands measure energy from the Visible (400 – 700 nm), Near Infrared (NIR) (760 – 1750 nm), Short-wave Infrared (SWIR) (1500-2350 nm) and Thermal Infrared (TIRS) (10.400 – 12.500 nm) regions (figure 3), which is further described in appendix IV.

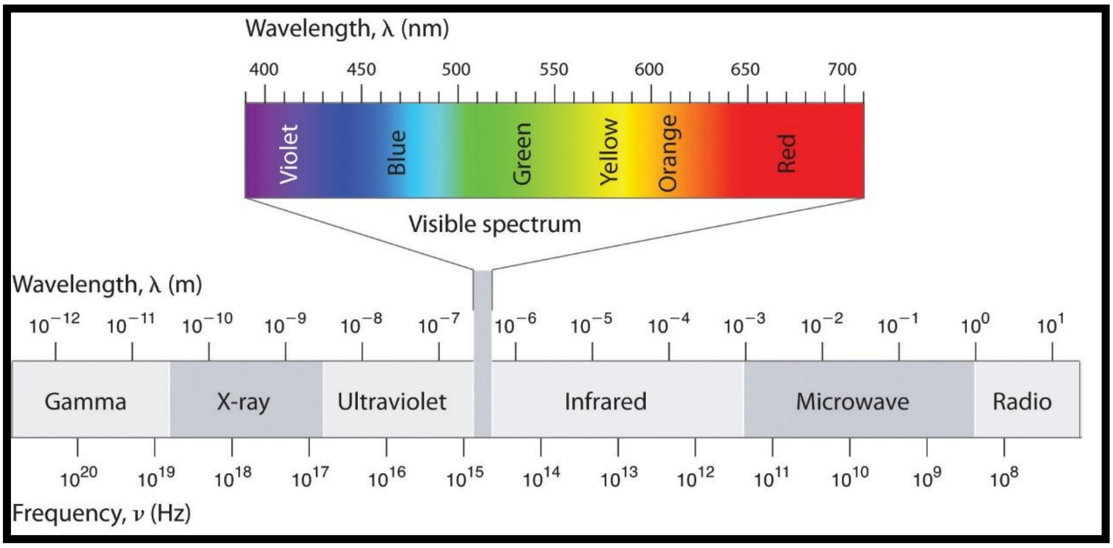

Figure 3: Diagram of the electromagnetic spectrum with indications of the wavelength, λ, and frequency, ν, of the most representative radiations from shorter and most energetic, cosmic rays, the longer and less energetic radio frequencies. A zoom detail of the optical part of the spectrum shows that light radiation is in the hundred nm and THz range of wavelengths and frequencies respectively (Abadal G., et al,2014)

Landsat bands can be sorted and combined in many ways to reveal different features on the earth's surface. A color composite is often made with three individual monochrome images (bands), each with their portion of electromagnetic reflectance spectrum and specifications (figure 4). The band stacks were expressed as a Red (R), Green (G), Blue (B) color combination and were used for image interpretation (NASA 2014).

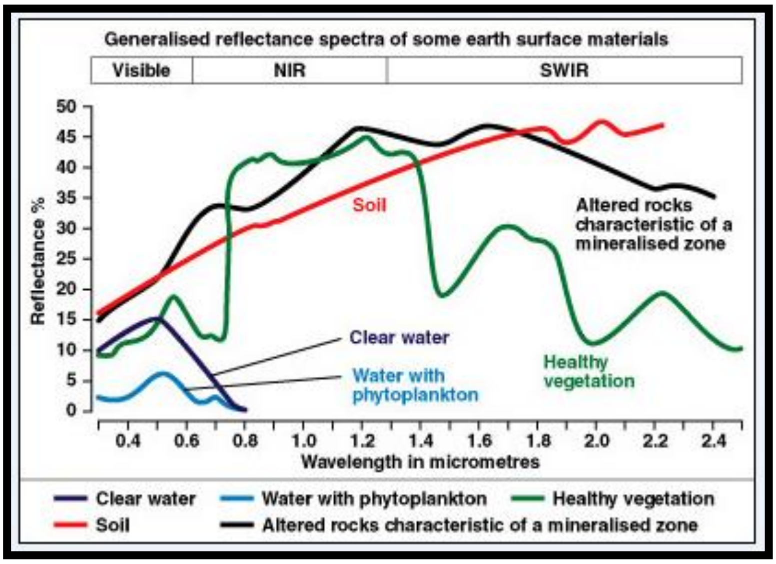

Figure 4: Electromagnetic Reflectance Spectrum (Source: https://www.usna.edu/Users/oceano/pguth/md_help/html/ref_spectra.htm)

The mangrove forest on the Landsat imagery was recognizable with a color composite of Near Infrared (NIR) band, Shortwave Infrared (SWIR) band, and Visible band. The Near Infrared band (NIR) is a very important part of the spectrum because it reflected the wavelengths of the healthy mangrove plants and emphasizes the mudbanks (NASA 2014). Besides, the Shortwave Infrared (SWIR) band is very sensitive to a soil moisture content which caused a darker color reflectance of the mangrove forest cover on the satellite imagery (USGS 2018). The visible band was used to recognize water in and near the mangrove forest cover. The whole is further described in appendix V.

3. MATERIALS AND METHOD

3.1 Study Area

The study areas, Paramaribo and Coronie, are part of the expansive coastal plain including mangrove forests in the coastal estuaries.

3.1.1 Paramaribo

Paramaribo, the capital city of Suriname, is the only urban region in Suriname with the largest population group of the entire country. Most of the inhabitants are concentrated in the coastal mangrove area of the district. Besides the influence of urbanization and industrialization in the “Noord - Paramaribo” area, the coast is also liable to coastal erosion in the “Weg naar Zee” region (Erftemeijer and Teunissen 2009; UNDP 2011; SBB 2014; Moe Soe Let 2016).

To monitor the regeneration and destruction of the mangrove forest cover, the Paramaribo study area was demarcated as following:

- The Hydro Mask – trace of 2009 (research by Valentien Moe Soe Let) as Northern boundary
- The Southern boundary of the Mangrove USGS 2011 – Suriname Map as Southern boundary
- The districts border of Paramaribo and Coronie as Western boundary
- The districts border of Paramaribo and Commewijne as Eastern boundary

The boundaries of the Paramaribo study area are illustrated in figure 5.

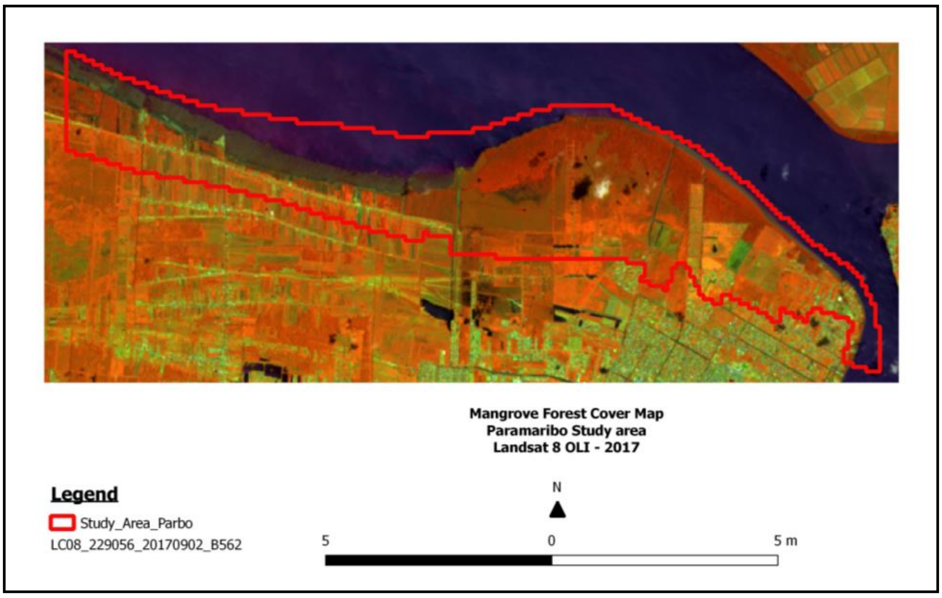

Figure 5: Illustration of the Paramaribo study area with all the boundaries

3.1.2 Coronie

Coronie is a rural district of Suriname where areas along the coastline have been established as a Nature Reserve (Coppename monding) and MUMA’s (Bigi Pan and North Coronie). Despite the protected areas, the mangrove vegetation along the coast of Coronie faced a lot of anthropogenic (dike construction) and natural (erosion) impacts. These significant impacts cause a loss of valuable habitat, coastal protection, and biodiversity (Erftemeijer and Teunissen 2009; UNDP 2011; SBB 2014).

To monitor the regeneration and destruction of the mangrove forest cover, the Coronie study area was demarcated using the following borders:

- The Hydro Mask – trace of 2009 (research by Valentien Moe Soe Let) as Northern boundary
- The “Oost-West Verbinding” road as Southern boundary
- The districts border of Coronie and Saramacca as Western boundary
- The districts border of Coronie and Nickerie as Eastern boundary

The boundaries of the Coronie study area are illustrated in figure 6.

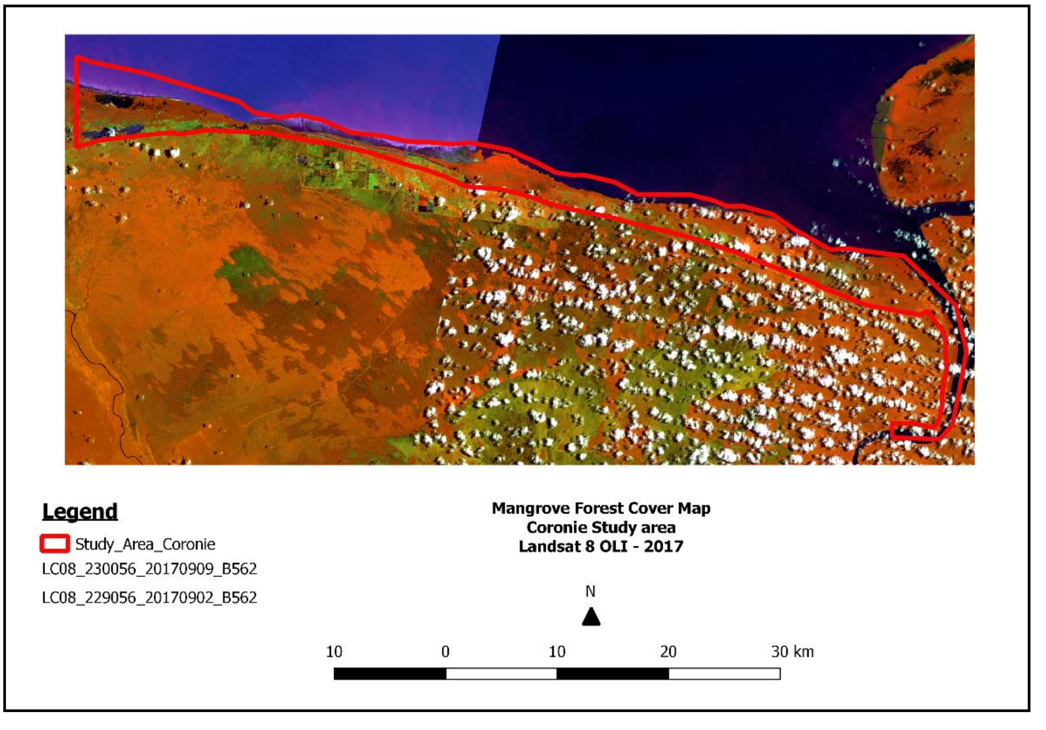

Figure 6: Illustration of the Coronie study area with all the boundaries

3.2 Data collection and software

3.2.1 Satellite and Ancillary data

The Suriname coast map has 3 scenes that are covered with a Landsat image with a specific code for the path and the row for each scene. For example, Paramaribo is in the 229th path and the 56th row (figure 7) and is described as “229056”.

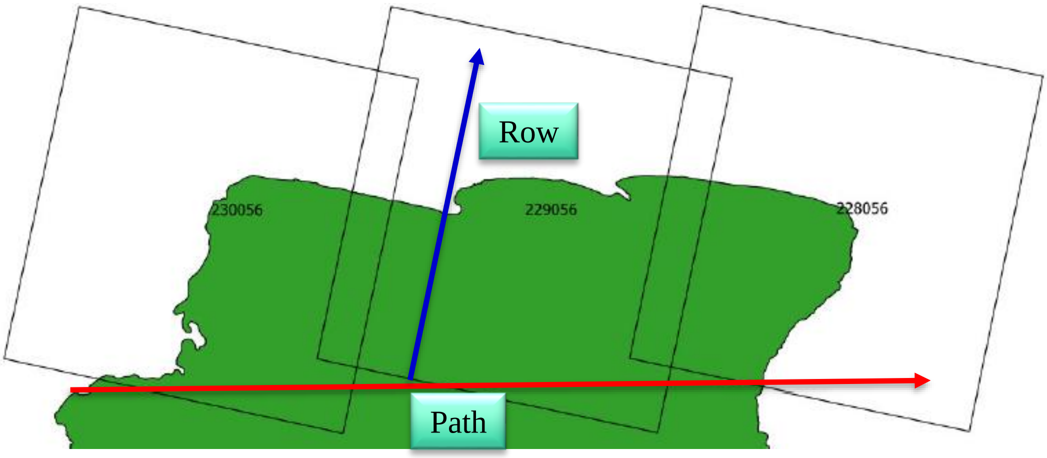

Figure 7: Landsat scene division for the coast of Suriname

The Landsat imagery covers 2009, 2014 and 2017 of Paramaribo and Coronie study areas. These freely available Landsat 5 TM and Landsat 8 OLI scenes for the study area are on the paths 229/ 230 and row 56. The 11 images, which are described in table 3, were being collected from the United States Geological Survey (USGS) – New Bulk downloader and Remote Pixel websites with a maximum cloud coverage of 50 % in the study areas.

Table 1: An overview of all downloaded Landsat images along with cloud fill data

SATELLITE/ YEAR	TYPE DATA	PATH	ROW	SENSOR	DATE	SCENE LIST
LANDSAT 8		229	56	OLI	20170902	LC08_L1TP_229056_20170902_20170916_01_T1
2017	Fill	229	56	OLI	20171004	LC08_L1TP_229056_20171004_20171014_01_T1
		230	56	OLI	20170909	LC08_L1TP_230056_20170909_20170927_01_T1
2014		229	56	OLI	20140926	LC08_L1TP_229056_20140926_20170419_01_T1
	Fill	229	56	OLI	20140521	LC08_L1TP_229056_20140521_20170422_01_T1
	Fill	229	56	OLI	20141012	LC08_L1TP_229056_20141012_20170418_01_T1
	Fill	229	56	OLI	20141028	LC08_L1TP_229056_20141028_20170418_01_T1
	Fill	230	56	OLI	20140917	LC08_L1TP_230056_20140917_20170419_01_T1
		230	56	OLI	20141019	LC08_L1TP_230056_20141019_20170418_01_T1
LANDSAT 5	Fill	229	56	TM	20090912	LT05_L1TP_229056_20090912_20161021_01_T1
2009		229	56	TM	20090928	LT05_L1TP_229056_20090928_20161020_01_T1
		230	56	TM	20091106	LT05_L1TP_230056_20091106_20161023_01_T1

This research also used available maps such as the Ecosystem map Teunissen (1978), the Preliminary Vegetation Map (1998), the Forest Cover Map SarVision (2010), the Global Distribution of Mangroves USGS map (2011) and the Dynamics of of the coastline and the relationship to mangrove using Remote Sensing by V. Moe Soe Let (2016) as reference. These maps are stored in the database of FCMU for the interpretation of the resulting final mangrove maps of Paramaribo and Coronie. Bing Aerial, Google Earth, reports, and literature were also used as support materials for identification of the mangrove forest on the satellite images.

3.2.2 Field data

During the field research, land cover data was being gathered. The locations, where the data collection took place, were first marked on a satellite image and distributed over the visualized mangrove forest cover. In the end, the markers were uploaded in a GARMIN GPS-instrument. The field materials were the map with the planned points to visit (Appendix VI), the GARMIN GPS-instrument, a camera, and datasheets. Data that was being recorded, included:

- Different mangrove types: Black mangrove (*Avicennia germinans* - Parwa), Red mangrove (*Rhizophora mangle* - Mangro) and White mangrove (*Laguncularia racemosa* - Akira) which are shown in appendix VII.
- Location and direction (North, South, West or East) of the mangroves.
- General information (title) of each picture that was captured on every planned point.

3.2.3 Software

For this research QGIS 2.18.1 had been used for the whole processing and QGIS 2.10 was only used to work with the Orpheo toolbox for classification purposes. Quantum Geographic Information System (QGIS) is an open-source desktop software product with several plugins that can be used to visualize, manage, edit, analyze and compose maps with geographic data.

3.3 Methods

According to the purpose of this thesis, a historical assessment was done on the changes of the mangrove forest cover for the years 2009, 2014 and 2017. At first, the extent of the mangrove forest cover within the study areas for all three years were being analyzed with the use of available Landsat images and field validation data. At the end of this research, a significant difference in the area was being analyzed between the classified mangrove forest cover maps of 2009, 2014 and 2017, through a mathematical combination of pixel by pixel for Paramaribo and Coronie.

3.3.1 Mangrove forest cover 2009 - 2017

The methodology was adopted for three main steps, to know pre-processing, core-processing and post-processing. In the pre-processing, the downloaded surface reflectance (SR) images were being prepared for further processing. By implementing the Cloud Masking 18.2.6 plugin for removing the clouds and clouds shadow, which were the most unavoidable obstacles on optical satellite imagery, from each of the downloaded bands (USGS 2017; Foga, et al. 2017). In the core-processing, the SVM Classifier was used for classifying the mangrove forest The SVM classifier had three steps toward mangrove classification, which were:

- **Compute Images Statistics:**
  This application computes a global mean and standard deviation for each band of the clipped images and optionally saves the results as an XML file. The output XML file was used as an input for the Train Images Classifier application to normalize samples before learning.

- **Train SVM Image Classifier:**
  This application performed a classifier training on the color composites and Region of Interests (ROI's) were being built for each class. The dataset of the ROI's was split into validation data and training data. To agree with the output, the Confusion Matrix and the Kappa Index (which must be near 1) must be evaluated.

- **Create Image Classification:**
  This application performs an image classification based on the output of the SVM classifier

The classification was done along with other subclasses, known as Hydrology, Forest, Urban area and Bare soil. The classes are defined in table 6 as follows:

Table 2: Definitions of the classes

Class	Name	Definition
0	No data	Areas outside the study areas
1	Hydrology	Defines the presence of water in the study area and, consequently, Atlantic Ocean, rivers and swamp areas.
2	Mangrove forest	The area of forest and other wooded land consisting of salt-tolerant trees or shrubs, generally exceeding five meters in height at maturity, and which normally grows above mean sea level in the intertidal zone of marine coastal environments, or estuarine margins (Duke, 1992; SBB, 2014).
3	Forest	Land mainly covered by trees which might contain shrubs, palms, bamboo, grass and vines, in which tree cover predominates with a minimum canopy density of 30%, a minimum canopy height (in situ) of 5 meters at the time of identification, and a minimum area of 1.0 ha (SBB, 2014).

4	Urban area	Areas that are concentrated with population, villages, towns or cities with differentiated infrastructure in rural areas, with a density of streets, dams, houses, buildings and other public facilities (SBB, 2016)
5	Bare soil	These are areas that do not conform to any of the above subjects, as would be sandbars, rocky outcrops and others

In the post-processing, the classified image was adjusted using the Sieve tool followed by a manual correction by the interpreter. The Sieve tool was used to generalize and reduce pixel misclassifications. Knowing that the human eyes were the best remote sensor, in the end, the mangrove vector layers underwent a visual check and manual corrections carried out by the interpreter. The entire process is detailed in appendix VIII.

3.3.2 Validation of the mangrove maps 2009-2017

The accuracy assessment was done by comparing each pixel of the remotely sensed classification with ground truth data (Congedo 2018). The accuracy assessment is based on error matrices. An error matrix is sorted in columns and rows and the values represent numbers of pixels. The Columns contain reference data, while the rows contain data of the classified map (Congalton and Green 2004). An example of an error matrix is shown in table 7. The error matrix is further described in appendix IX.

Table 3: Example of an error matrix

		j = Columns (Reference)			Row total
		1	**2**	**k**	N_{i+}
i = Rows (Classification)	**1**	$\mathbf{N_{11}}$	N_{12}	N_{1k}	N_{1+}
	2	N_{21}	$\mathbf{N_{22}}$	N_{2k}	N_{2+}
	K	N_{k1}	N_{k2}	$\mathbf{N_{kk}}$	N_{k+}
Column total	N_{+j}	N_{+1}	N_{+2}	N_{+k}	**N**

3.3.3 Change detection of the mangrove forest cover 2009-2017

The mangrove change detection included a comparative analysis of independently produced mangrove classification maps, produced for the three different time intervals (2009-2014, 2014-2017 and 2009-2017). This comparison is done through a mathematical combination of pixel by pixel. The output has been represented as a matrix showing the values of three different stages of mangrove: mangrove-destruction, mangrove-regeneration, and mangrove-stabilization. Additionally, a spatial image is generated showing the changes in the mangrove forest cover. This was the final step of the remote sensing historical assessment on the changes in the mangrove forest cover for the years 2009, 2014 and 2017.

4. RESULTS

The classification results represented the mangrove forest, including the areas of mangrove removals within Paramaribo and Coronie study areas for the years 2009, 2014 and 2017. The mangrove forest cover change detection was carried out using the mangrove map results for three different intervals 2009-2014, 2014-2017 and 2009-2017.

4.1 Extraction of the Mangrove Forest Cover 2009 - 2017

The three processes pre-, core- and post-processing used to generate the maps showing the spatial distribution of the mangrove forest cover in Paramaribo and Coronie, with an accuracy between 97 – 100 %. The following results of the mangrove extraction within Paramaribo in 2017 gives an illustration of the whole process. Also, the results of Paramaribo in 2009 and 2014 and Coronie in 2009, 2014 and 2017 are detailed in appendix X.

Figure 8 illustrates the result of the pre-processing of Paramaribo in 2017. The prepared image was derived from the Landsat 8 OLI image of September 2, 2017 and refilled with data of the image of October 4, 2017.

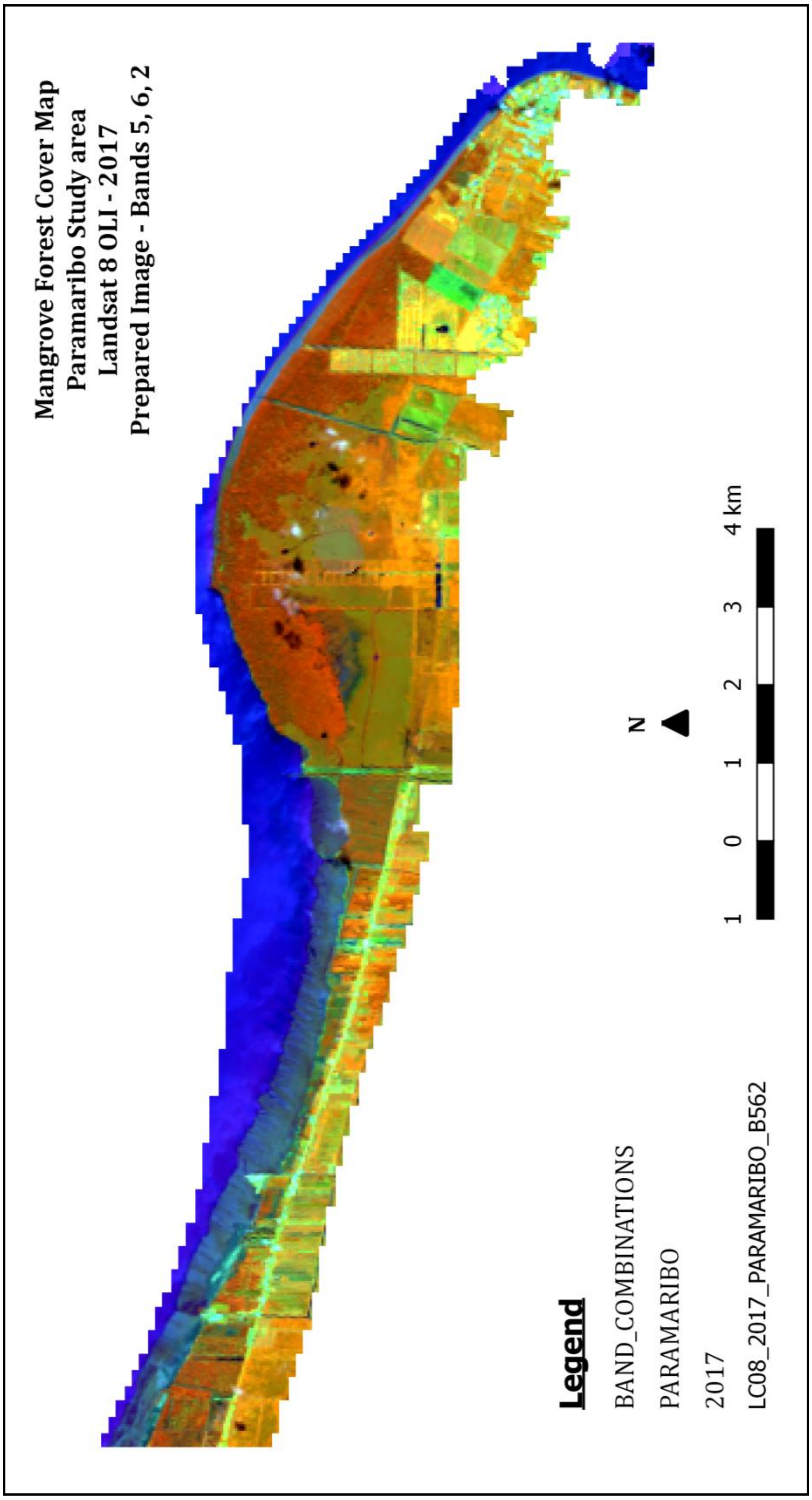

Figure 8: Prepared image of Paramaribo derived from Landsat 8 OLI in 2017 with a band combination of 5, 6, 2

In the following step, Regions of interest (ROI’s) were drawn based on reference data, which has been illustrated in figure 9.

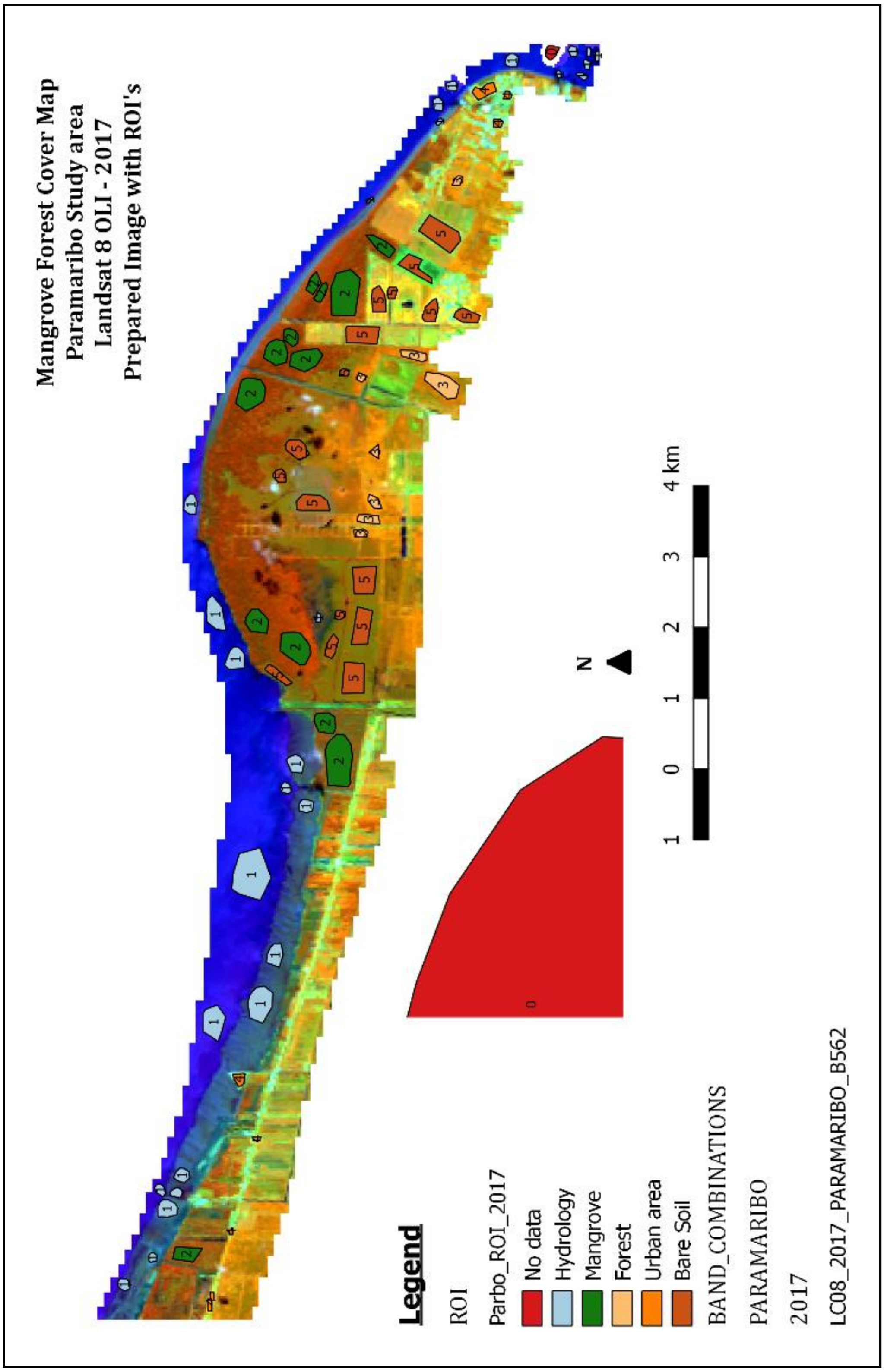

Figure 9: Prepared image of Paramaribo in 2017 with drawn ROI's

The image underwent the SVM classifier which is illustrated figure 10.

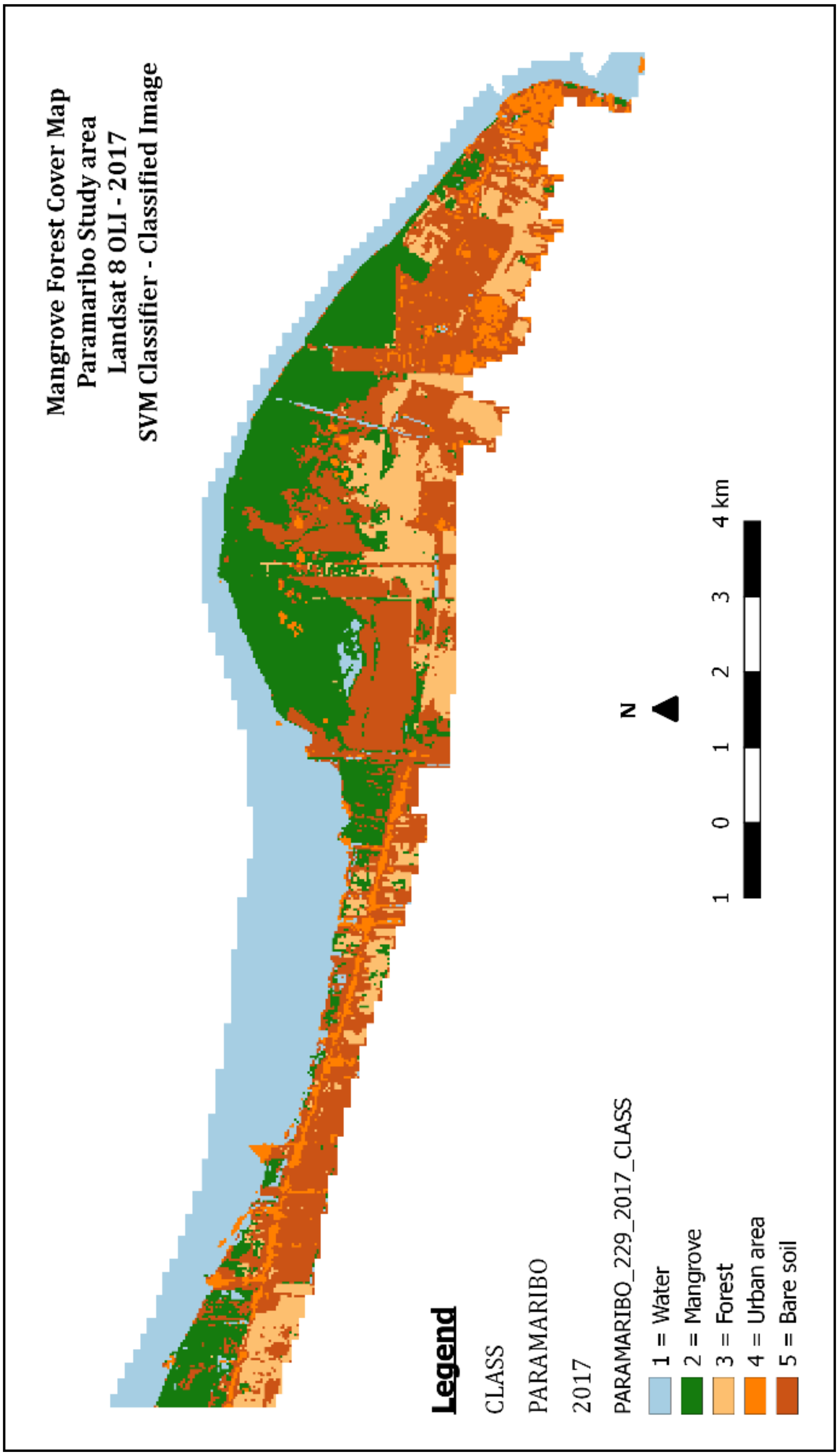

Figure 10: The classified image of Paramaribo in 2017 as result of the SVM classifier

In the final process, the classified image was filtered and manually adjusted. Figure 11 gives an illustration of the adjusted image.

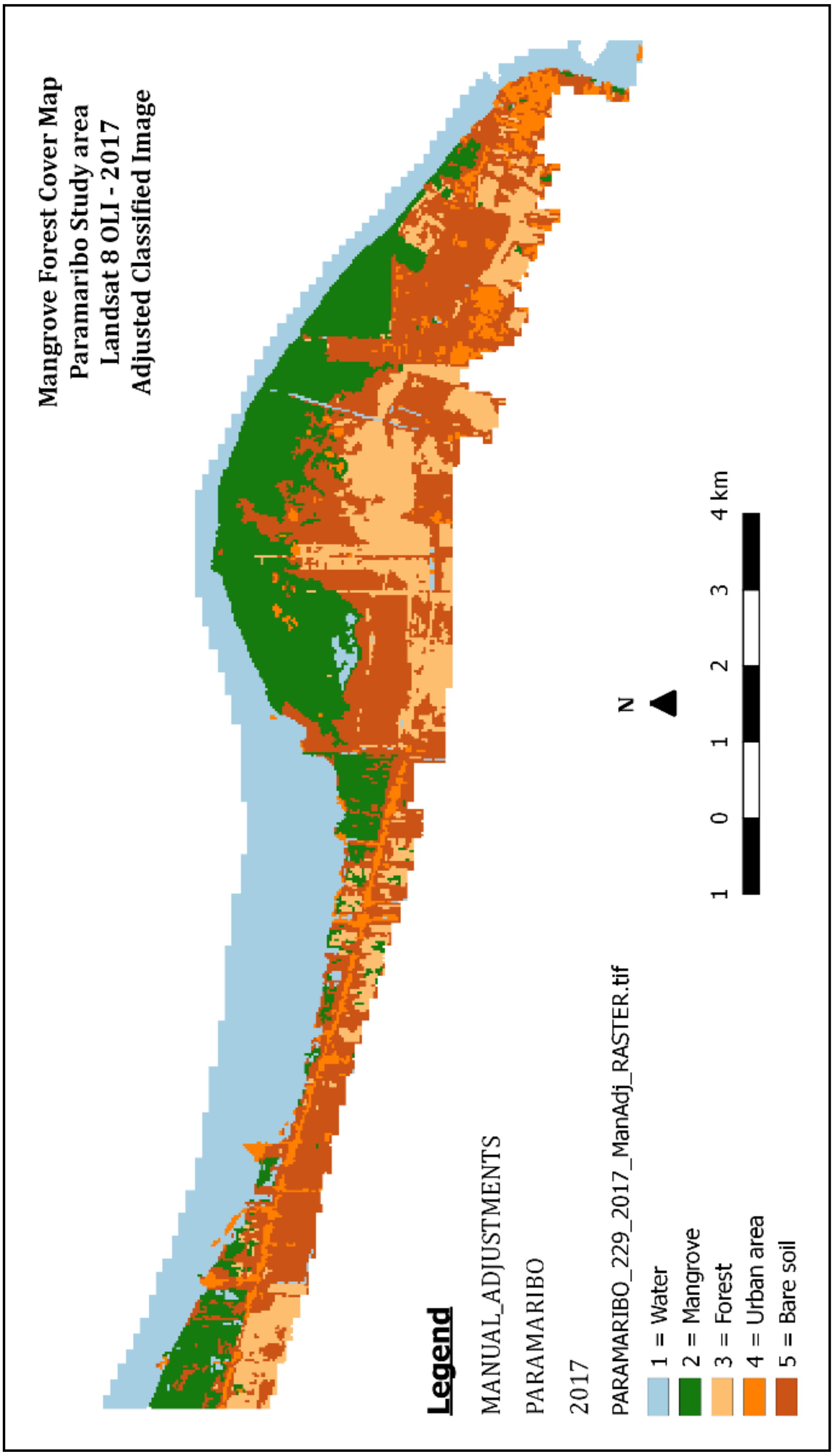

Figure 11: Filtered and manual adjusted classified image of Paramaribo in 2017

Validating the classified image with reference data produced an error matrix in several pixels, which is demonstrated in table 10.

Table 4: The produced error matrix of the classified Paramaribo map for 2017 in pixels

PARAMARIBO 2017		Reference						
		Hydrology	Mangrove	Forest	Urban area	Bare soil	Total	user Accuracy (%)
Classification	Hydrology	14449	0	0	0	0	14449	100
	Mangrove forest	15	9804	895	0	0	10714	91,50644017
	Forest	0	0	5635	0	0	5635	100
	Urban area	0	0	0	2504	0	2504	100
	Bare soil	0	0	0	0	14406	14406	100
	Total	14464	9804	6530	2504	14406	47708	
	Producer Accuracy (%)	99,896294	100	86,294028	100	100		
	Kappa hat Class (%)	97,463265						
	Overall Accuracy (%)	98,092563						

According to the error matrix between the remotely sensed classification and the reference data, the total number of correct pixels (diagonal) and the total number of pixels in the error matrix gave an overall accuracy of 98 %. Subsequently, the measured agreement between the two data gave a kappa hat of 97 %. Also, did the error matrix showed that 895 pixels of the forest class and 15 pixels of the hydrology class were misclassified into the mangrove forest class (Figure 12). The misclassification occurred because of unrecognizable ROI boundaries between the classes. After a comparison of the remotely sensed classification and the reference data, the producer's accuracy of the mangrove class was 99,37 % which indicates a good result of the classification. In the end, the user's accuracy was 98,89 % that gave the reliability and probability of the mangrove class on the map that represents the category on the ground.

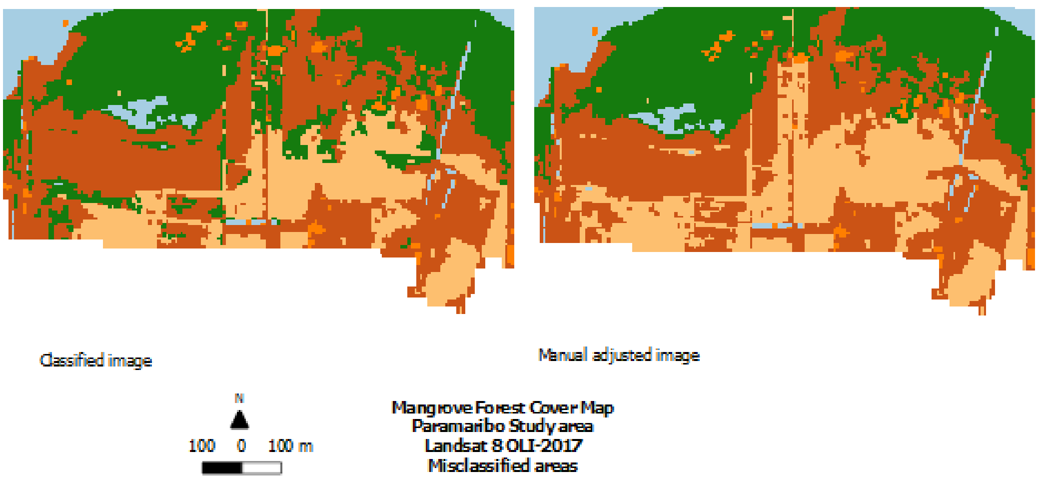

Figure 12: Misclassification 1 - Paramaribo 2017

In the end, the mangrove class was extracted, which is shown in figure 13 as the mangrove map of Paramaribo in 2017.

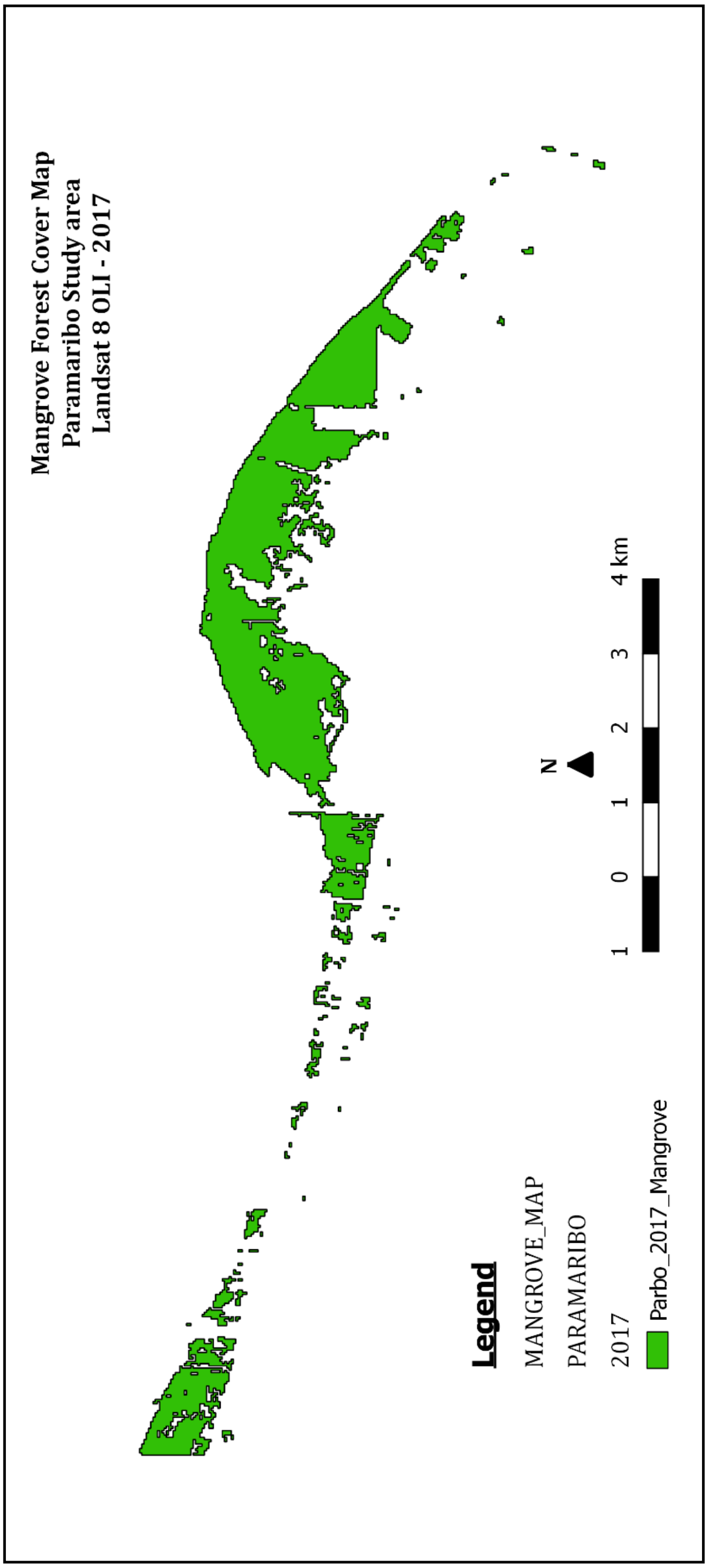

Figure 13: The extracted mangrove map of Paramaribo in 2017

According to the results, the mangrove forest cover of Paramaribo in 2017 was extended over an area of 882.36 ha and was 0.77 % of the total mangrove forest cover of Suriname.

Table 5 indicates the mangrove area (ha) of Paramaribo and Coronie over the years 2009, 2014 and 2017 related to the total mangrove area of Suriname (%) which was 115000 ha (FAO 2010; Kainuma, et al. 2011; WWF 2018; FCMU 2019).

Table 5: Overview of the mangrove area (ha) of Paramaribo and Coronie in 2009, 2014 and 2017 in relation with the total mangrove area of Suriname (%)

	Year	Mangrove area (ha)	Mangrove area of Suriname (%)
Paramaribo	2009	851.76	0.74 %
	2014	805.32	0.70 %
	2017	882.36	0.77 %
Coronie	2009	10,347.48	9 %
	2014	8,034.66	6.99 %
	2017	9,167.22	7.97 %

4.2 Mangrove Change Detection

4.2.1 Paramaribo

According to the results of the Paramaribo study area in 2009, 2014 and 2017 described in section 4.1 showed significant rates of mangrove loss due to extensive land use (urbanization, agriculture, industrialization) and periodic absence of mudflats. Large changes took place near the coast of the "Weg naar Zee" region with a constant erosion of overgrown mudflats caused by the "Guyana Stream", which is illustrated in figure 14.

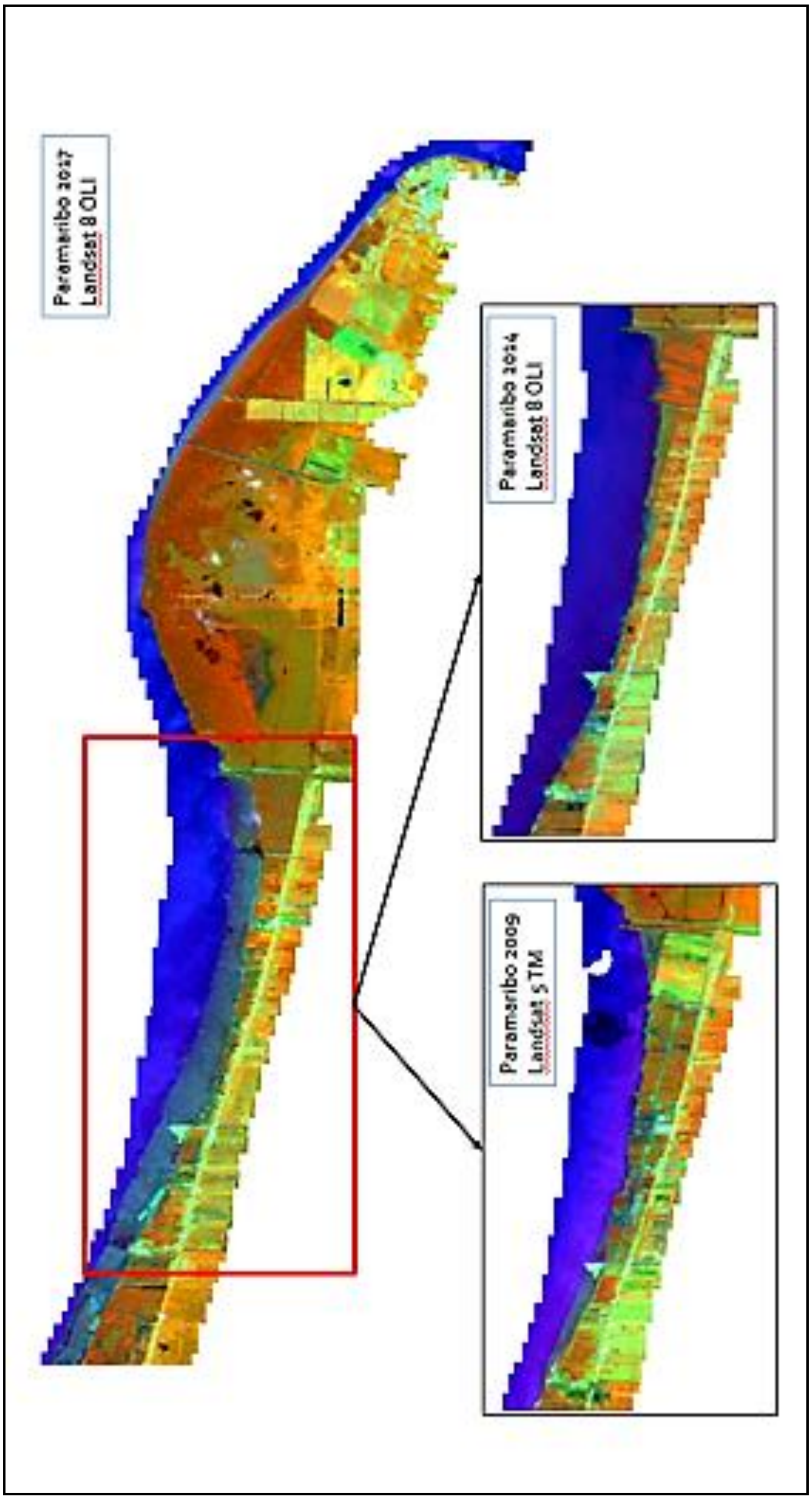

Figure 14: Overview of the "Weg naar Zee" region, the most affected area in Paramaribo

Figure 15 shows the changes in area (ha) of the mangrove forest in Paramaribo from 2009 - 2014.

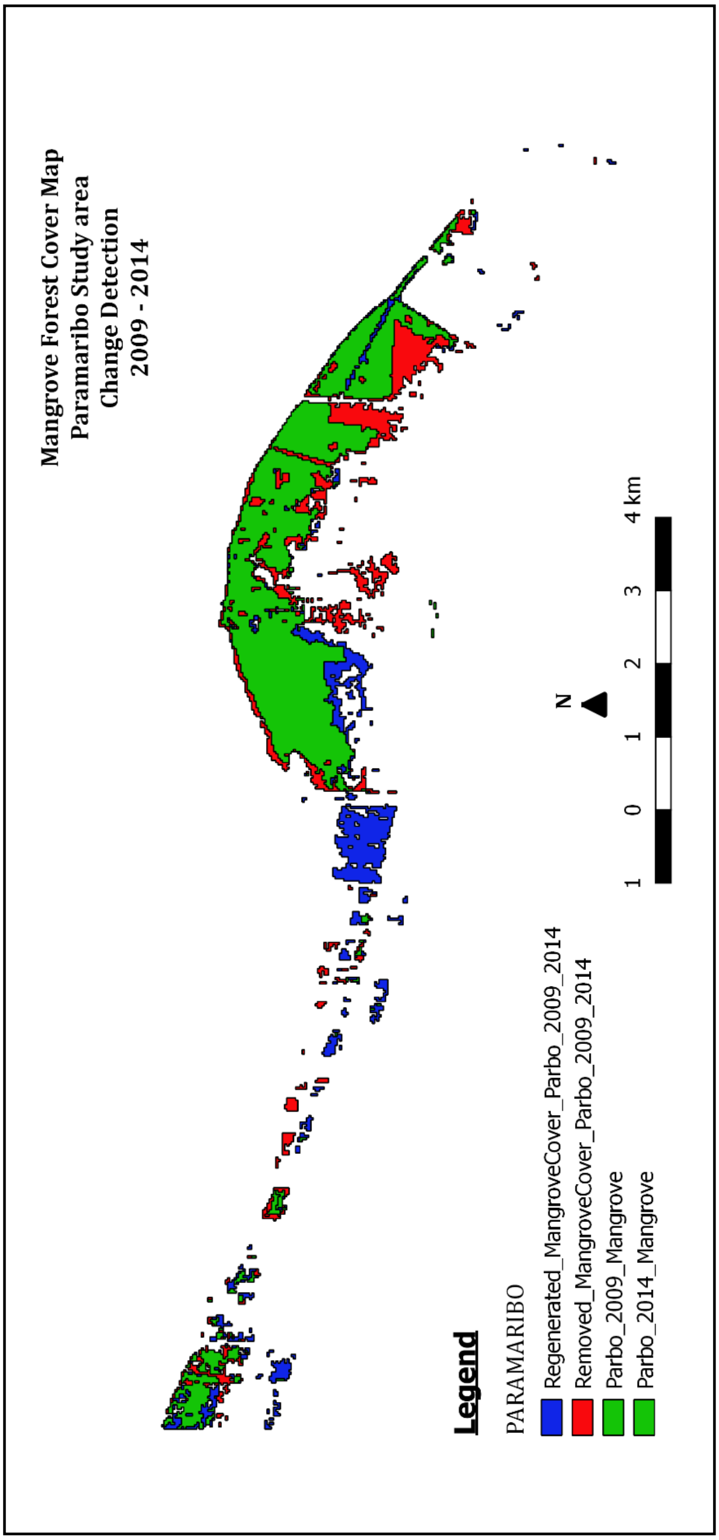

Figure 15: Change detection map of Paramaribo for the period 2009 - 2014

Figure 16 shows the changes in area (ha) of the mangrove forest in Paramaribo from 2014 - 2017.

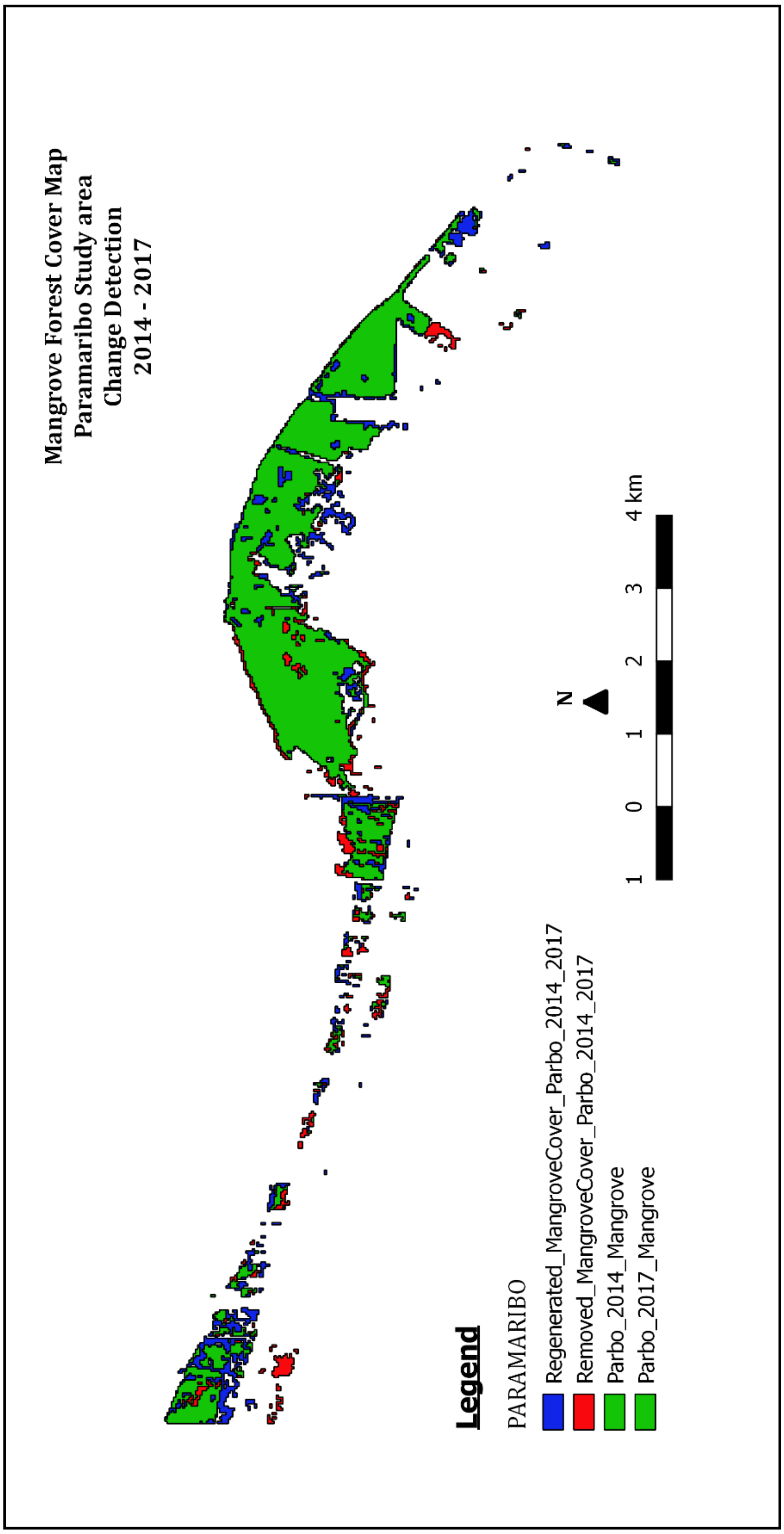

Figure 16: Change detection map of Paramaribo for the period 2014 – 2017

Figure 17 shows the changes in area (ha) of the mangrove forest in Paramaribo from 2009 - 2017.

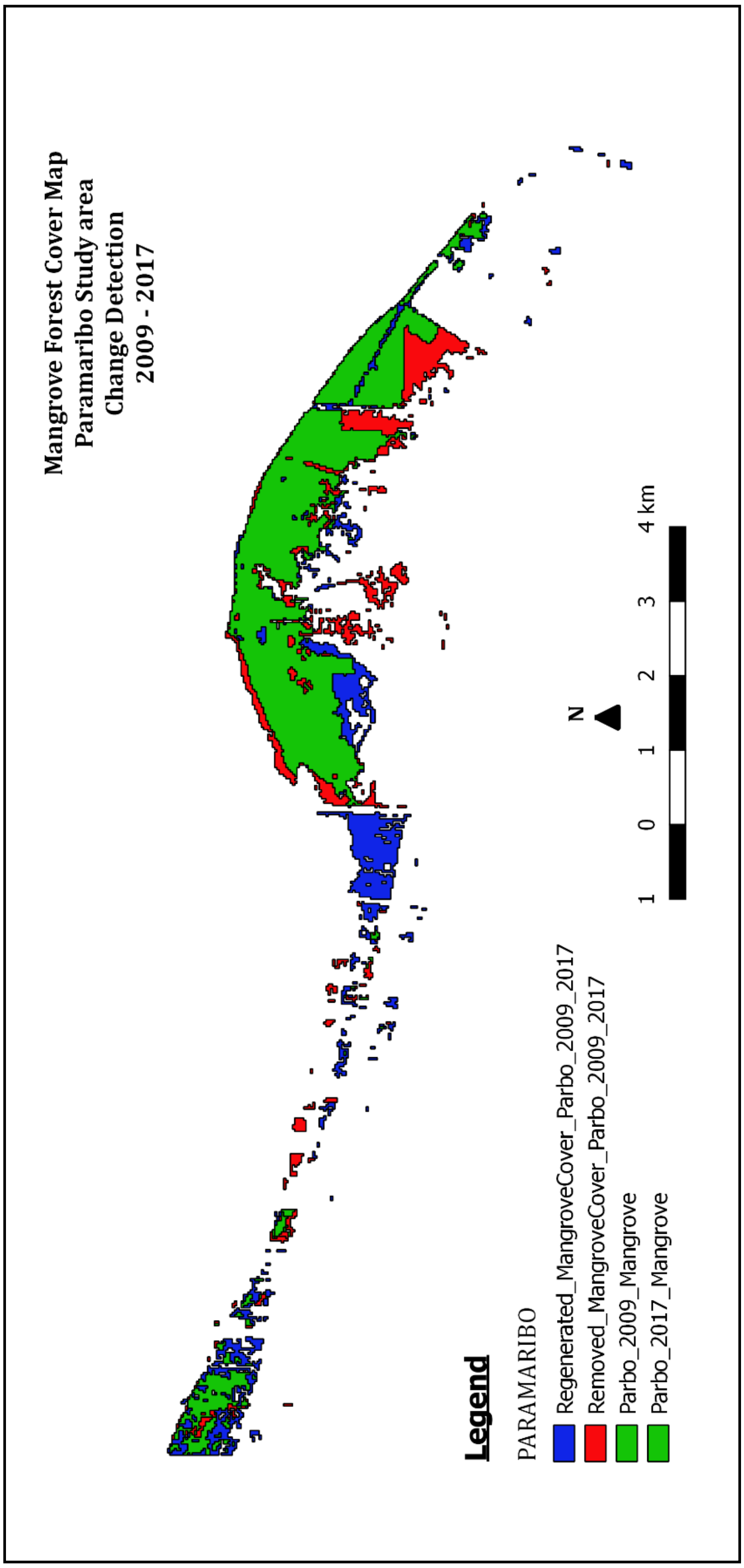

Figure 17: Change detection map of Paramaribo for the period 2009 – 2017

The loss of mangrove, between 2009 – 2017, was 205.29 ha, while 229.50 ha recovered naturally or was newly planted. During the period 2009-2014, 225.27 ha of the mangrove changed to non-mangrove but recovered with 183.33 ha. The loss of mangrove, which was 102.06 ha, reduced in the period 2014-2017 with regeneration of 164.88 ha mangrove forest in the Paramaribo study area. Figure 18 gives an overview of the mangrove forest cover area (ha) change of Paramaribo from 2009 till 2017.

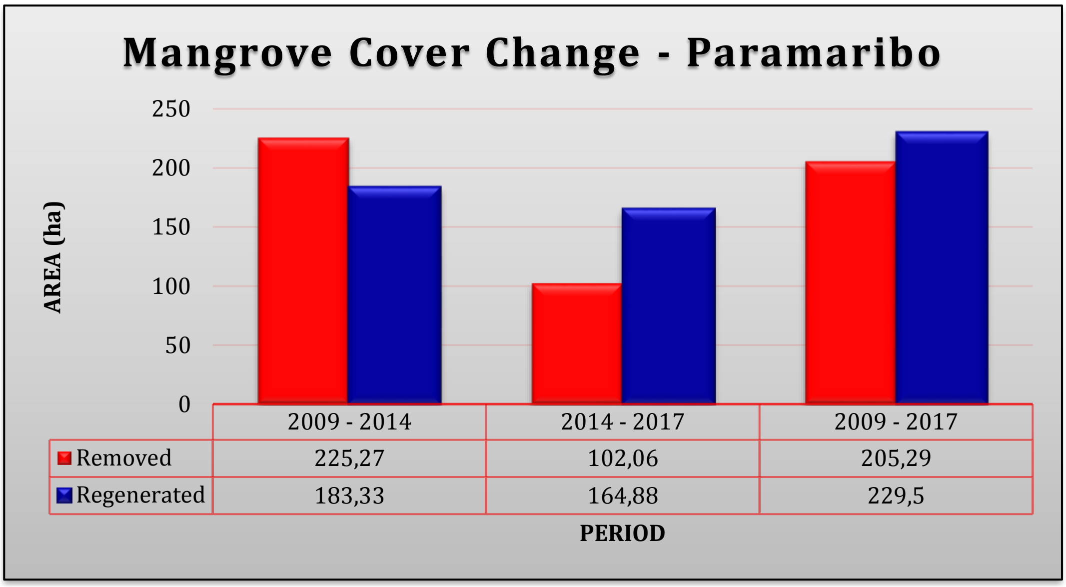

Figure 18: Overview of the mangrove forest cover area (ha) change of Paramaribo from 2009 till 2017

Also, the regenerated and removed mangrove areas, calculated for each period, were used to estimate the yearly changed mangrove net area in hectares divided over 8 years. According to table 6, the yearly regenerated and removed mangrove net area was respectively 43.52 ha and 40.92 ha which were sequentially 4.93 % and 4.64 % of the Paramaribo mangrove area in 2017. Estimations showed that the mangrove forest would yearly change with a regenerated area of 2.61 ha, which was 0.30 % of the Paramaribo mangrove area in 2017.

Table 6: Calculation of the yearly regenerated and removed mangrove net area in hectares of the Paramaribo study area

	Year	Regenerated	Removed	Changed area
PARAMARIBO (ha)	2009	Reference		
	2014	183.33	225.27	-41.94
	2017	164.88	102.06	62.82
Total net mangrove area		348.21	327.33	20.88
Yearly net mangrove area		43.52	40.92	2.61

4.2.2 Coronie

Substantial areas of mangroves near the coast of Coronie were cleared for the “Sea Dike” construction, near-coastal agriculture plantations, road construction, which led to heavy coastal erosion. Along with this, a reducing vitality of the mangrove forest cover took place because of salt intrusions and hydrological disturbances, which is illustrated in figure 19.

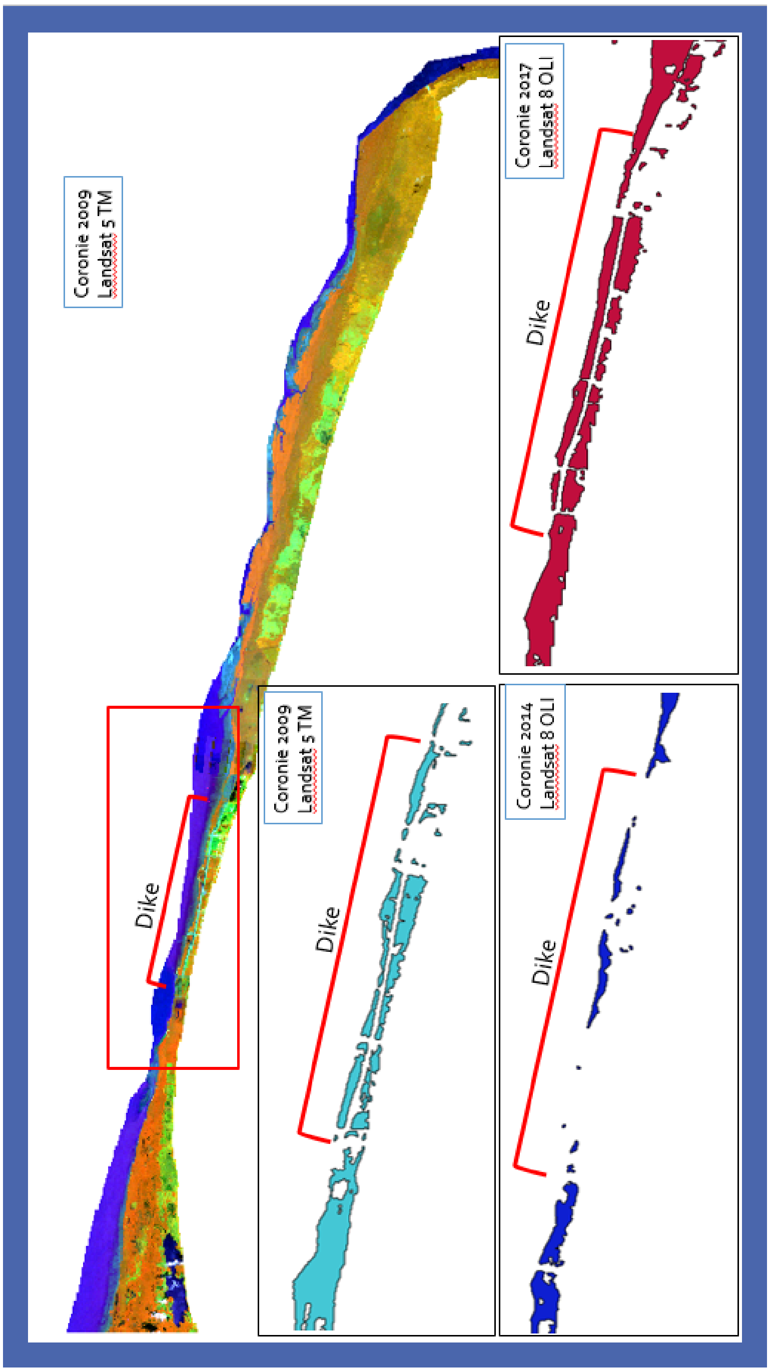

Figure 19: Overview of the most affected area in Coronie

Figure 20 shows the changes in area (ha) of the mangrove forest in Coronie from 2009 - 2014.

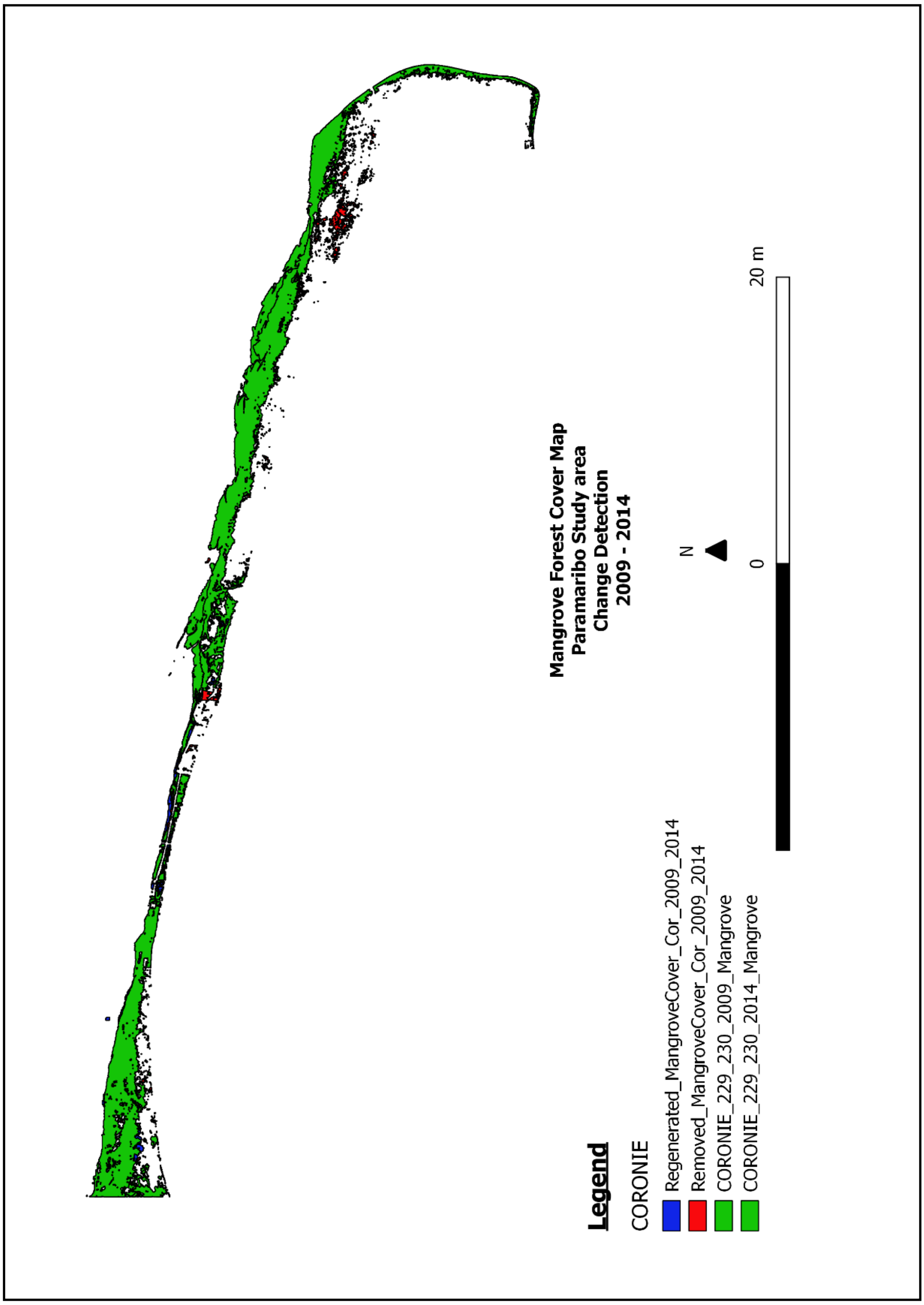

Figure 20: Change detection map of Coronie for the period 2009 – 2014

Figure 21 shows the changes in area (ha) of the mangrove forest in Coronie from 2014 - 2017.

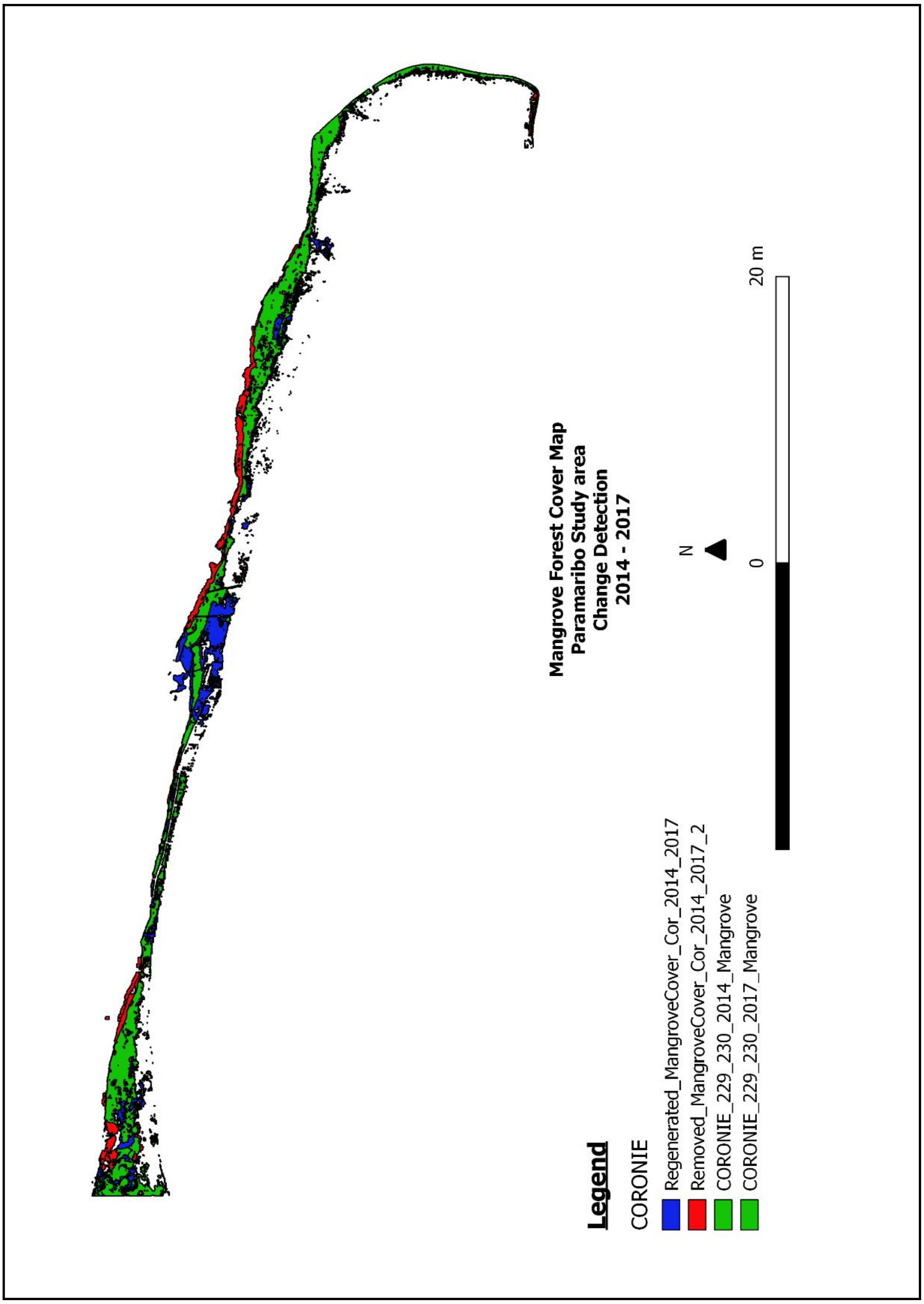

Figure 21: Change detection map of Coronie for the period 2014 - 2017

Figure 22 shows the changes in area (ha) of the mangrove forest in Coronie from 2009 - 2017.

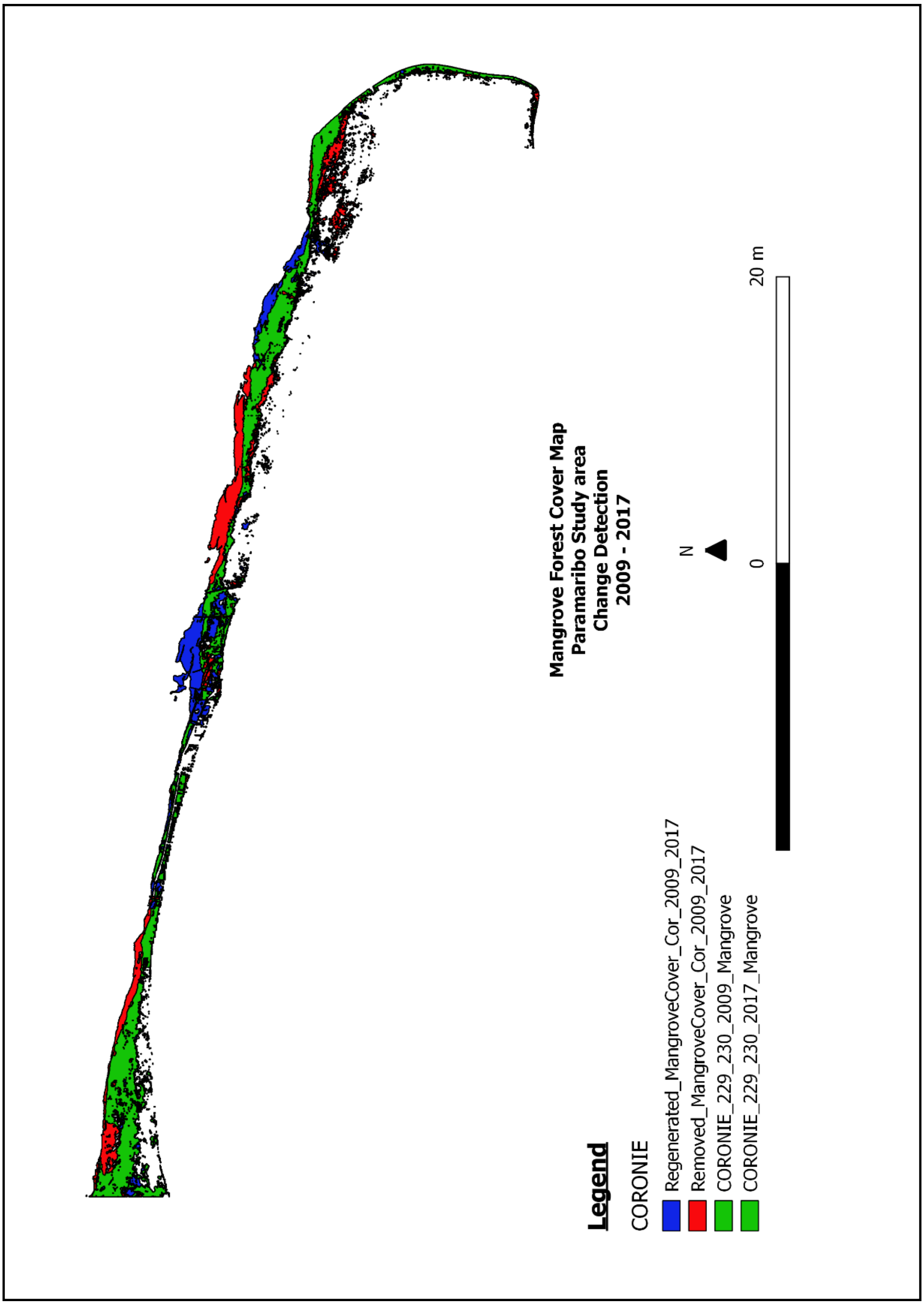

Figure 22: Change detection map of Coronie for the period 2009 – 2017

The change of the mangrove forest cover in the Coronie study area in three past periods, 2009-2014, 2014-2017 and 2009-2017 represented a loss of the mangrove forest by approximately 3846.90 ha. The most loss of 1954.95 ha, from mangrove area to non-mangrove area, was detected in the decade 2014 to 2017 but recovered with 2796.46 ha mangrove forest. Figure 23 illustrates the change of the mangrove forest cover in the Coronie study area.

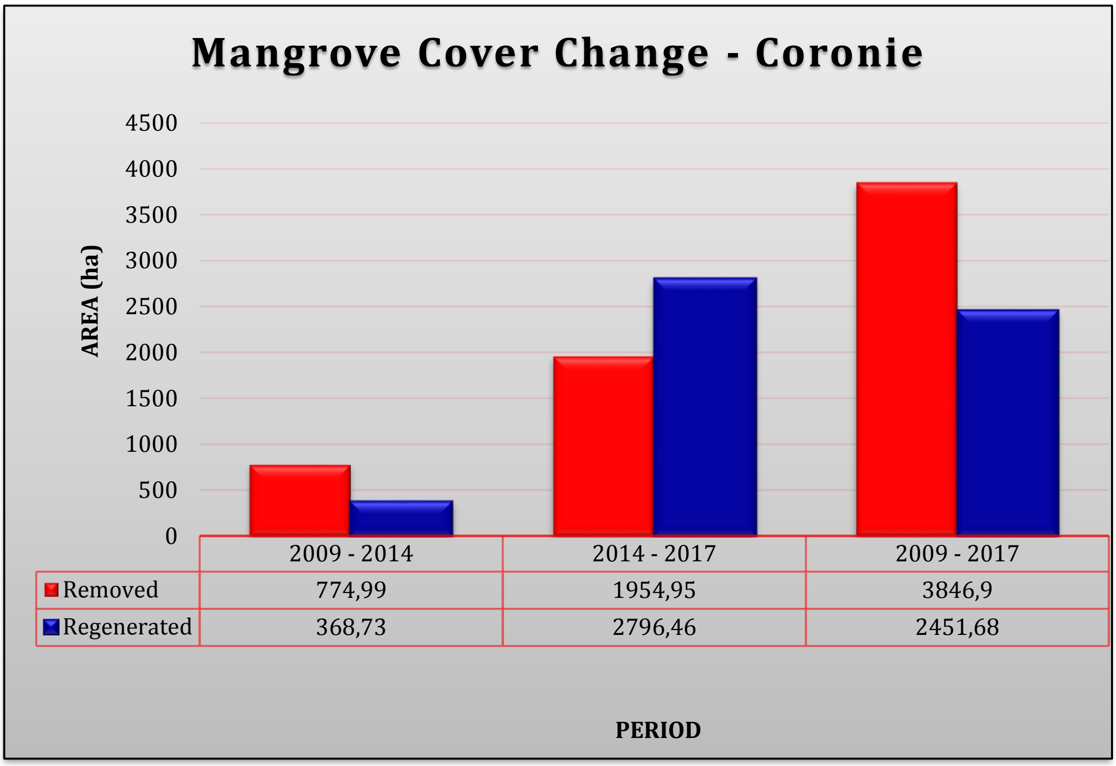

Figure 23: Overview of the mangrove forest cover change of Coronie

Also, the regenerated and removed mangrove areas, calculated for each period, were used to estimate the yearly changed mangrove net area in hectares divided over 8 years. According to table 7, the yearly regenerated and removed mangrove net area was respectively 395.65 ha and 341.24 ha which were sequentially 4.32 % and 3.72 % of the Coronie mangrove area in 2017. Estimations showed that the mangrove forest would yearly change with a recovered area of 54 ha, which was 0.59 % of the Coronie mangrove area in 2017.

Table 7: Calculation of the yearly regenerated and removed mangrove net area in hectares of the Coronie study area

CORONIE (ha)	**Year**	**Regenerated**	**Removed**	**Changed area**
	2009	Reference		
	2014	368.73	774.99	-406.26
	2017	2796.46	1954.95	841.51
Total net mangrove area		3165.19	2729.94	435
Yearly net mangrove area		395.65	341.24	54

5. CONCLUSION

Remote sensing was successfully applied to extract the mangrove forest cover of Paramaribo and Coronie based on characteristics, uniqueness, and distribution as well as reflectance values and spectral properties of the mangrove forest cover in the Landsat images of 2009, 2014 and 2017. The mangrove forest cover of Paramaribo in 2009, 2014 and 2017 extended over, respectively 0.74 % (851.76 ha), 0.70 % (805.32 ha) and 0.77 % (882.36 ha) of the total mangrove forest area in Suriname. Also, the mangrove forest cover of Coronie in 2009, 2014 and 2017 extended over, respectively 9 % (10.347.48 ha), 6.99 % (8034.66 ha) and 7.97 % (9167.22 ha) of the total mangrove forest area in Suriname. The mangrove change detection analysis indicated significant changes between the mangrove forest cover of 2009, 2014 and 2017 for Paramaribo and Coronie. The largest change of mangrove to non-mangrove for Paramaribo was detected during the period 2009 – 2014, which was 225.27 ha and regenerated of about 183.33 ha. The significant changes of the mangrove forest cover in Coronie were during the period 2014 - 2017 that represented a loss by approximately 1954.95 ha but recovered of about 2796.46 ha. The Paramaribo mangrove forest underwent a yearly change with a regenerated area of 2.61 ha, which was 0.30 % of the Paramaribo mangrove area in 2017 and the Coronie mangrove forest would yearly change with a recovered area of 54 ha, which was 0.59 % of the Coronie mangrove area in 2017. The regeneration of the mangrove forest was natural grown or newly planted. On the other hand, loss of the mangrove forest cover as a result of anthropogenic activities, such as urbanization, industrialization, agricultural, fishery, and infrastructure, but also because of natural activities, such as heavy coastal erosion caused by the Guyana stream, salt intrusions, hydrological disturbances and periodic absence of mudflats.

RECOMMENDATION

Despite the importance of the mangrove forest, comprehensive and reliable information on their spatial extent was missing which is crucial for monitoring the changes in the mangrove forest cover. The overall efforts in this research showed the effectiveness of the proposed method used for investigating the spatiotemporal changes of the mangrove forest. This data could provide planners with invaluable quantitative information for sustainable management of mangrove ecosystems in Suriname by maintaining their environment, ecological and socio-economic benefits.

Monitoring of mangrove forest in Suriname would provide estimates on the extent and conditions of mangrove. According to Erftemeijer and Teunissen (2009) this should be happening at regular intervals of 3-5 years in the problem areas and 5-10 years nationwide. But it is recommended to monitor each year in the problem areas and 3-5 years nationwide.

When monitoring the mangrove forest, it is recommended to use Sentinel 2A images (launched in 2015) with a high spatial resolution (10 m) over land and coastal areas than Landsat images (30 m).

Before getting into the field, it is recommended to use drones, it provides higher temporal resolution images, even clouds could not be an obstacle, especially when working in a humid tropical climate. Drones can be used for getting a better overview of the field and the accessibility for field visitors.

Through time the software gets modernizing including the plugins that were used for extracting the mangrove forest. It is recommended to keep working with the updated versions of QGIS and plugins.

REFERENCES

Abadal, G, and et al. 2014. "Electromagnetic Radiation Energy Harvesting - The Rectenna Based Approach. Ch 1."

Agency European Space, ESA. 2017. *Copernicus observing the earth.* december 7. Accessed april 17, 2018. https://www.esa.int/Our_Activities/Observing_the_Earth/Copernicus/Overview4.

Augustinus, P. G. E. F. 1978. "The Changing Shoreline of Surinam (South America)."

Bock, M, and G Krause. 2006. "Remote Sensing of Mangrove Forest Structure and Dynamics."

Canada, Natural Resources. 2015. *Fundamentals of Remote Sensing - Introduction.* November 19. Accessed Augustus 9, 2018. http://www.nrcan.gc.ca/node/9363.

Congalton, R. G., and K. Green. 2004. "Remote Sensing and GIS Accuracy Assessment."

Congedo, Luca. 2018. "Semi-Automatic Classification Plugin."

Dan, T. T., C. F. Chen, S. H. Chiang, and S. Ogawa. 2016. "Mapping and change analysis in mangrove forest by using Landsat imagery." *Remote Sensing and Spatial Information Sciences, Volume lll-8* 8.

Ellison, J., V. Jungblut, P. Anderson, and C. Slaven. 2012. "Manual for Mangrove Monitoring in the Pacific Islands Region."

Erftemeijer, P, and P Teunissen. 2009. "Analysis of problems and solutions for the management of mangrove forests." Suriname, 3 - 8.

FAO. 2010. „Global Forest Resources Assessment."

FCMU, Forest Cover Monitoring Unit -. 2015. "Overview Mangrove Forest Area."

Humboldt State University, Geospatial Online. 2017. *GSP 216 Introduction to Remote Sensing.* Accessed July 24, 2018. http://gsp.humboldt.edu/OLM/Courses/GSP_216_Online/lesson2-1/surface.html.

ICZM-EPA, Guyana Forestry Commission and Integrated Coastal Zone Management. 2012. „National Mangrove Management Action Plan."

JARS. 1993. *Remote Sensing Note. Japan Association on Remote Sensing.* Accessed 2018. http://www.jars1974.net/pdf/rsnote_e.html.

Kainuma, Mami, Lorna Collins, Francisca Blasco-Takali, en Francois Blasco. 2011. *Atlas Mundial de los Manglares (World Atlas of Mangroves).*

Kanniah, K, A Sheikhi, A Cracknell, H Goh, K Tan, C Siong Ho, and F Rasli. 2015. "Satellite Images for Monitoring Mangrove Cover Changes in a Fast Growing Economic Region in Southern Peninsular Malaysia." *remote sensing ISSN 2072-4292.*

Kauffman, J. B., and D. C. Donato. 2012. "Protocols for the measurement, monitoring and reporting of structure, biomass and carbon stocks in mangrove forests." 1.

Kuenzer, Claudia, Andrea Bluemel, Steffen Gebhardt, Tuan Vo Quoc, and Stefan Dech. 2011. "Remote Sensing of Mangrove Ecosystems: A Review." *Remote Sensing ISSN 2072-4292* 878-928.

Moe Soe Let, V. 2016. „Study on the dynamics of the coastline of Suriname and the relationship to mangrove using Remote Sensing."

NASA. 2013. *Landsat 7 Science Data User's Handbook.* Accessed July 9, 2018. http://landsathandbook.gsfc.nasa.gov.

Noordam, D. 2010. „Environmental Impact Assessment of production development of the Tambaredjo North-West oil field in Suriname."."

Polidori, Laurent. 2008. "Remote Sinsing and Coastal Ecosystem Monitoring in French Guiana: Research and Achievements over a decade." *Commission VIII, WG VIII/4.*

Rene, Somopawiro, Matai Rewiechand, Crabbe Sarah, Djojodikromo Mark, Paloeng Consuela, and Svensson Sara. 2015. "Global Forest Resources Assessment ." Country report.

Richards, J. A., and X. Jia. 2006. In *Remote Sensing Digital Image Analysis: An Introduction*. Berlin, Germany.

SBB. 2014. "Baseline Mangrove Forest Suriname."

SBB. 2014. „Suriname National Plan for Forest Cover Monitoring (FCM Plan)."

SBB. 2016. "NFMS Roadmap - Status and Plans for Suriname's National Forest Monitoring System."

UNDP. 2011. "Suriname Coastal Protected Area Management."

UNDP. 2011. „Suriname Coastal Protection Area Management."

USGS. 2018. *Landsat Missions - What are the best spectral bands to use for my study?* October 18. Accessed November 13, 2018. https://landsat.usgs.gov/what-are-best-spectral-bands-use-my-study.

USGS, U.S. Department of the Interior - U.S. Geological Survey. 2018. *Landsat Missions.* April 25. Accessed Augutus 11, 2018. https://landsat.usgs.gov/what-are-band-designations-landsat-satellites.

WWF. 2018. *Eastern Soth America: Coastal French Guiana, Suriname, Guyana and southeastern Venezuela.* Geopend April 26, 2018. https://www.worldwildlife.org/ecoregions/nt1411.

APPENDICES

Appendix I: The Forest Cover Monitoring Unit (FCMU)

Land cover and land use (changes) in Suriname are being monitored by the Forest Cover Monitoring Unit (FCMU) of the Foundation for Forest Management and Production Control (SBB). The FCMU was established in 2012 within the ACTO-project "Monitoring the forest cover in the Amazon region" to contribute to the strengthening of the National Forest Monitoring System (NFMS), by generating information regarding changes in forest cover (SBB 2014; SBB 2016)). A vision for the National Forest Monitoring System (NFMS) of Suriname was developed by multiple stakeholders in 2014, in the context of formulating a National Plan for Forest Cover Monitoring:

Vision: "Suriname monitors forest cover changes in the whole country in close collaboration with multiple stakeholders, using modern technologies and local community participation in a system that provides the national and international community with the most updated and reliable information about forest cover, which is used to enforce governance on deforestation, forest degradation, land tenure and land use (changes), to sustainably manage the forest resources while maintaining resilience of forest ecosystems."

The Satellite Land Monitoring System (SLMS) is one of the components of NFMS that encompasses forest cover monitoring using Remote Sensing information. The methods used by the FCMU include the use of open-source software and freely available satellite images (SBB. 2016).

Appendix II: Components of Remote Sensing

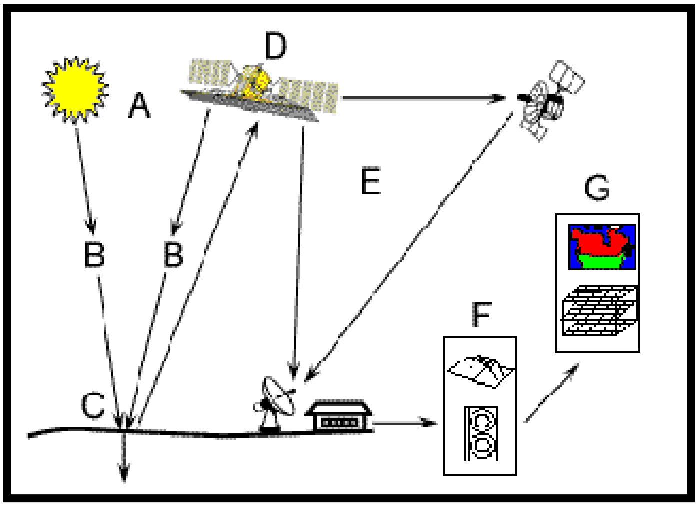

Figure II-1: Overview of the Remote Sensing system (Natural Resources Canada 2015)

The components of remote sensing in figure II-1 are described as follow (Canada 2015):

- **The Energy Source or Illumination (A)** can be the sun or a satellite sensor which illuminates or provides electromagnetic energy to an earth object.
- **Radiation and the Atmosphere (B)** is the interaction of the energy from source to earth object and from earth object to satellite sensor. While traveling, the energy also encounters the atmosphere.
- **Interaction with the target (C)** is depending on the properties of the earth object and the radiation.
- **Recording of energy by the sensor (D)** is the collection of electromagnetic radiation, which has been scattered by or radiated from the earth object, by a satellite sensor.
- **Transmission, Reception and Processing (E)** occurs when the receiving and processing station conceives the recorded energy by the sensor and transmits it into an image.
- **Interpretation and Analysis (F)** is visually, digitally or electronically extraction of information about the earth object from the image.
- **Application (G)** is the final process of remote sensing, which is accomplished when the extracted information is used due to better understand it and disclose new information.

Appendix III: Data within the Forest Cover Monitoring Unit (FCMU)

Within the FCMU forest cover and deforestation maps have been made for 2000, 2000-2009, 2009-2013 and 2013-2014 (Figure III-1). The area covered with these maps remains constant over the years, amongst others to determine the deforestation rate and forest coverage compared to a constant area. This means that the area subjected to coastal dynamics is not completely included. So, there is no complete coverage of mangrove forest within these maps.

Nevertheless, during the above-mentioned collaborative study, more detailed mapping of the coastal area can be carried out, including the area subjected to coastal dynamics, with a special focus on mangrove forest, but eventually also including other land and forest cover/use types. It will be done in a way that it is linked to the forest cover monitoring system of the whole country.

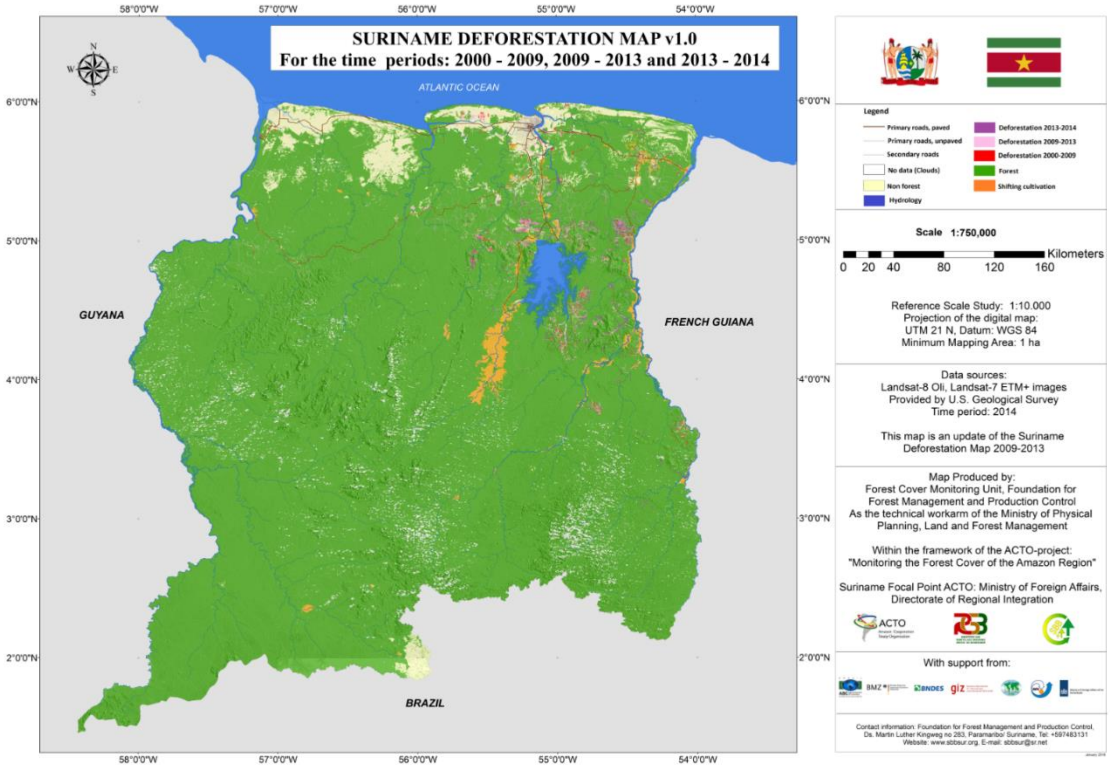

Figure III-1: Deforestation map for the time periods of 2000-2009, 2009-2013 and 2013-2014

Global Distribution of Mangroves USGS (2011)

Figure III-2: Global distribution of mangrove forests using Global Land Survey (GLS) data and the Landsat archive (USGS)

Description

This dataset shows the global distribution of mangrove forests, derived from earth observation satellite imagery (Figure III-2). The dataset was created using Global Land Survey (GLS) data and the Landsat archive. Approximately 1000 Landsat scenes were interpreted using hybrid supervised and unsupervised digital image classification techniques. The mangrove area of Suriname within this dataset is 74552 ha. See Giri et al. (2011) for full details.

Temporal range

1997-2000

Limitations

Results were validated using existing distribution data and published literature. Note that small patches (< 900-2,700 sq.-m) of mangrove forests cannot be identified using this approach. This methodological approach had several challenges, such as cloud cover and noise. There may also be areas where land cover was misclassified.

Preliminary vegetation map (CELOS/Narena- 1998)

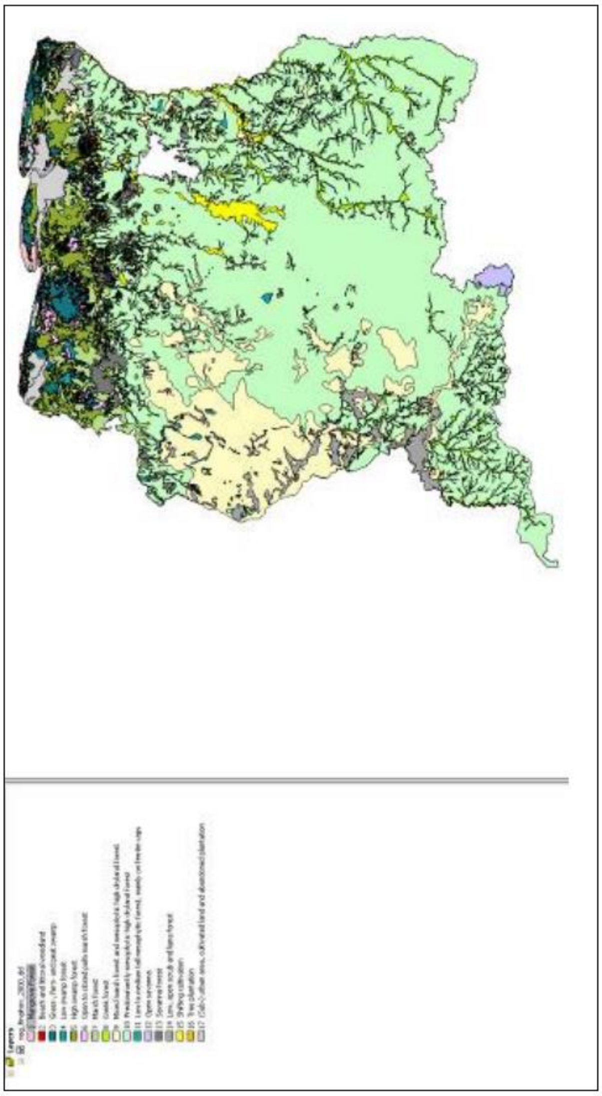

Figure III-3: Preliminary vegetation map (CELOS/Narena- 1998)

Description

CELOS/Narena made a preliminary vegetation map, based on field observations and landsat images (Figure III-3). Mangrove forest is also classified on this map. A total area of 114.400 ha of mangrove forest was delineated on this map.

Limitations

The report explaining which methodology was used to produce this map, is missing.

Forest Cover Map SarVision (2010)

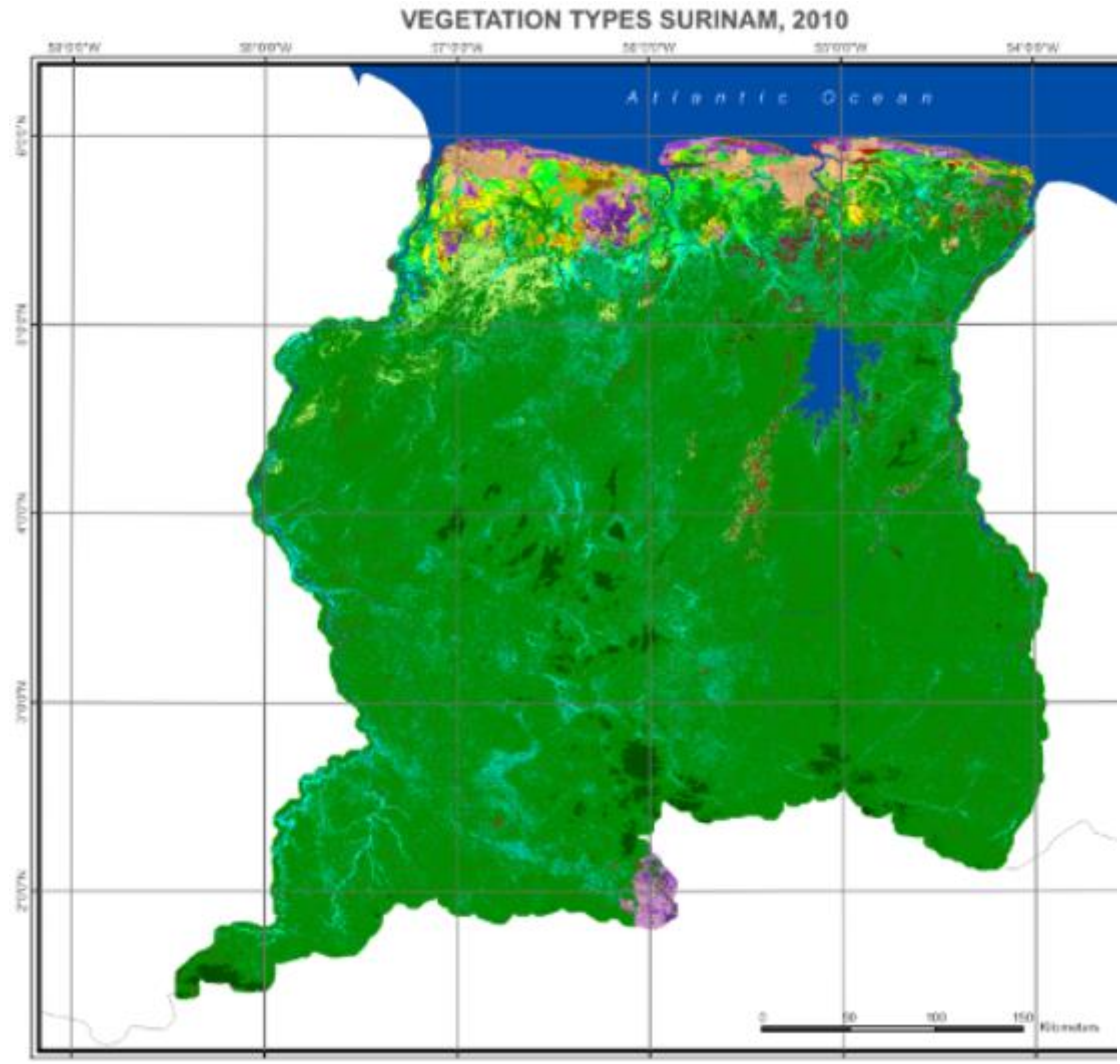

Figure III-4: The vegetation map of Suriname in 2010 carried out by SarVision and Wageningen University, the Netherlands

Figure III-5: The mangrove forest area on the vegetation map in 2010 carried out by SarVision and Wageningen University, the Netherlands

Description

The vegetation map for the whole country of Suriname is carried out by SarVision and Wageningen University, the Netherlands (Figure III-4). This assignment is commissioned by Conservation International Suriname within the framework of the KfW REDD+ project. The map is based on ALOS PALSAR radar satellite images at 50m resolution. Advanced techniques for radiometric correction, relief correction to reduce topographic effects, radar image mosaicking and radar image classification have been applied in the creation of this map. The mangrove area within this map, which is illustrated in figure III-5, was 40238 ha.

Limitations

This type of qualitative validation is done using the available preliminary vegetation map of Suriname developed by K. Tjon, from the Centre for Agricultural Research in Suriname (CELOS), NARENA. The map is an indicative map but for the validation of the radar derived map it appears to be appropriate because of the similarities in the legends.

Ecosystem Map Teunissen

Figure III-6: The mangrove forest on the ecosystem map of Suriname produced by Teunissen/ Stinasu in 1978 with aerial photographs (Central Bureau for Aerial Survey, Paramaribo, 1970-1973) and reconnaissance soil maps (Department of Soil Survey, Paramaribo, 1978)

Description

Ecosystem map for the coastal part of Suriname produced by Teunissen / Stinasu 1978 with aerial photographs (Central Bureau for Aerial Survey, Paramaribo, 1970-1973) and reconnaissance soil maps (Department of Soil Survey, Paramaribo, 1978) (Figure III-6). The mangrove area according to this map is 55506 ha.

Study on the dynamics of the coastline and the relationship to mangrove using Remote Sensing by V. Moe Soe Let in the context of a thesis research

To know which area of Suriname is not subject to coastal dynamics (and remains constantly when reporting on area change, as for the National Communication), we made a time series of how the coastline moves for the time period of 1984-2014. The Landsat satellite image archive makes it possible to do historical analyses to monitor the coast in the time period of 1984-2014. Using a semi-automatic classification method, land and hydrology are distinguished from each other with a supervised classification, followed by manual adjustment to improve the classification. This same method is used to detect mangrove in the coastal area with RADAR imagery. Results indicate that the area of interest of Suriname is growing and mangrove detected on the RADAR imagery has a close link with the areas with a high land-acquisition rate (Table III-1).

Table III-1: Growing area of interest of Suriname, with a net area acquisition

Mangrove detected on Radar in areas with land acquisition	**Area (ha)**
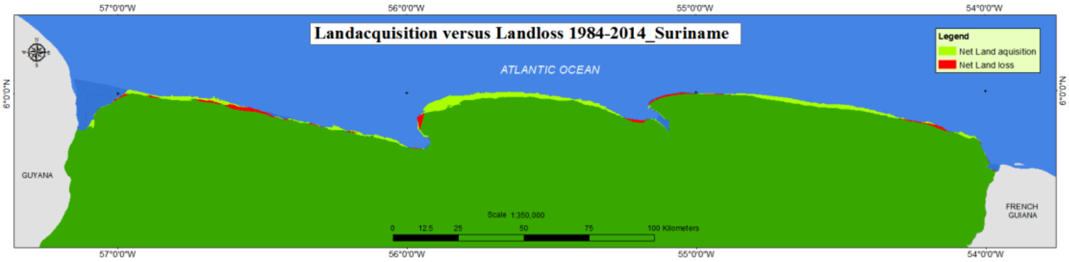 Figure. Areas with a net land acquisition versus areas with a net land loss	Net Land acquisition: 32989.07 Net land loss: 14216.20
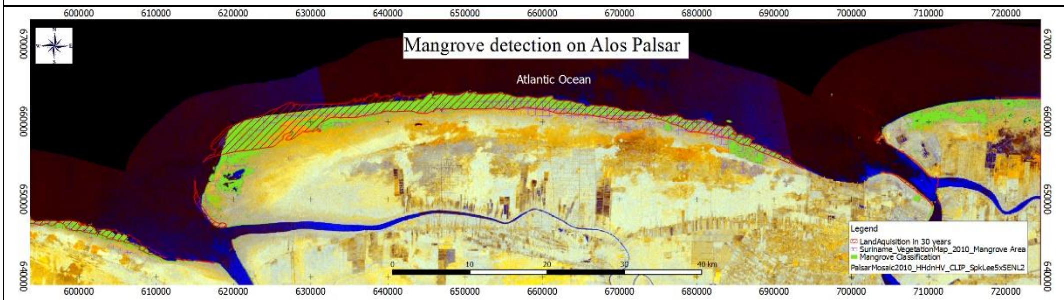 Figure. Mangrove detection on Alos Palsar	Mangrove in study area: 17079.54
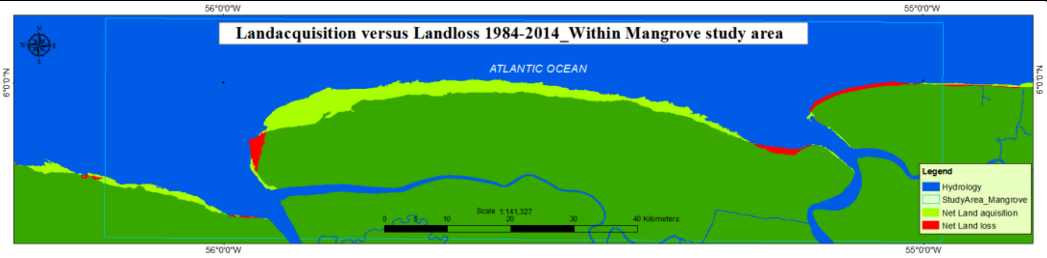 Figure. Land acquisition from 1984-2014 within the study area to detect mangrove	Land acquisition within mangrove study area: 17128.84

Conclusion

Mangrove is growing in the areas where land acquisition takes place. With this information, an extrapolation can be made for the area of mangrove for the whole country. The mangrove area in the period 1984-2014 is then equal to the net land acquisition with an area of 32989.07 ha. This is an underestimation because base on field knowledge, we know that mangrove can also be older than 30 years.

Table III-2: Range of data sources with different areas of mangroves

Data Source	**Area(ha)**
UNEP- Global Distribution of Mangroves –USGS 1997-2000	74552
SarVision – Forest Cover Map 2010	40238
Teunissen – Ecosystem Map 1978	55506
Spalding, M., Kainuma, M. and Collins, L. 2010. World atlas of mangroves. Earthscan, London, UK	50978
FRA 2015 report on mangrove area 2010 (based on preliminary vegetation map of CELOS/Narena)	114400
Study on the dynamics of the coastline and the relationship to mangrove using Remote Sensing (1984-2014) by V.Moe Soe Let	32989

Appendix IV: Band Information of Landsat 5 TM and Landsat 8 OLI

The Landsat 5 TM has 7 spectral bands with a spectral resolution of 30 m for bands 1-5 and 7, while band 6 (Thermal Infrared band) has a resolution of 120 m but is resampled to 30 m pixels which is given in table IV-1.

Table IV-1: Landsat 5 TM band information (USGS 2018)

LANDSAT 5 TM			
Bands	**Name**	**Wavelength (um)**	**Resolution (m)**
Band 1	Visible	0.45 – 0.52	30
Band 2	Visible	0.52 – 0.60	30
Band 3	Visible	0.63 – 0.69	30
Band 4	Near Infrared	0.76 – 0.90	30
Band 5	Near Infrared	1.55 – 1.75	30
Band 6	Thermal	10.40 – 12.50	120
Band 7	Mid - Infrared	2.08 – 2.35	30

The Landsat 8 OLI has 11 spectral bands with a spatial resolution of 30 m for bands 1 - 7 and 9, 15 m for band 8 (Panchromatic band) and 100*30 m for bands 10 and 11 (Thermal Infrared band 1 and 2) that is given in table IV-2.

Table IV-2: Landsat 8 OLI band information (USGS 2018)

LANDSAT 8 OLI			
Bands	**Name**	**Wavelength (um)**	**Resolution (m)**
Band 1	Ultra-Blue (coastal/ aerosol)	0.435 – 0.451	30
Band 2	Blue	0.452 – 0.512	30
Band 3	Green	0.533 – 0.590	30
Band 4	Red	0.636 – 0.673	30
Band 5	Near Infrared (NIR)	0.851 – 0.879	30
Band 6	Shortwave Infrared (SWIR) 1	1.566 – 1.651	30
Band 7	Shortwave Infrared (SWIR) 2	2.107 – 2.294	30
Band 8	Panchromatic	0.503 – 0.676	15
Band 9	Cirrus	1.363 – 1.384	30
Band 10	Thermal Infrared (TIRS) 1	10.60 – 11.19	100*(30)
Band 11	Thermal Infrared (TIRS) 2	11.50 – 12.51	100*(30)

Appendix V: Band Combination for The Mangrove Forest Cover

Across the whole reflectance spectrum, which is shown in section 2.2 figure 4, were “Healthy vegetation”, “Altered rocks characteristic of a mineralized zone” and “Soil” curves with the highest reflectance percentage (30 - 50 %) while “Clear Water” and “Water with phytoplankton” reflected only 10 % of energy (Humboldt State University 2017).

For identification of the mangrove forest cover on the Landsat images, for the year 2009 a color composite was being made of **B 4, 5, 1** for **Landsat 5 TM** and for the years 2014 and 2017 a color composite was being made of **B 5, 6, 2** for **Landsat 8 OLI**.

Mangrove forest and other forest types were being identified with the “Healthy vegetation” curve. According to the spectrum, **Band 4 (Landsat 5 TM) and Band 5 (Landsat 8 OLI)** or Near Infrared with a wavelength range of 0.851 - 0.879 um had the highest reflectance percentage of 40 - 45 %. This range is a very important part of the spectrum because it reflects the wavelengths of the healthy plants and emphasizes the mudbanks (NASA 2014).

Build areas, bare soils and infrastructure were being identified with the “Altered rocks characteristic of a mineralized zone” curve and “Soil” curve. According to the spectrum, **Band 5 (Landsat 5 TM) and Band 6 (Landsat 8 OLI)** with a wavelength range of 1.566 - 1.651 um had the highest peaks in both curves while “Healthy vegetation” had a trough in the curve at the same location. In the other bands rocks and soils have a similar color but only in SWIR they have a strong contrast (NASA 2014). According to USGS (2018) the SWIR band is very sensitive to soil moisture content. The mangrove forest cover has a high soil moisture content than other forest types which causes a darker color reflectance on the satellite imagery.

Sea water, river water and water in the mangrove forest were being identified with the “Clear Water” and “Water with phytoplankton” curves. According to the spectrum, **Band 1 (Landsat 5 TM) and Band 2 (Landsat 8 OLI)** with a wavelength range of 0.452 – 0.512 um were the visible blue bands and had the highest peak in this range for water.

Appendix VI: The field validation locations in the study areas

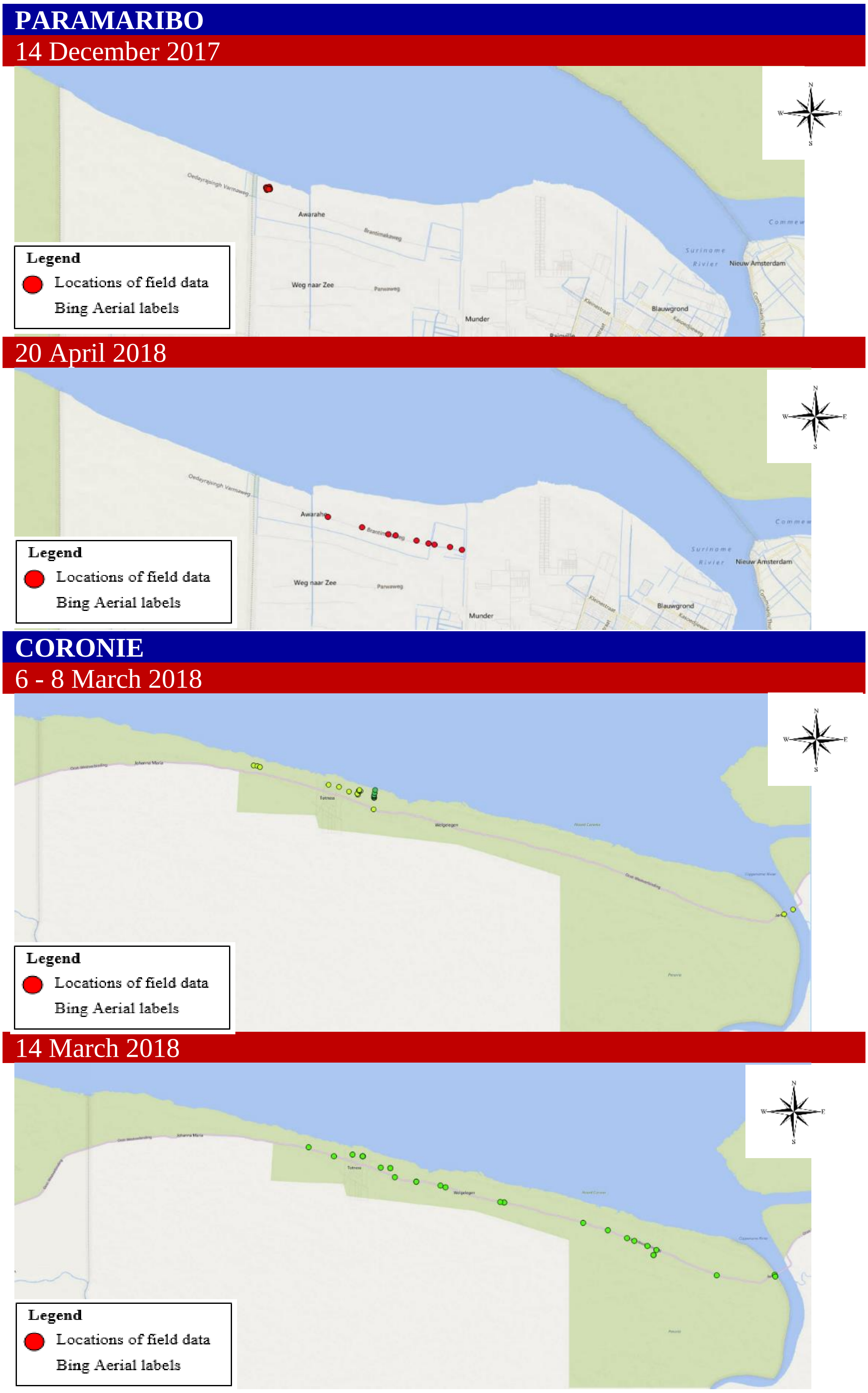

Figure VI-1: Overview of field validation locations in Paramaribo and Coronie

Appendix VII: Schematic view of the mangrove forest cover

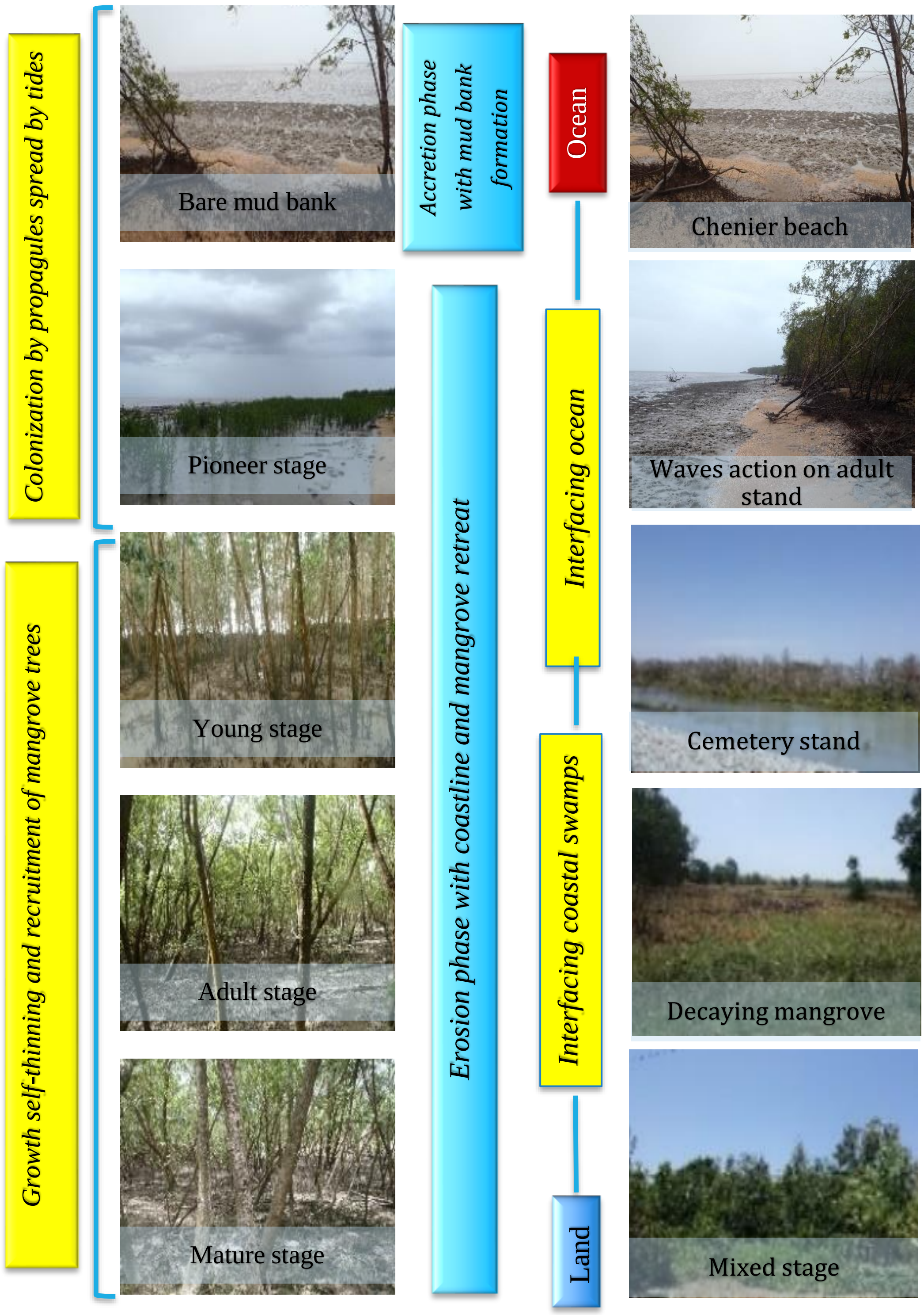

Figure VII-1: Overview of the mangrove forest cover along the coast of Suriname

Appendix VIII: Classification process

The methodology was adopted for three main steps, to know pre-processing, core-processing and post-processing (figure VIII-1).

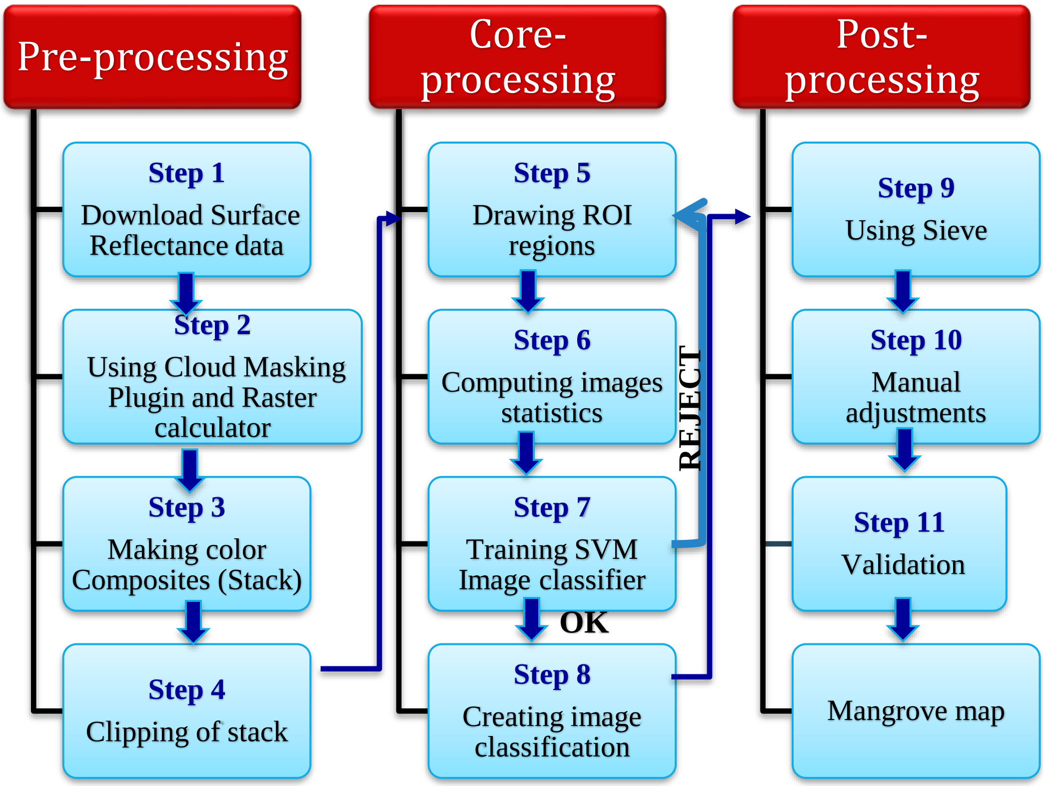

Figure VIII-1: Flow chart of the methodology used for extraction of the mangrove forest cover

Pre-processing

In the pre-processing, the downloaded surface reflectance (SR) images from United States Geological Survey (USGS) – New Bulk downloader were being prepared for further processing.

The second step was the **implementation of Cloud Masking 18.2.6 plugin** for removing the clouds and clouds shadow with three processes from each of the downloaded bands (USGS 2017). Clouds are the most unavoidable obstacles on optical satellite imagery (Foga, et al. 2017). Currently, Landsat SR data of each date contains a Pixel Quality Assessment band (pixel QA – band), generated by the CF Mask algorithm, to recognize cloud, cloud confidence, cloud shadow, snow/ice and water pixels in the imagery (USGS 2017). The Pixel QA band has accurate results for cloud, cloud shadow, snow/ice and water (USGS 2018). The Pixel QA is a band of 16 bits for Landsat 5 TM and Landsat 8 OLI, which is given in table VIII-1.

Table VIII-1: Landsat 5 TM and Landsat 8 OLI Pixel QA band attributes[1]

<table>
<tr><th>Bit</th><th>Bit value</th><th>Cumulative Sum</th><th>Landsat 5 TM Attribute</th><th>Landsat 8 OLI Attribute</th></tr>
<tr><td>0</td><td>1</td><td>1</td><td>Fill</td><td>Fill</td></tr>
<tr><td>1</td><td>2</td><td>3</td><td>Clear</td><td>Clear</td></tr>
<tr><td>2</td><td>4</td><td>7</td><td>Water</td><td>Water</td></tr>
<tr><td>3</td><td>8</td><td>15</td><td>Cloud Shadow</td><td>Cloud Shadow</td></tr>
<tr><td>4</td><td>16</td><td>31</td><td>Snow</td><td>Snow</td></tr>
<tr><td>5</td><td>32</td><td>63</td><td>Cloud</td><td>Cloud</td></tr>
<tr><td>6</td><td>64</td><td>127</td><td rowspan="2">Cloud Confidence
00 = none
01 = Low
10 = medium
11 = high</td><td rowspan="2">Cloud Confidence
00 = none
01 = Low
10 = medium
11 = high</td></tr>
<tr><td>7</td><td>128</td><td>255</td></tr>
<tr><td>8</td><td>256</td><td>511</td><td>Unused</td><td rowspan="2">Cirrus Confidence
00= not set
01 = low from OLI band 9 reflectance
10 = medium from OLI band 9 reflectance
11 = high from OLI band 9 reflectance</td></tr>
<tr><td>9</td><td>512</td><td>1023</td><td>Unused</td></tr>
<tr><td>10</td><td>1024</td><td>2047</td><td>Unused</td><td>Terrain Occlusion</td></tr>
<tr><td>11</td><td>2048</td><td>4095</td><td>Unused</td><td>Unused</td></tr>
<tr><td>12</td><td>4096</td><td>8191</td><td>Unused</td><td>Unused</td></tr>
<tr><td>13</td><td>8192</td><td>16383</td><td>Unused</td><td>Unused</td></tr>
<tr><td>14</td><td>16384</td><td>32767</td><td>Unused</td><td>Unused</td></tr>
<tr><td>15</td><td>32786</td><td>65553</td><td>Unused</td><td>Unused</td></tr>
</table>

The table below contains the pixel values of Landsat 5 TM and Landsat 8 OLI Pixel QA band.

Table VIII-2: Landsat 5 TM and Landsat 8 OLI Pixel QA band values[2]

Attribute	**Landsat 5 TM** *Pixel Value*	**Landsat 8 OLI** *Pixel Value*
Fill	1	1
Clear	66, 130	322, 386, 834, 898, 1346
Water	68, 132	324, 388, 836, 900, 1348
Cloud Shadow	72, 136	328, 392, 840, 904, 1350

[1] *Landsat 5 TM and Landsat 8 OLI Surface Reflectance Pixel QA band attributes* https://smbyc.bitbucket.io/qgisplugins/cloudmasking/cloud_filters/

[2] *Landsat 5 TM and Landsat 8 OLI Pixel QA band values* https://smbyc.bitbucket.io/qgisplugins/cloudmasking/cloud_filters/

Snow/Ice	80, 112, 144, 176	336, 368, 400, 432, 848, 880, 912, 944, 1352
Cloud	96, 112, 160, 176, 224	352, 368, 416, 432, 480, 864, 880, 928, 944, 992
Low cloud confidence	66, 68, 72, 80, 96, 112	322, 324, 328, 336, 352, 368, 834, 836, 840, 848, 864, 880
Medium cloud confidence	130, 132, 136, 144, 160, 176	386, 388, 392, 400, 416, 432, 900, 904, 928, 944
High cloud confidence	224	480, 992
Low confidence cirrus		322, 324, 328, 336, 352, 368, 386, 388, 392, 400, 416, 432, 480
High confidence cirrus		834, 836, 840, 848, 864, 880, 898, 900, 904, 912, 928, 944, 992
Terrain occlusion		1346, 1348, 1350, 1352

The cloud masking plugin has three sections. The first section was uploading the MTL file (Metadata file) for activating the plugin. In the second section, named "Filter to apply", only the Fmask and Pixel QA filters with bits between 5 and 9 were used. When multiple bits are selected the plugin marked all pixels for each bit, which means that all pixels that had cloud (bit 5) were marked as 1 (Fill), Cloud Confidence and Cirrus Confidence as 2-3. In the final section, named "Apply and Save", the generated cloud mask was applied to the color stack and created a mask, named **Enmask.** This mask had cloud areas with **pixel value** 0 and non-cloud areas with **pixel values** greater than 1.

The cloud areas with pixel value 0 were being filled, by using the raster calculator, with an image of the same year (Fill image) and further processed. A flow chart of the whole process is given in figure VIII-2 and is illustrated in table VIII-3.

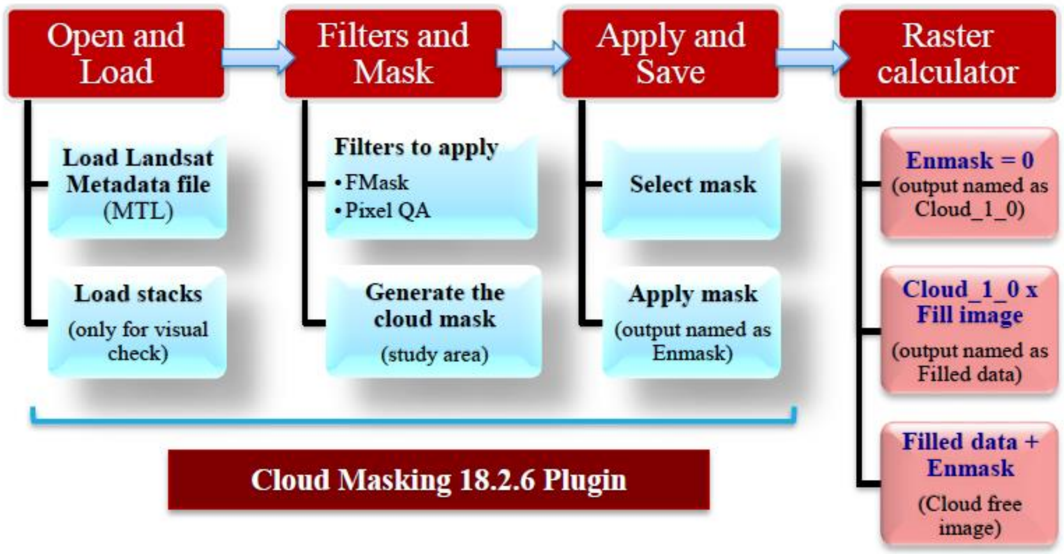

Figure VIII-2: Flow chart of generating a cloud free image with the Cloud Masking plugin and Raster calculator

Table VIII-3: An example of the processes with raster calculator and the produced images of Paramaribo-2017

Description	Spectral view
Stack before using the Cloud Masking plugin	
<u>Output of Cloud Masking 18.2.6</u> **Cloudmask** Cloud Pixel value is 1 - 4 and the rest has a value 0	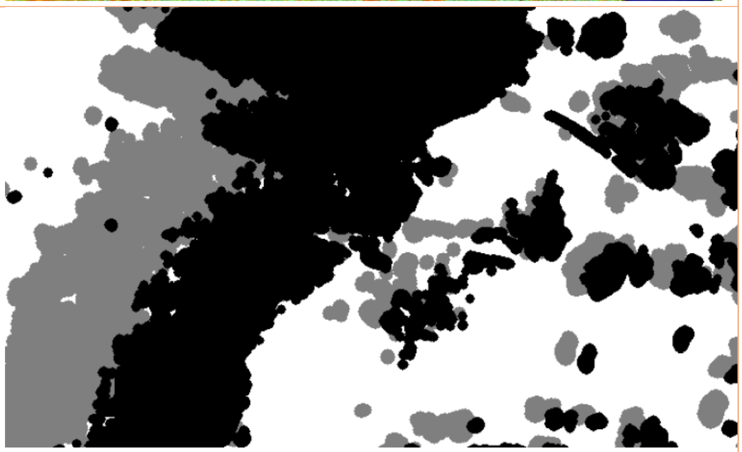
<u>Output of Cloud Masking 18.2.6</u> **Enmask** Cloud Pixel value is 0 and the rest has a value >1	

Raster Calculator **Enmask = 0** (output is named as Cloud_1_0) Cloud Pixel value is 1 (white) and the rest has a value 0 (black)	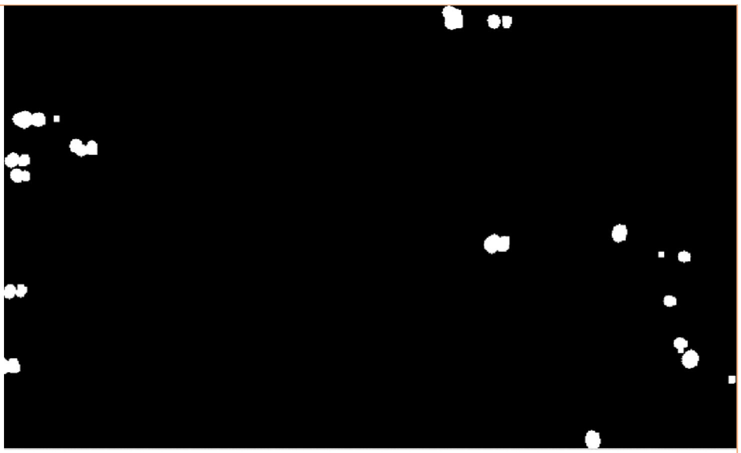
Raster Calculator **Clouds _1_0 * Fill image** (named as Filled data) Cloud Pixel value are filled with a fill image of the same year cloud >1 (white) and the rest has a value 0 (black)	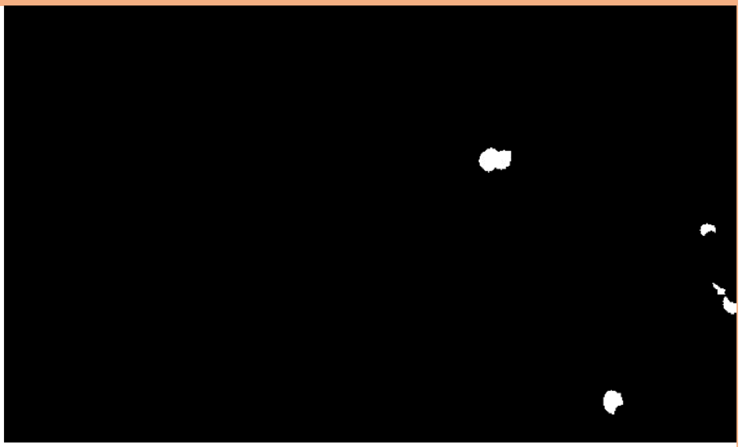
Raster Calculator **Filled_Data + Enmask** (Cloud free image) The value 0 are filled again with Enmask	

Stack after using the Cloud Masking plugin	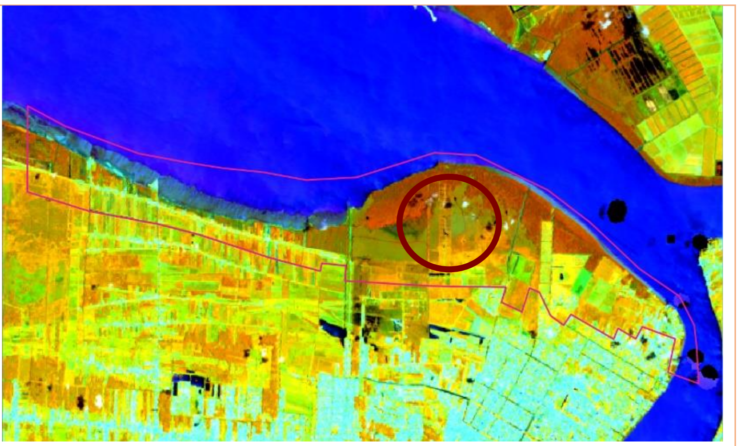

In the third step, a color composite of **B 4, 5, 1** for the year 2009 (**Landsat 5 TM)** and **B 5, 6, 2** for the years 2014 and 2017 (**Landsat 8 OLI)** were being created. In the final step of Pre – processing the study areas were being clipped out of the produced color composites.

Core – processing

The SVM classifier had three steps toward mangrove classification, which were:

- **Compute Images Statistics**

This application computes a global mean and standard deviation for each band of the clipped images and optionally saves the results as an XML file. The output XML file was used as an input for the Train Images Classifier application to normalize samples before learning.

- **Train SVM Image Classifier**

This application performed a classifier training on the color composites and Region of Interests (ROI's) were being built for each class. The dataset of the ROI's was split into validation data and training data. To agree with the output, the Confusion Matrix and the Kappa Index (which must be near 1) must be evaluated.

- **Create Image Classification**

This application performs an image classification based on the output of the SVM classifier. First the input image is chosen, where after the Image Statistics file (.xml) and the Model file (.txt) are loaded. In the end the Output Image Classification is saved in the destined directory.

Post - processing

In the post-processing, the classified image was adjusted using the Sieve tool followed by a manual correction by the interpreter. The Sieve tool eliminated raster polygons smaller than the provided threshold size (which is 2) in pixels and substituted them with pixel value (which is 4) of the largest neighbor polygon. The Sieve tool uses the nearest neighborhood algorithm to generalize and reduce pixel misclassifications. For the final adjustments the raster layers were converted into vector layers using the color composites as background. Knowing that the human eyes are the best remote sensor at the end, the mangrove vector layers underwent a visual check and manual corrections carried out by the interpreter.

Appendix IX: Validation of the mangrove maps 2009-2017

An example of an error matrix is shown in table IX-1.

Table IX-1: Example of an error matrix

		j = Columns (Reference)			Row total
		1	**2**	**k**	N_{i+}
i = Rows (Classification)	**1**	**N_{11}**	N_{12}	N_{1k}	N_{1+}
	2	N_{21}	**N_{22}**	N_{2k}	N_{2+}
	K	N_{k1}	N_{k2}	**N_{kk}**	N_{k+}
Column total	N_{+j}	N_{+1}	N_{+2}	N_{+k}	**N**

The N_{i+} (1) are classified samples into category i in the remotely sensed classification and N_{+j} (2) are the classified samples into category j in the reference data set, that was computed as follows:

$$N_{i+} = \sum_{j=1}^{k} N_{ij} \quad (1) \qquad and \qquad N_{+j} = \sum_{i=1}^{k} N_{ij} \quad (2)$$

Overall accuracy, divides the total number of correct pixels(diagonal) by the total number of pixels in the error matrix, between remotely sensed classification and reference data, which was computed as follows:

$$\text{Overall accuracy} = \frac{\sum_{i=1}^{k} N_{ii}}{N} \quad (3)$$

Producer's accuracy (j) shows how well a certain area can be classified and User's accuracy gives the reliability and probability of a pixel class on the map that represents the category on the ground. These were computed by:

$$j = \frac{N_{jj}}{N_{+j}} (4) \qquad and \qquad i = \frac{N_{ii}}{N_{i+}} (5)$$

The Kappa (K_{hat}) measures the agreement between the remotely sensed classification map and reference data and was computed by:

$$K_{hat} = \frac{N \sum_{i=1}^{k} x_{ii} - \sum_{i=1}^{k} (x_{i+} \times x_{+j})}{N^2 - \sum_{i=1}^{k} (x_{i+} \times x_{+j})} \quad (6)$$

Appendix X: Extraction of the mangrove forest cover 2009-2017

X.1 Mangrove Map of Paramaribo in 2009

Figure X-1-1 illustrates the result of the pre-processing of Paramaribo in 2009. The prepared image was derived from the Landsat 5 TM image of September 28, 2009 with a cloud coverage of 1% and the clouds were refilled with data of the image of September 12, 2009.

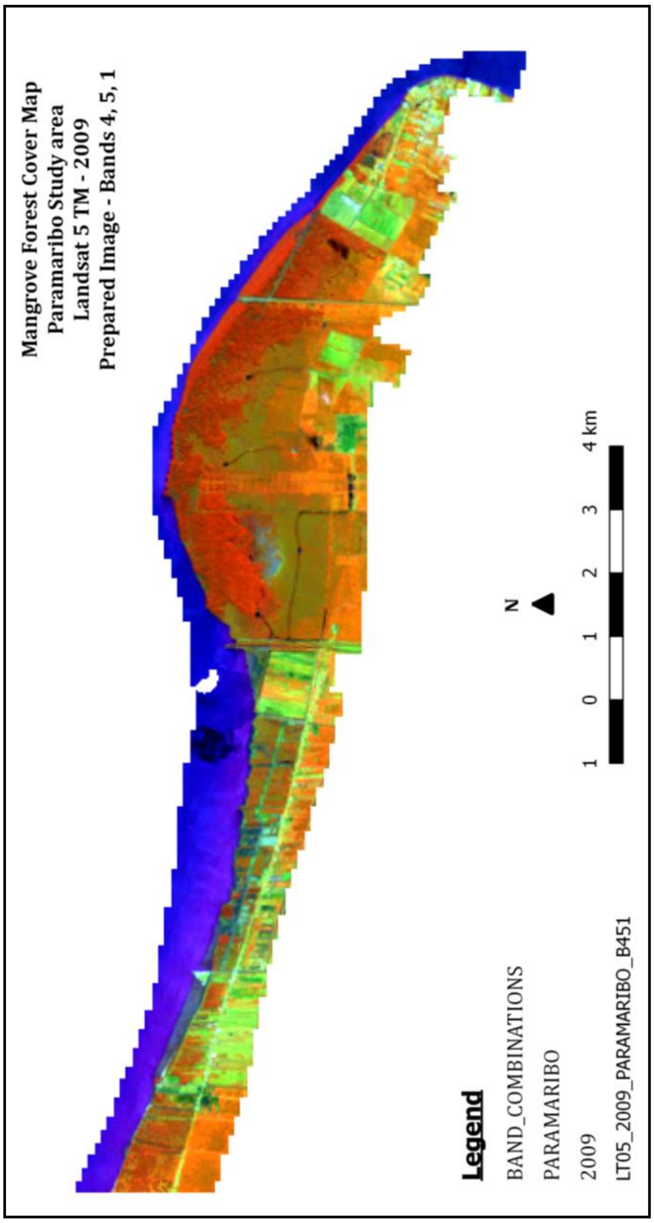

Figure X-1-1: Prepared image of Paramaribo derived from Landsat 5 TM in 2009 with a band combination of 4, 5, 1

In the following step, Region of interest (ROI) were drawn, which has been illustrated in figure X-1-2.

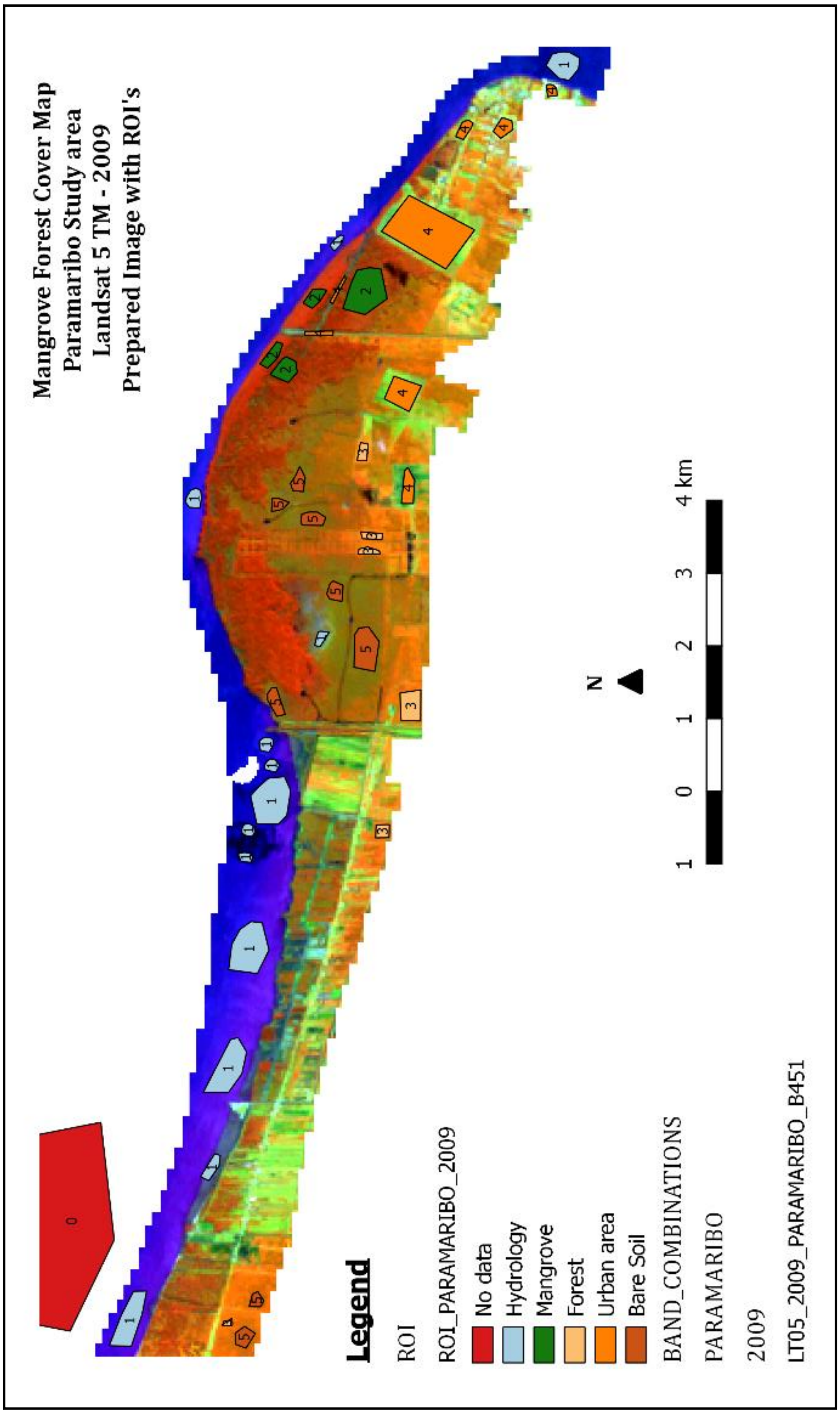

Figure X-1 2: Prepared image of Paramaribo in 2009 with drawn ROI's

The image underwent the SVM classifier which is illustrated figure X-1-3.

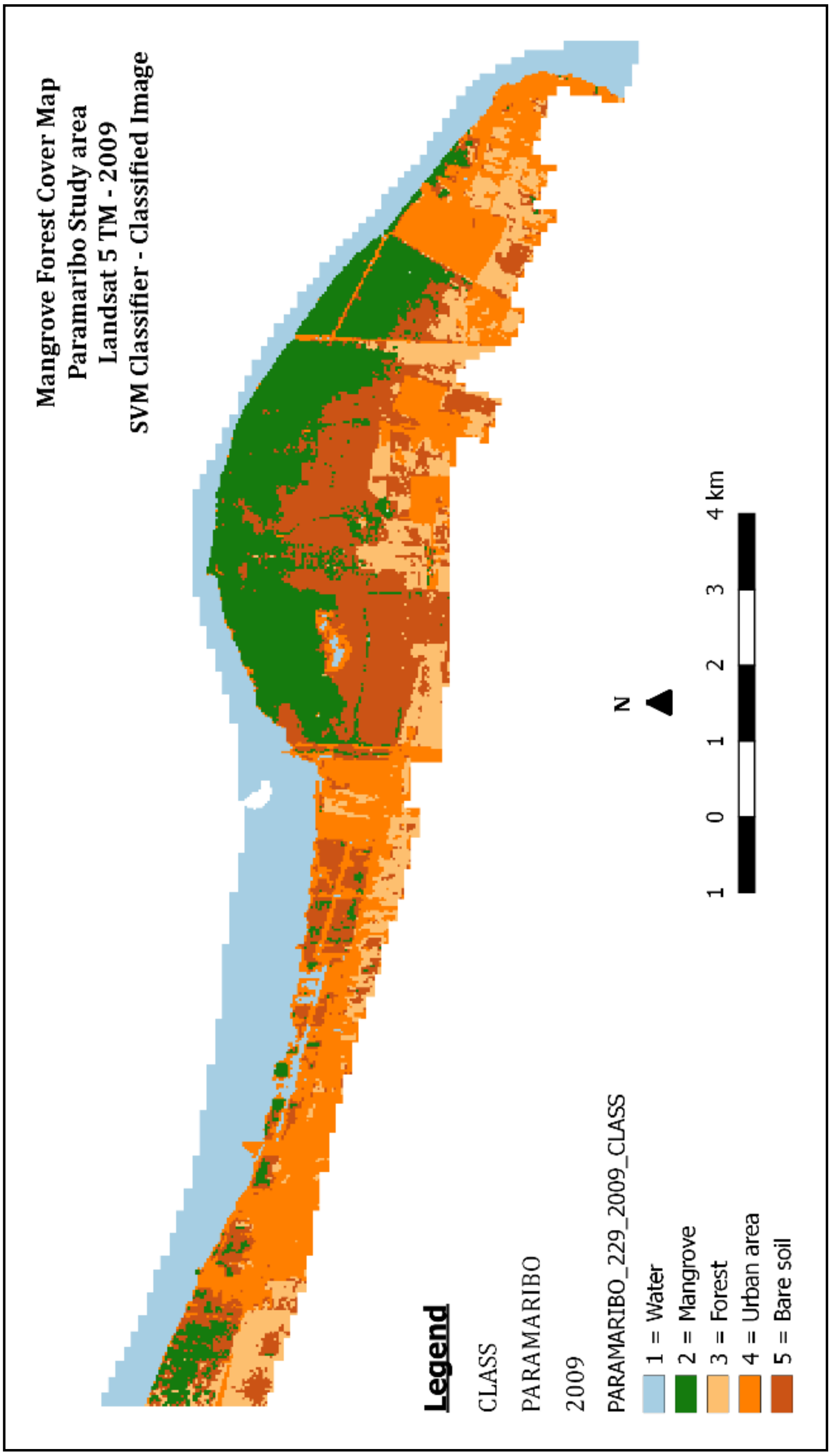

Figure X-1-3: The classified image of Paramaribo in 2009 as result of the SVM classifier

In the final process the classified image was filtered and manual adjusted. Figure X-1-4 gives an illustration of the adjusted image.

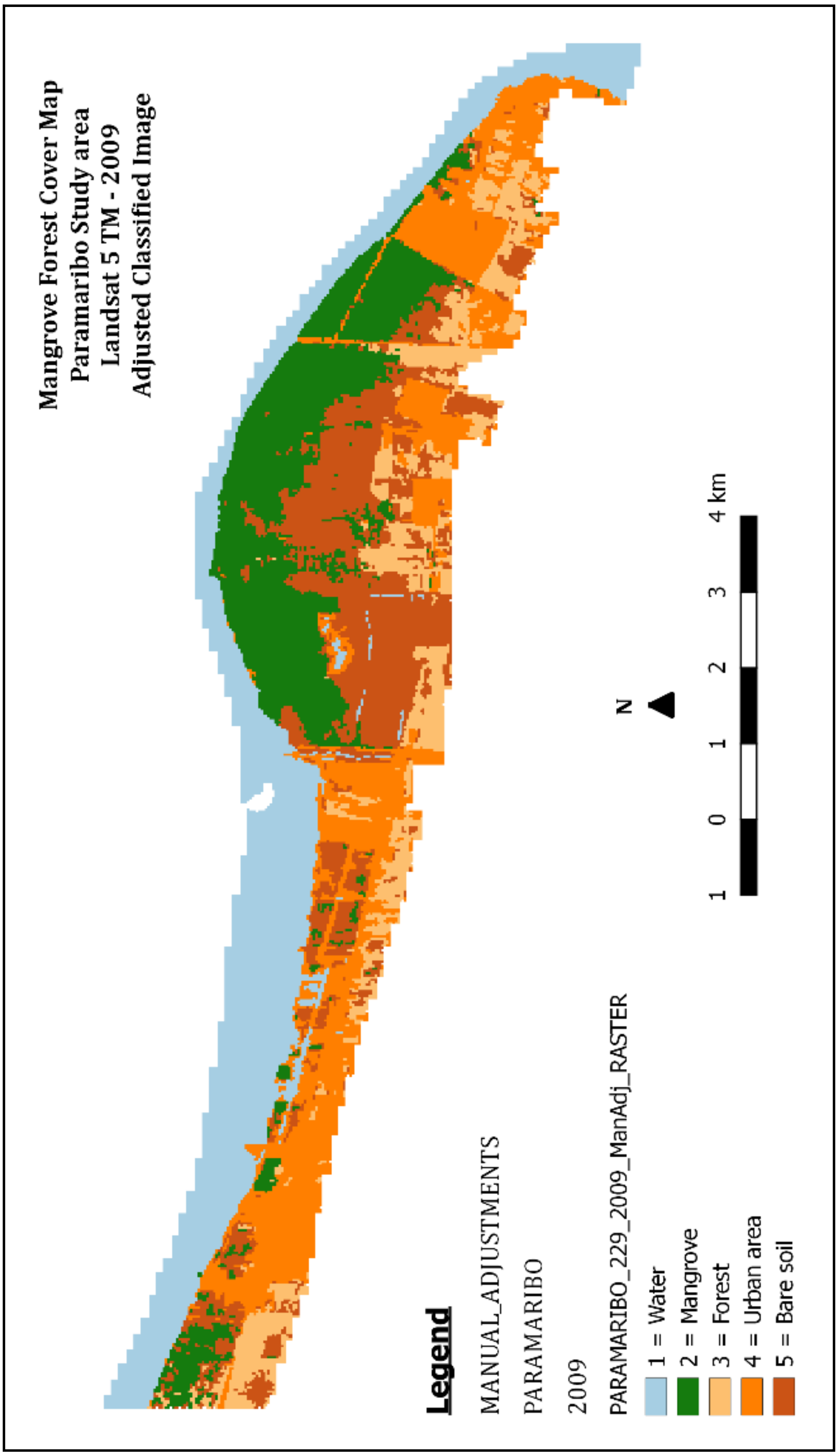

Figure X-1-4: Filtered and manual adjusted classified image of Paramaribo in 2009

Validating the classified image of Paramaribo in 2009 with reference data produced an error matrix in number of pixels, which is demonstrated in table X-1-1.

Table X-1-1: The produced error matrix of the classified Paramaribo map for 2009 in pixels

PARAMARIBO 2009		Reference						
		Hydrology	Mangrove	Forest	Urban area	Bare soil	Total	user Accuracy (%)
Classification	Hydrology	12281	0	0	0	0	12281	100
	Mangrove forest	106	9404	0	0	0	9510	98,88538381
	Forest	0	0	5554	0	0	5554	100
	Urban area	0	0	0	10619	0	10619	100
	Bare soil	0	60	0	0	9710	9770	99,38587513
	Total	12387	9464	5554	10619	9710	47734	
	Producer Accuracy (%)	99,1442641	99,3660186	100	100	100		
	Kappa hat Class (%)	99,5592798						
	Overall Accuracy (%)	99,6522395						

According to the error matrix between the remotely sensed classification and the reference data, the total number of correct pixels (diagonal) and the total number of pixels in the error matrix gave an overall accuracy of 99 %. Subsequently, the measured agreement between the two data gave a kappa hat of 99 %. Also, did the error matrix showed that 106 pixels of the hydrology class were misclassified into the mangrove forest class (Figure X-1-5). Also, 60 pixels of the mangrove forest class were misclassified into the bare soil class (Figure X-1-6). The misclassification occurred because of wrong color identification by the SVM classifier. After comparison of the remotely sensed classification and the reference data, the producer's accuracy of the mangrove class was 99 % that indicates how well the area was classified. At the end, the user's accuracy was 99 % that gave the reliability and probability of the mangrove class on the map that represents the category on the ground.

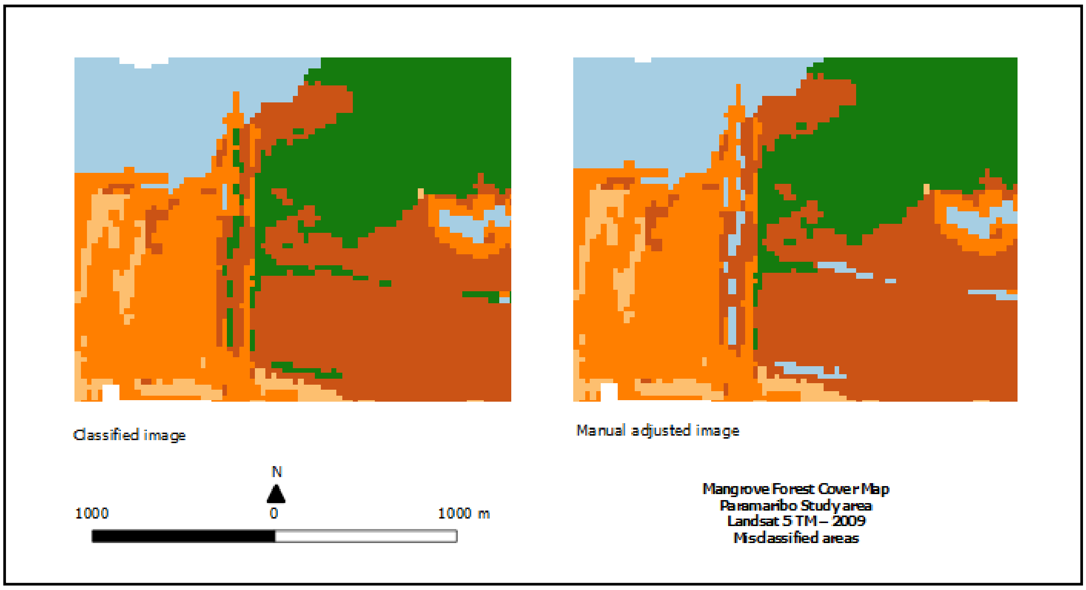

Figure X-1-5: Misclassification 1 - Paramaribo 2009

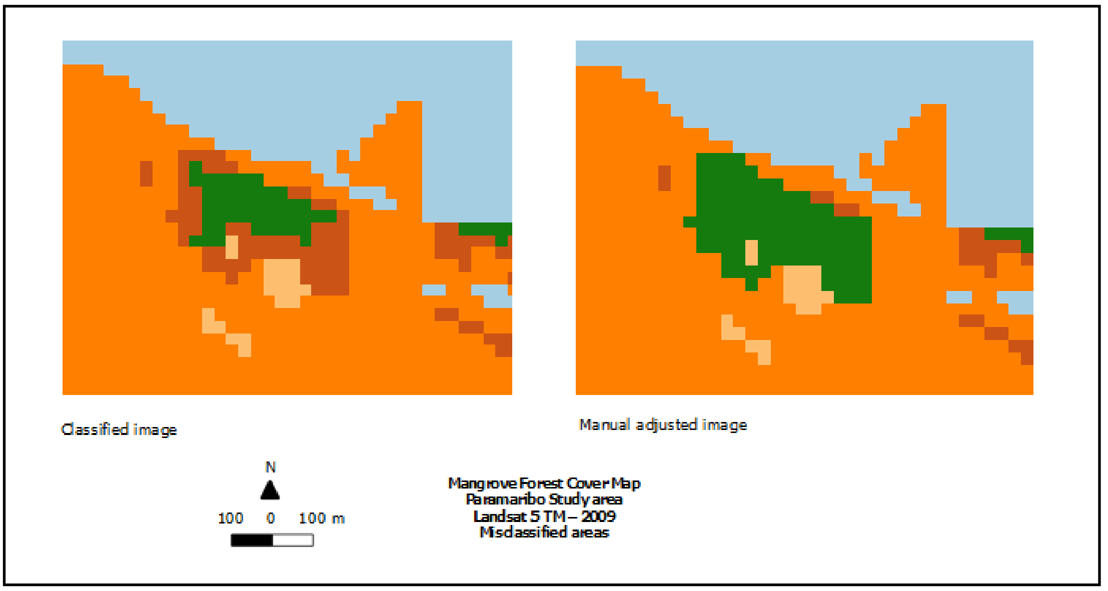

Figure X-1-6: Misclassification 2 - Paramaribo 2009

In the end, the mangrove class was extracted, which is shown in figure X-1-7 as the mangrove map of Paramaribo in 2009.

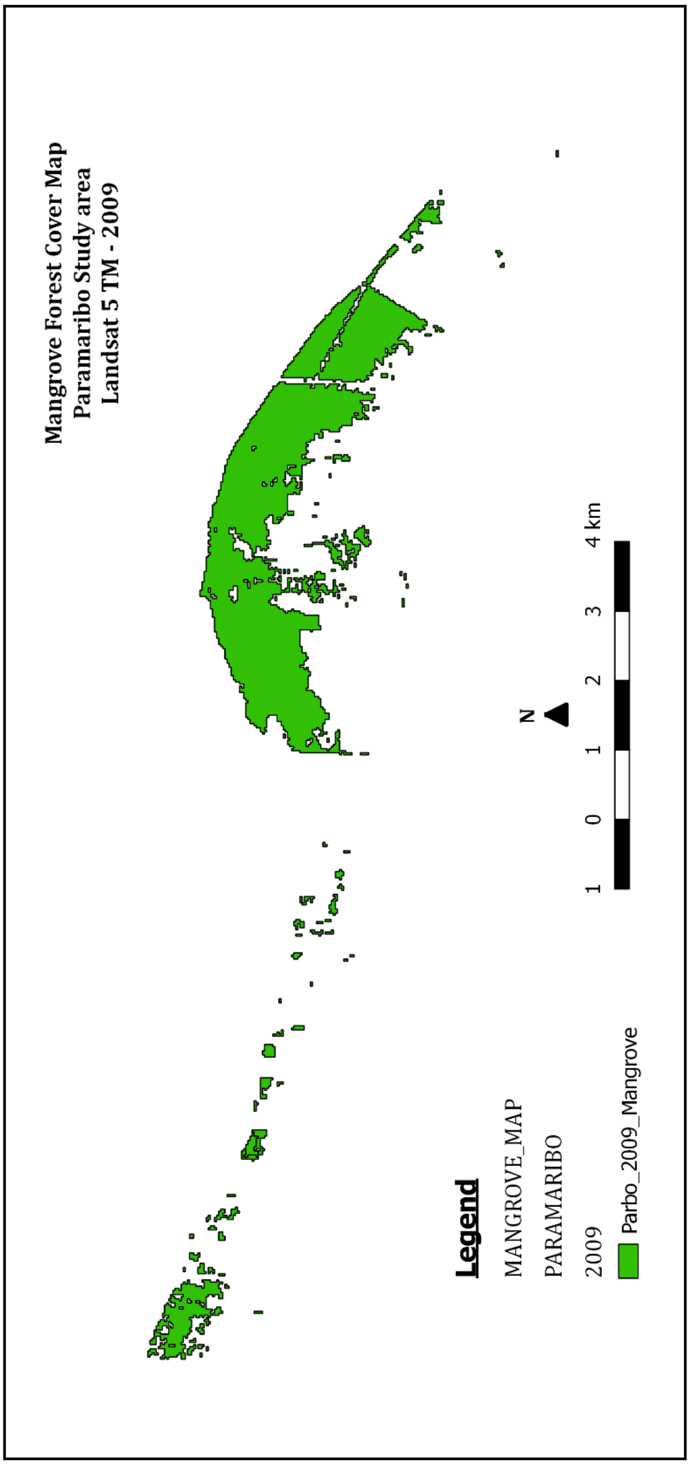

Figure X-1-7: The extracted mangrove map of Paramaribo in 2009

According to the results, the mangrove forest cover of Paramaribo in 2009 was extended over an area of 852 ha and was 0,74 % of the total mangrove forest cover of Suriname.

X.2 Mangrove Map of Paramaribo in 2014

Figure X-2-1 illustrates the result of the pre-processing of Paramaribo in 2014. The prepared image was derived from the Landsat 8 OLI image of September 26, 2014 with a cloud coverage of 2.4 % and the clouds were refilled with data of the image of May 21, 2014, October 12, 2014 and October 28, 2014.

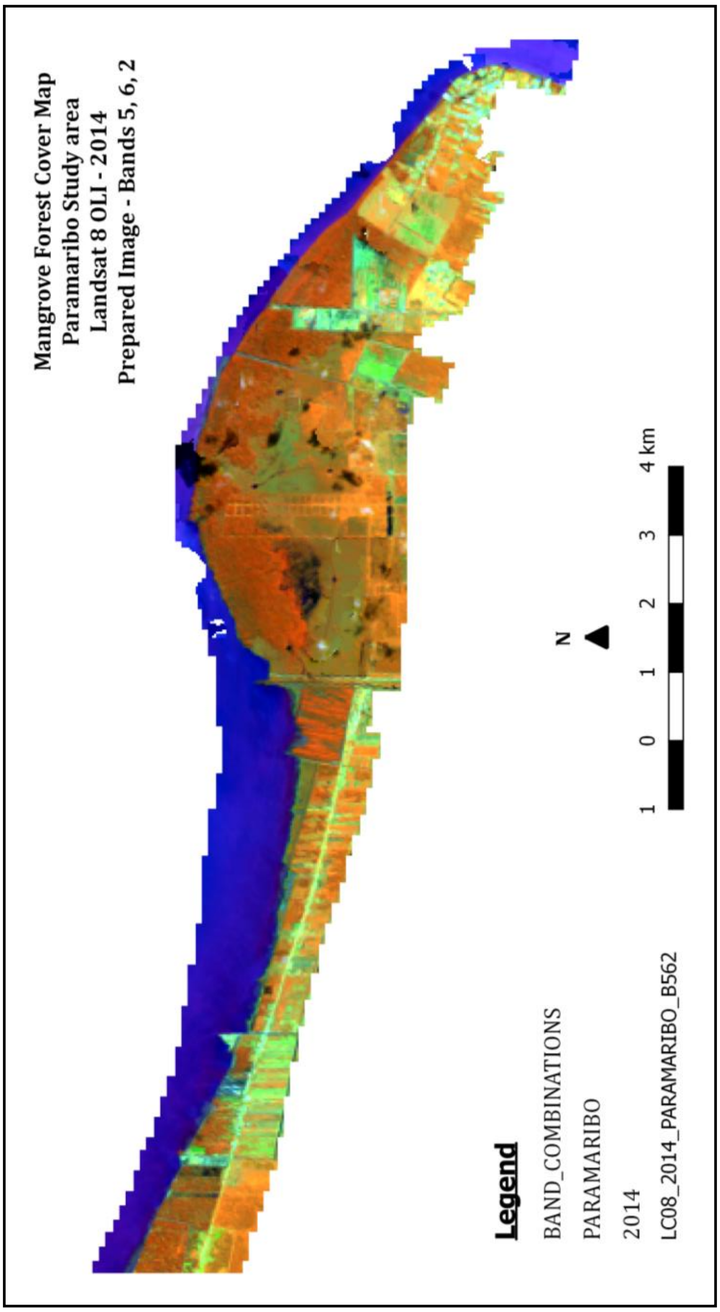

Figure X-2-1: Prepared image of Paramaribo derived from Landsat 8 OLI in 2014 with a band combination of 5, 6, 2

In the following step, Region of interest (ROI) were drawn, which has been illustrated in figure X-2-2.

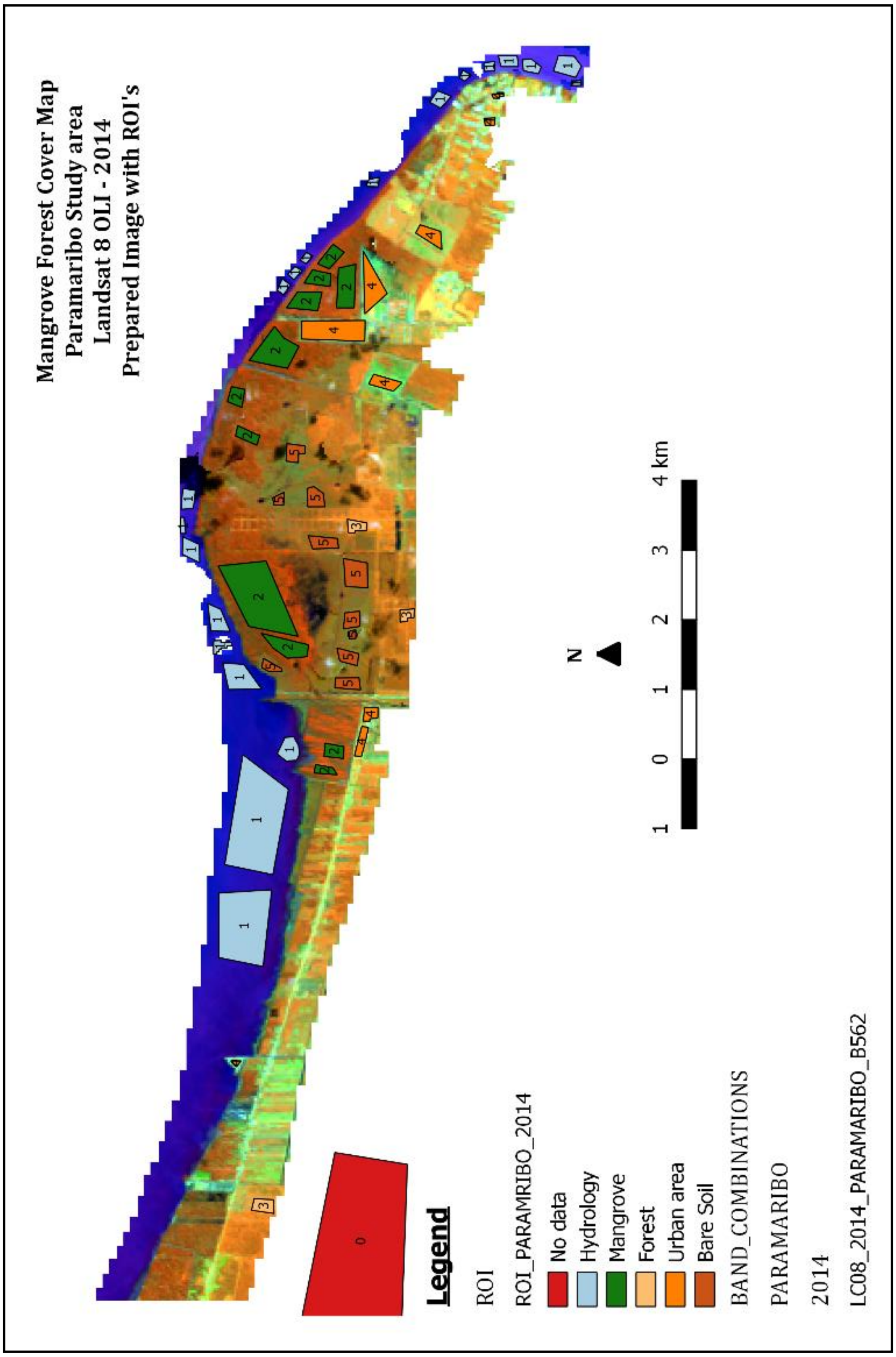

Figure X-2-2: Prepared image of Paramaribo in 2014 with drawn ROI's

The image underwent the SVM classifier which is illustrated figure X-2-3.

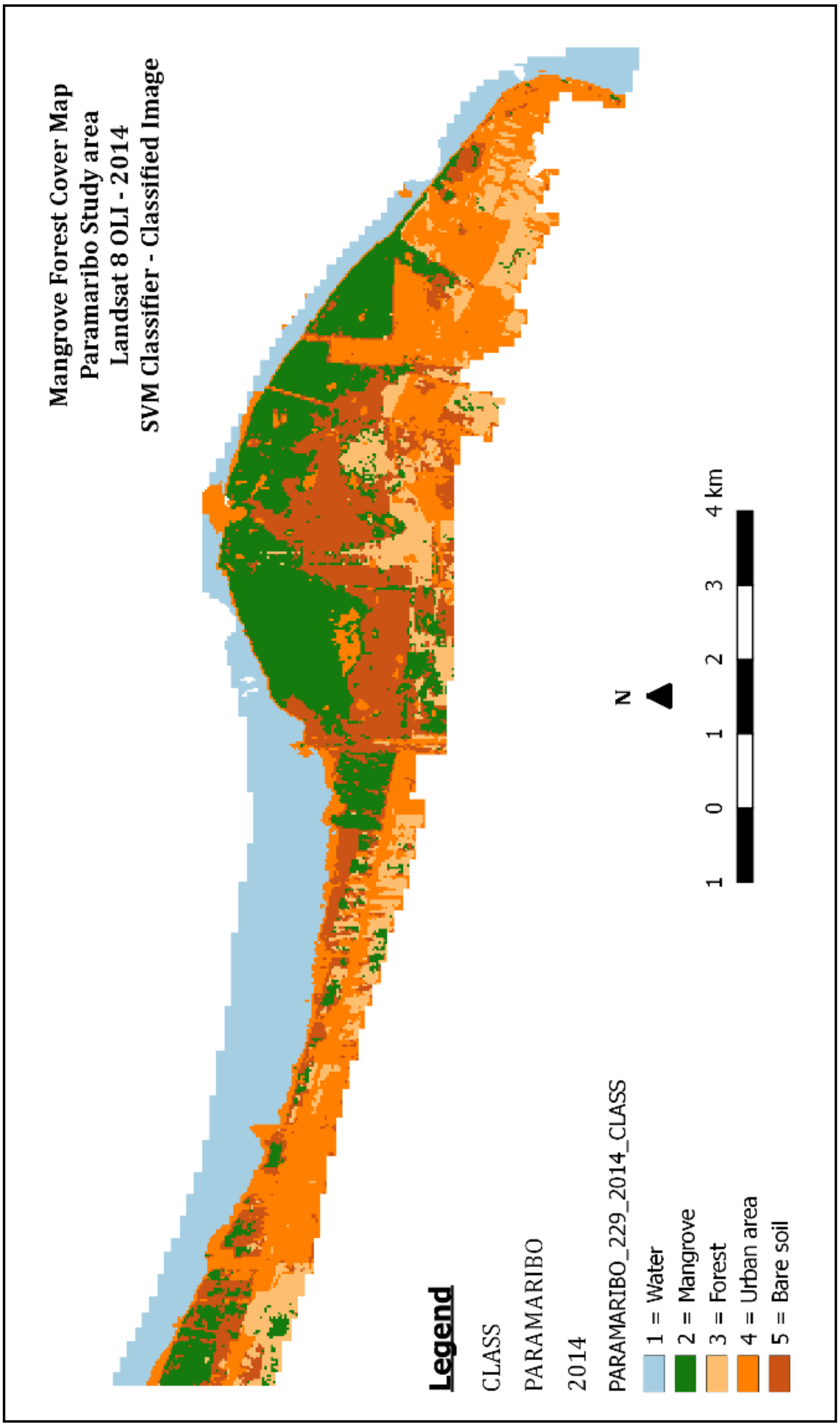

Figure X-2-3: The classified image of Paramaribo in 2014 as result of the SVM classifier

In the final process the classified image was filtered and manual adjusted. Figure X-2-4 gives an illustration of the adjusted image.

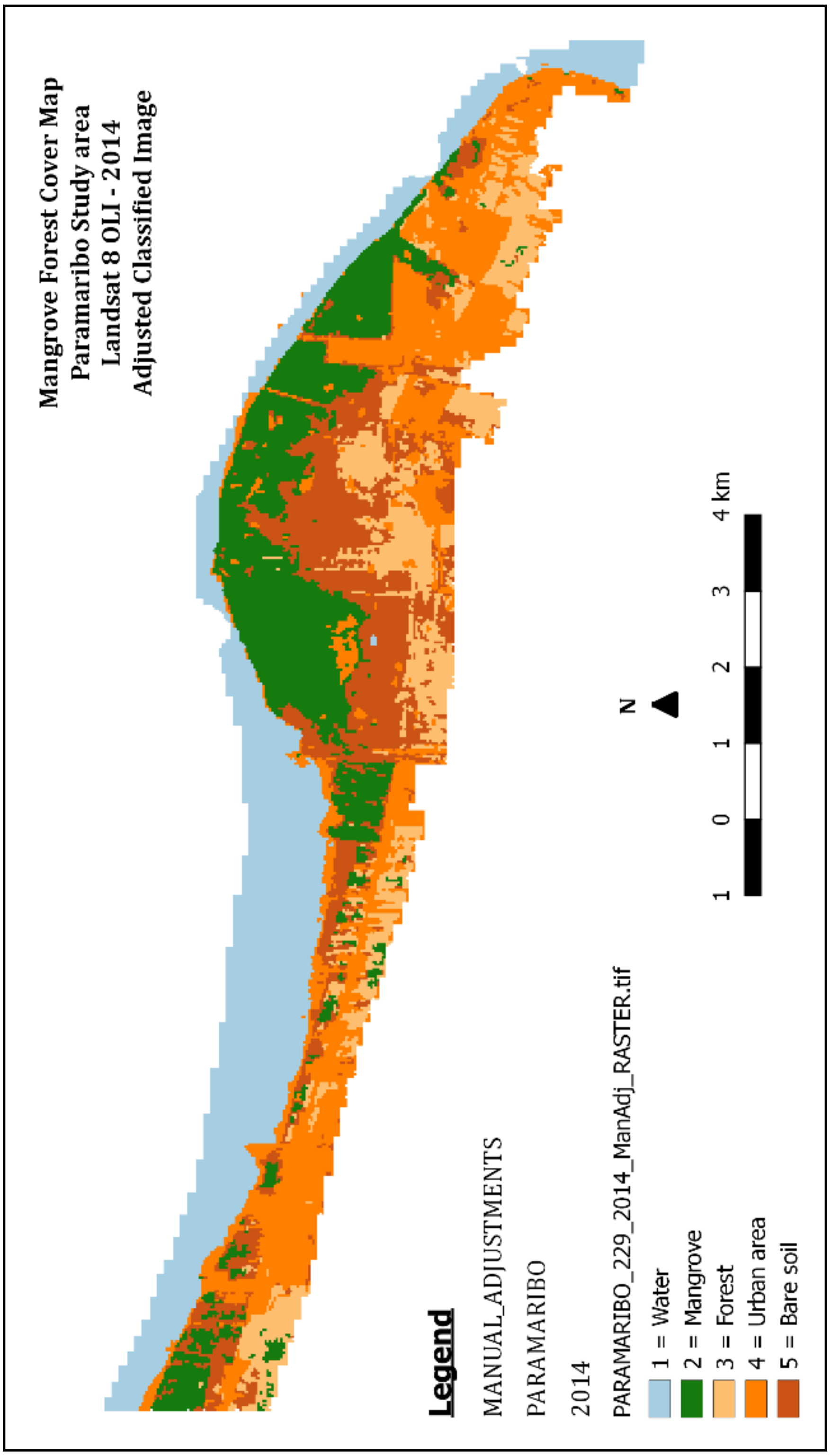

Figure X-2-4: Filtered and manual adjusted classified image of Paramaribo in 2014

Validating the classified image with reference data produced an error matrix in number of pixels, which is demonstrated in table X-2-1.

Table X-2-1: The produced error matrix of the classified Paramaribo map for 2014 in pixels

PARAMARIBO 2014		Reference						
		Hydrology	Mangrove	Forest	Urban area	Bare soil	Total	user Accuracy (%)
Classification	Hydrology	11853	0	0	0	0	11853	100
	Mangrove forest	10	8873	925	62	0	9870	89,89868288
	Forest	0	0	5367	0	0	5367	100
	Urban area	197	72	0	11612	0	11881	97,73588082
	Bare soil	0	3	0	0	8446	8449	99,96449284
	Total	12060	8948	6292	11674	8446	47420	
	Producer Accuracy (%)	98,283582	99,161824	85,298792	99,468905	100		
	Kappa hat Class (%)	96,607059						
	Overall Accuracy (%)	97,323914						

According to the error matrix between the remotely sensed classification and the reference data, the total number of correct pixels (diagonal) and the total number of pixels in the error matrix gave an overall accuracy of 97 %. Subsequently, the measured agreement between the two data gave a kappa hat of 97 %. Also, did the error matrix showed that 925 pixels of the forest class, 62 pixels of the urban class and 10 pixels of the hydrology class were misclassified into the mangrove forest class (Figure X-2-5). Also, 72 pixels and 3 pixels of the mangrove forest class were misclassified, into the urban class and the bare soil class (Figure X-2-6). The misclassification was caused due to cloud fill data that had a darker color preview than the prepared image. After comparison of the remotely sensed classification and the reference data, the producer's accuracy of the mangrove class was 99 % that indicates how well the area was classified. At the end, the user's accuracy was 90% that gave the reliability and probability of the mangrove class on the map that represents the category on the ground.

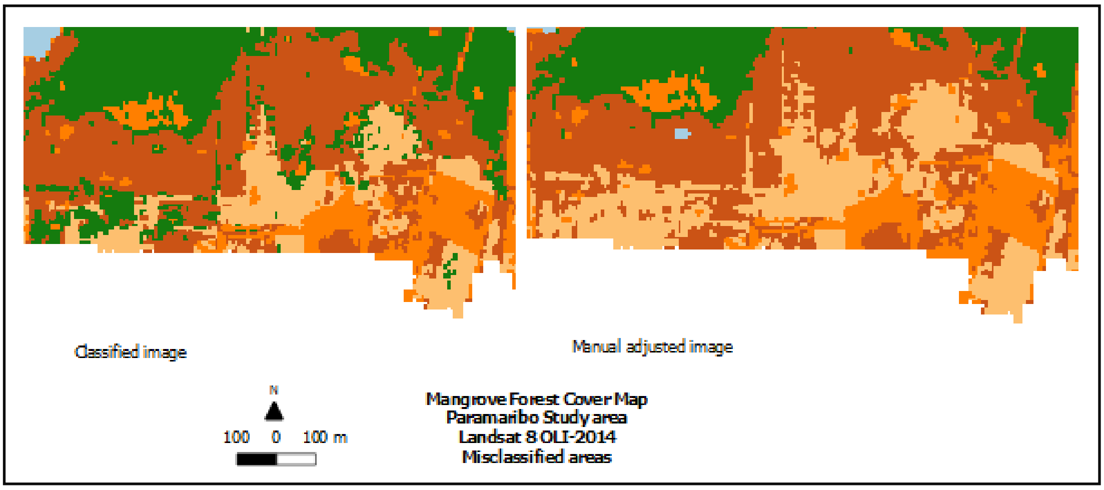

Figure X-2-5: Misclassification 1 - Paramaribo 2014

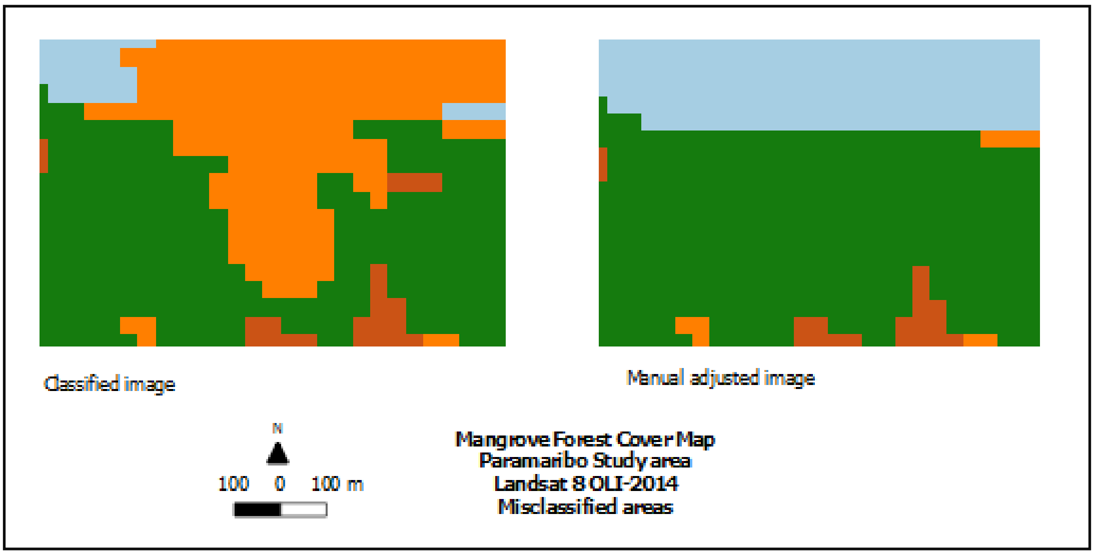

Figure X-2-6: Misclassification 2 - Paramaribo 2014

In the end, the mangrove class was extracted, which is shown in figure X-2-7 as the mangrove map of Paramaribo in 2014.

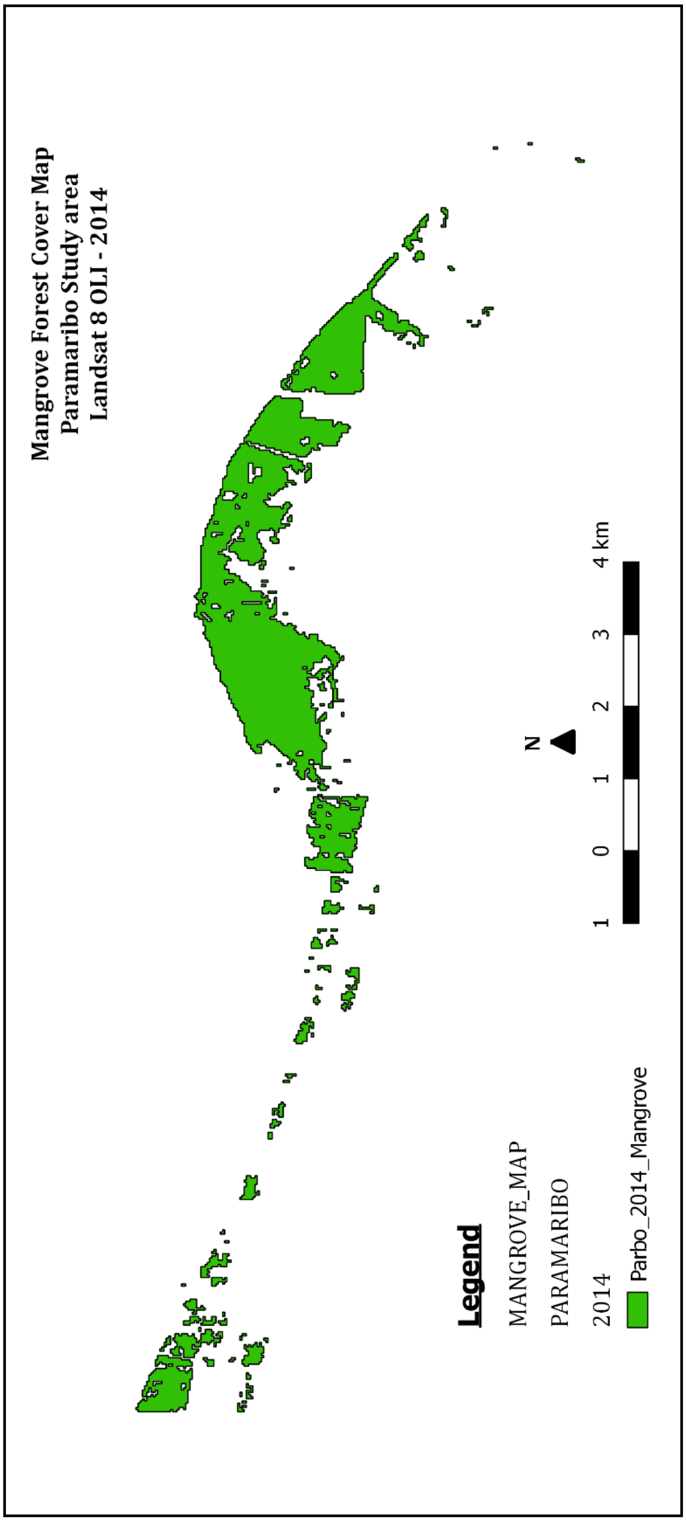

Figure X-2-7: The extracted mangrove map of Paramaribo in 2014

According to the results, the mangrove forest cover of Paramaribo in 2014 was extended over an area of 805 ha and was 0,70 % of the total mangrove forest cover of Suriname.

X.3 Mangrove Map of Coronie in 2009

Figure X-3-1 illustrates the result of the pre-processing of Coronie in 2009. The prepared image was derived from the Landsat 5 TM image of September 28, 2009 (scene 229/56) and November 6, 2009 (scene 230/56) with cloud coverage of, respectively, 1 % and 2 %. The clouds were refilled with data of the image of September 12, 2009 for scene 229/56.

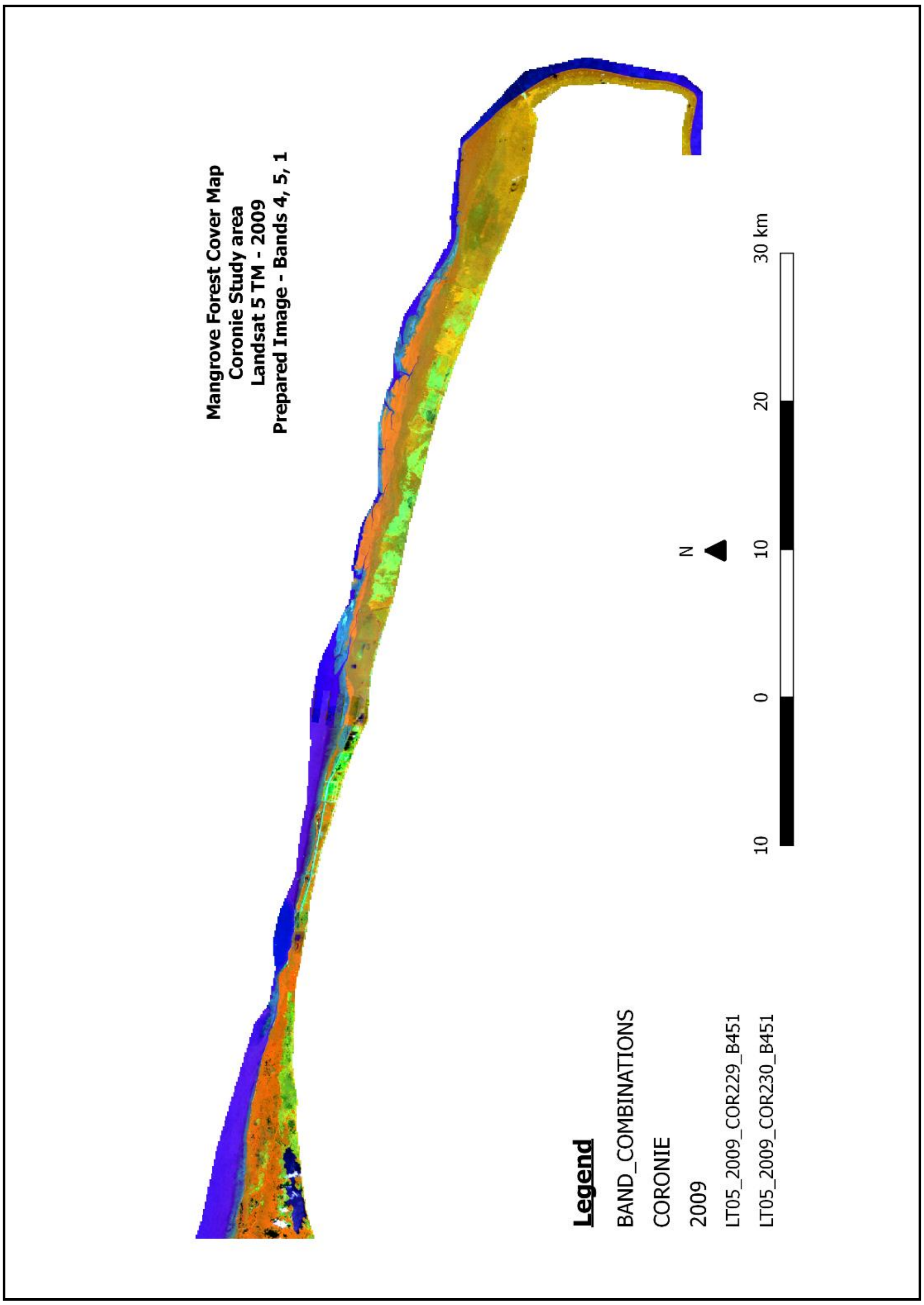

Figure X-3-1: Prepared image of Coronie derived from Landsat 5 TM in 2009 with a band combination of 4, 5, 1

In the following step, Region of interest (ROI) were drawn, which has been illustrated in figure X-3-2.

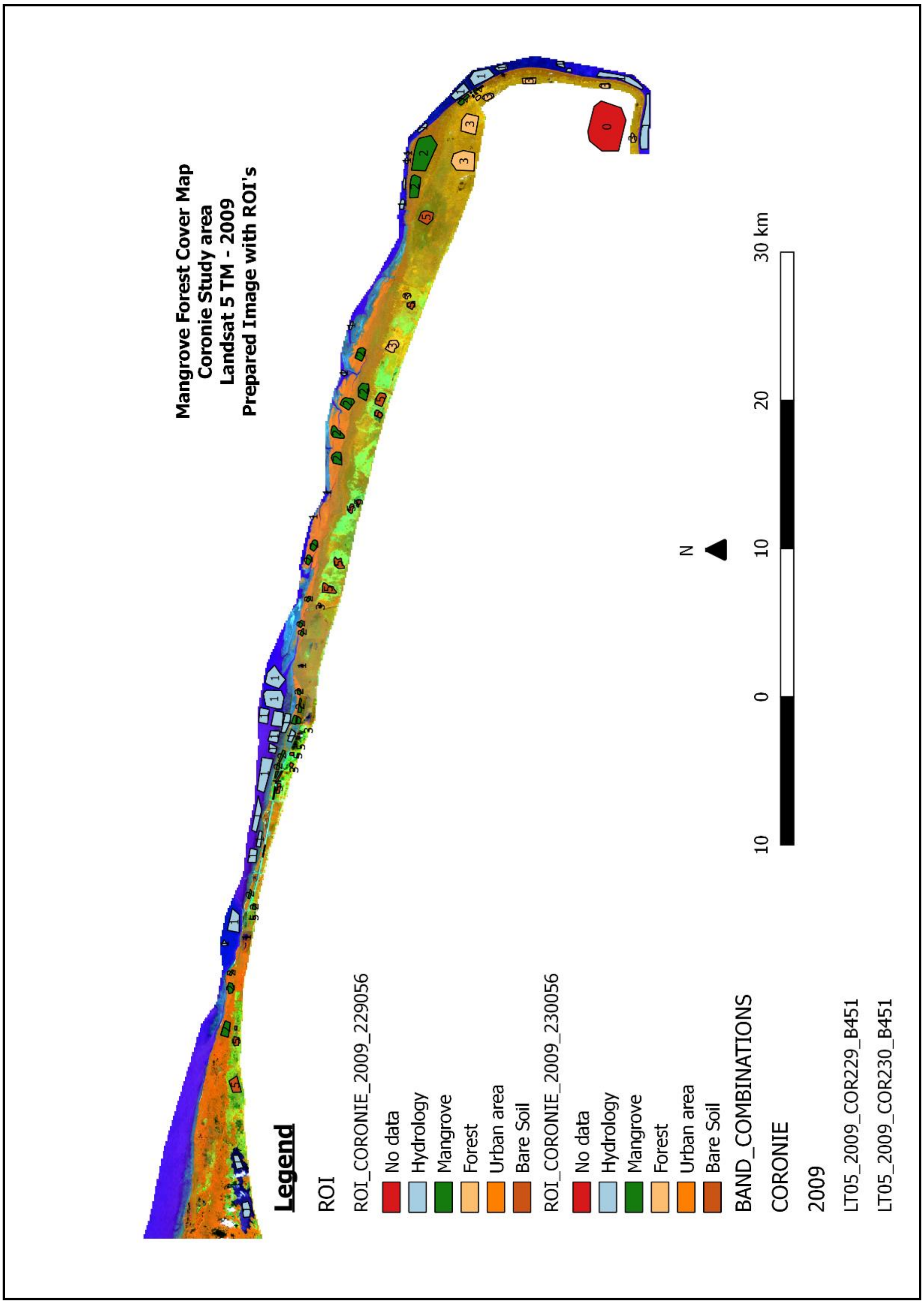

Figure X-3-2: Prepared image of Coronie in 2009 with drawn ROI's

The image underwent the SVM classifier which is illustrated figure X-3-3.

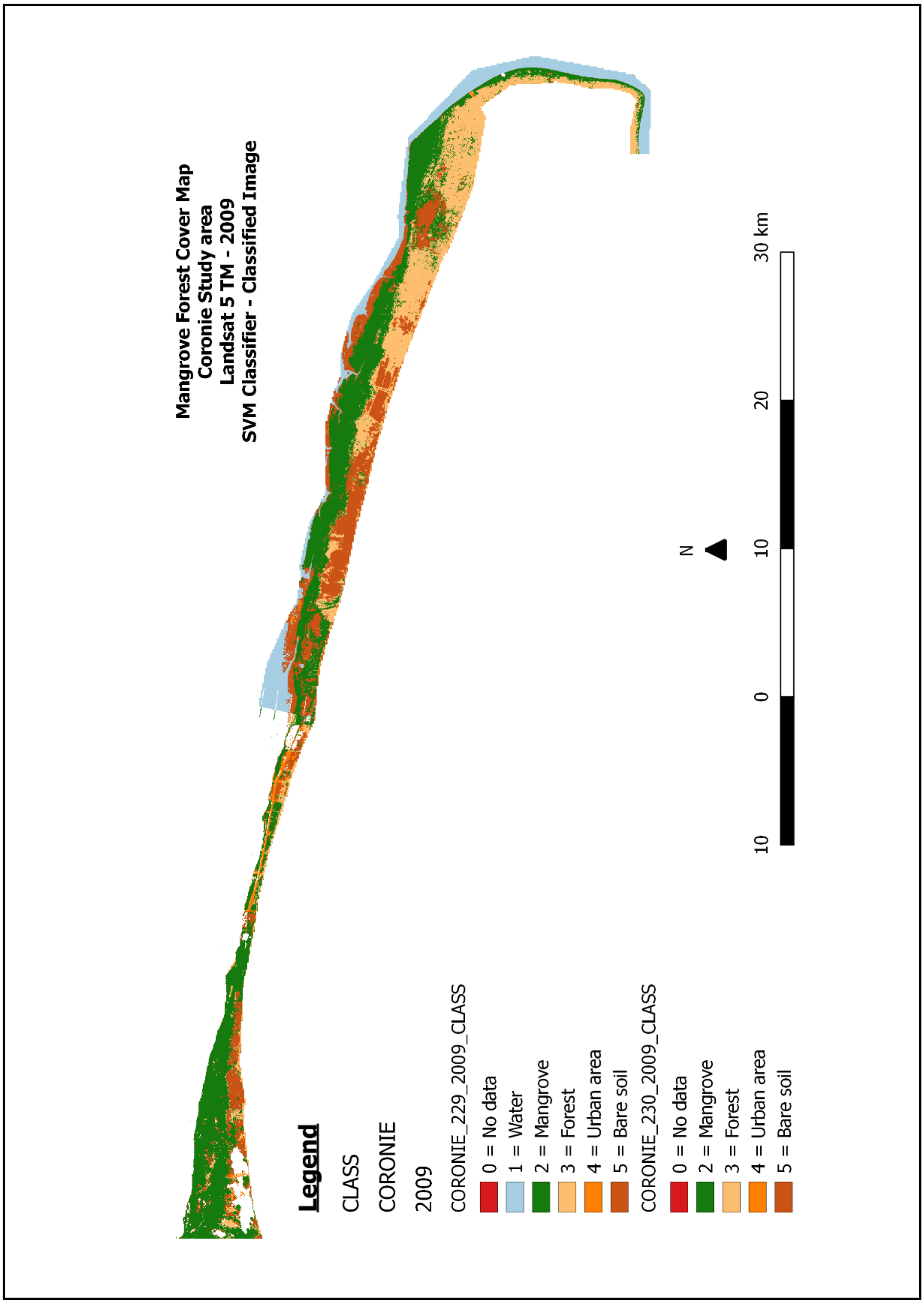

Figure X-3-3: The classified image of Coronie in 2009 as result of the SVM classifier

In the final process the classified image was filtered and manual adjusted. Figure X-3-4 gives an illustration of the adjusted image.

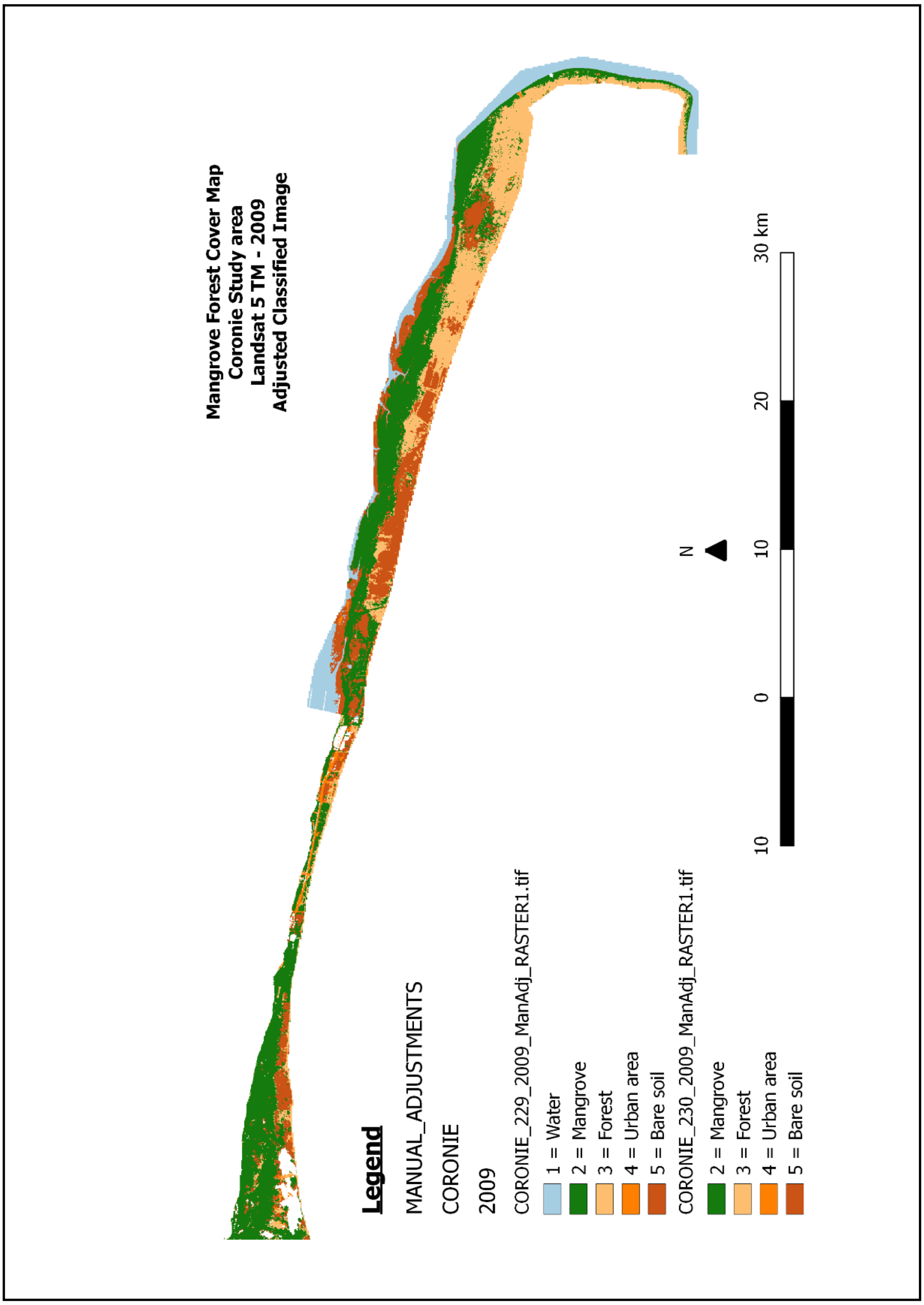

Figure X-3-4: Filtered and manual adjusted classified image of Coronie in 2009

NN

Validating the classified image with reference data produced an error matrix in number of pixels for scene 229056 and 230056, which is demonstrated respectively in table X-3-1 and X-3-2.

Table X-3-1: The produced error matrix of the classified Coronie map for 2009, scene 229056 in pixels

CORONIE 2009 - 229056		Reference						
		Hydrology	Mangrove	Forest	Urban area	Bare soil	Total	user Accuracy (%)
Classification	Hydrology	34041	0	0	0	0	34041	100
	Mangrove forest	0	68867	0	0	7	68874	99,98983651
	Forest	0	0	54279	0	0	54279	100
	Urban area	0	0	0	689	0	689	100
	Bare soil	0	1	0	0	45502	45503	99,99780234
	Total	34041	68868	54279	689	45509	203386	
	Producer Accuracy (%)	100	99,9985479	100	100	99,9846184		
	Kappa hat Class (%)	99,9946559						
	Overall Accuracy (%)	99,9960666						

Table X-3-2: The produced error matrix of the classified Coronie map for 2009, scene 230056 in pixels

CORONIE 2009 - 230056		Reference						
		Hydrology	Mangrove	Forest	Urban area	Bare soil	Total	user Accuracy (%)
Classification	Hydrology	73011	2	0	0	0	73013	99,99726076
	Mangrove forest	0	46102	0	0	0	46102	100
	Forest	0	0	7288	0	0	7288	100
	Urban area	0	0	0	3532	0	3532	100
	Bare soil	0	0	0	0	12441	12441	100
	Total	73011	46104	7288	3532	12441	142376	
	Producer Accuracy (%)	100	99,995662	100	100	100		
	Kappa hat Class (%)	99,997739						
	Overall Accuracy (%)	99,9985953						

According to the error matrix of scene 229056 and 230056 between the remotely sensed classification and the reference data, the total number of correct pixels (diagonal) and the total number of pixels in the error matrix gave an overall accuracy of 99 % for both scenes. Subsequently, the measured agreement between the two data gave a kappa hat of 99%. Also, did the error matrix showed that 7 pixels of the bare soil class in scene 229056 were not classified, because of the failure of the scan line corrector (Figure X-3-5). After comparison of the remotely sensed classification and the reference data, the producer's accuracy of the mangrove class for Coronie was 99 % that indicates how well the area was classified. At the end, the user's accuracy was 99 % that gave the reliability and probability of the mangrove class on the map that represents the category on the ground.

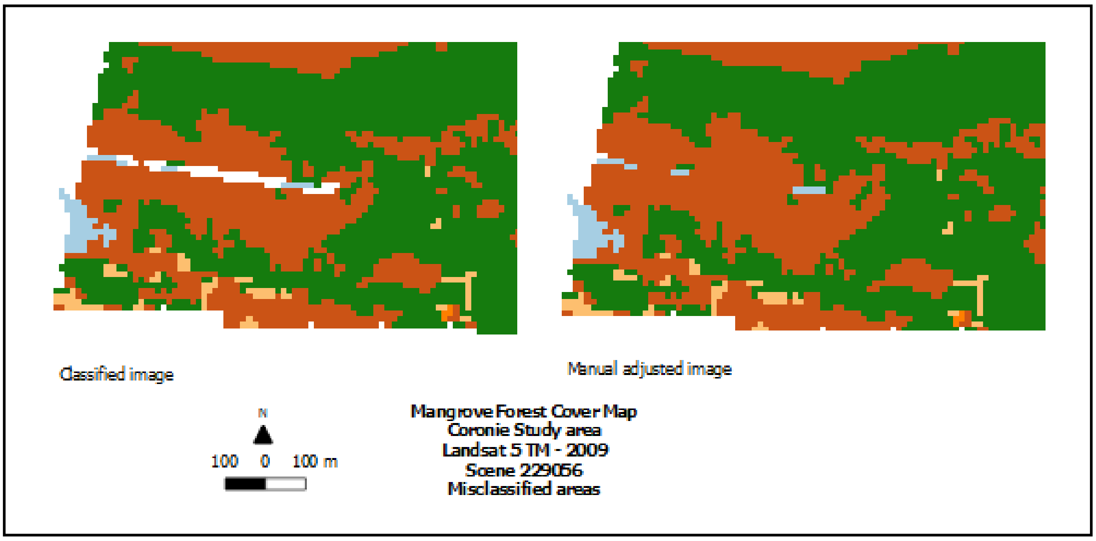

Figure X-3-5: Misclassification - Coronie 2009, Scene 229056

In the end, the mangrove class was extracted, which is shown in figure X-3-6 as the mangrove map of Coronie in 2009.

According to the results, the mangrove forest cover of Coronie in 2009 was extended over a total area of 10347 ha and was 9 % of the total mangrove forest cover of Suriname.

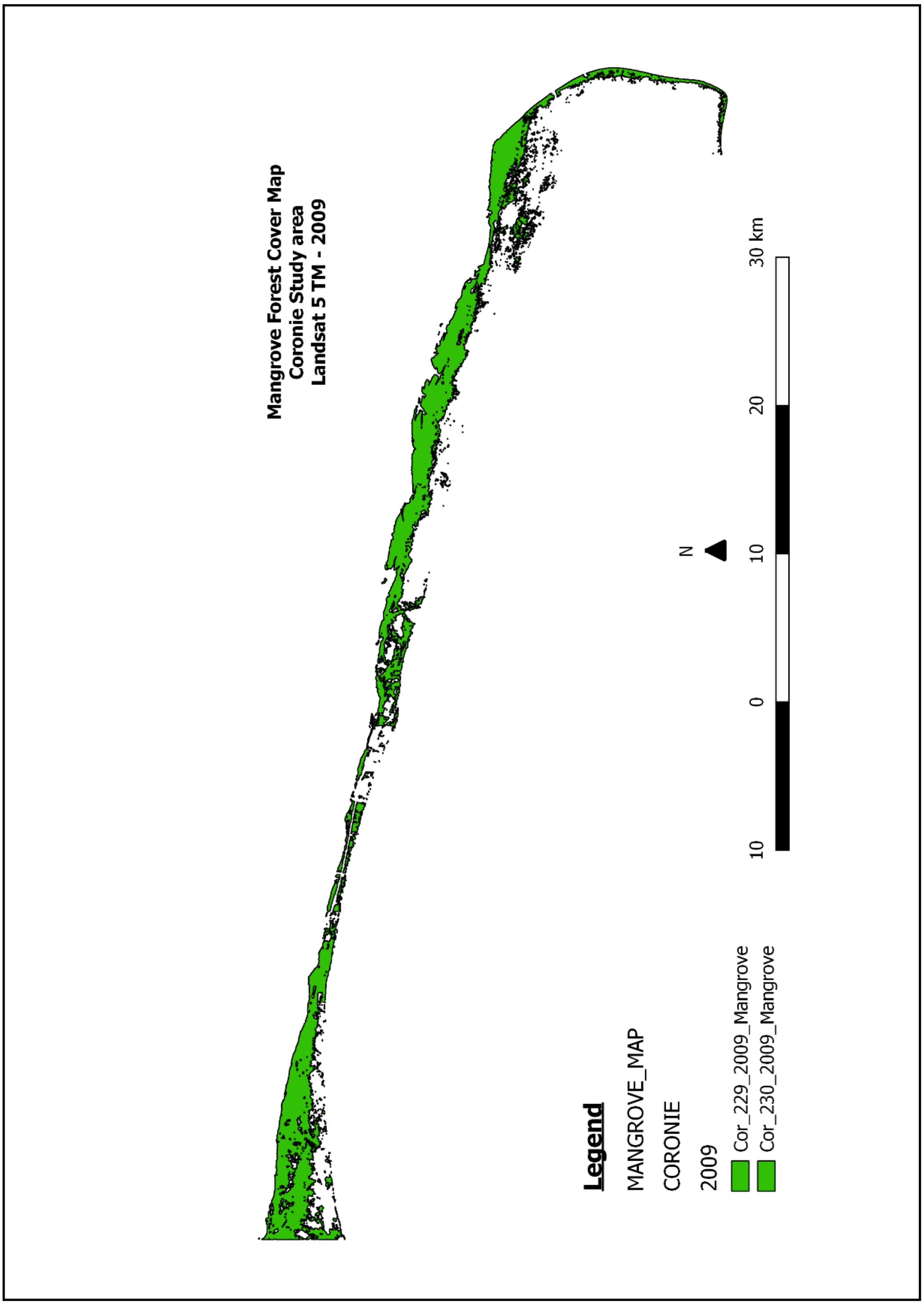

Figure X-3-6: The extracted mangrove map of Coronie in 2009

X.4 Mangrove Map of Coronie in 2014

Figure X-4-1 illustrates the result of the pre-processing of Coronie in 2014. The prepared image was derived from the Landsat 8 OLI image of September 26, 2014 (scene 229/56) and October 19, 2017 (scene 230/56) with cloud coverage of, respectively, 2.4 % and 9.18 %. The clouds were refilled with data of the image of May 21, 2014, October 12, 2014 and October 28, 2014 for scene 229/56 and September 17, 2014 for scene 230/56.

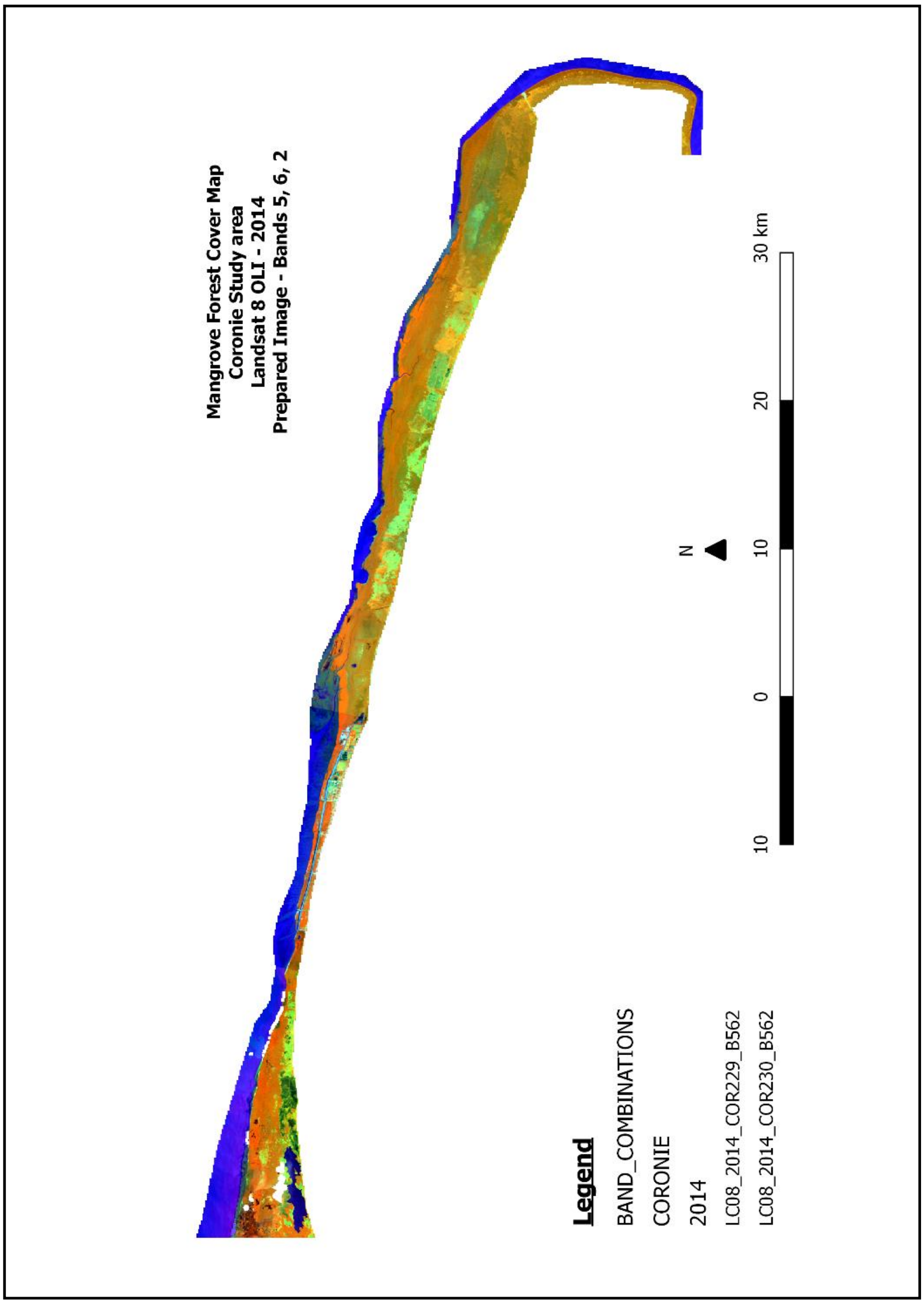

Figure X-4-1:Prepared image of Coronie derived from Landsat 8 OLI in 2014 with a band combination of 5, 6, 2

In the following step, Region of interest (ROI) were drawn, which has been illustrated in figure X-4-2.

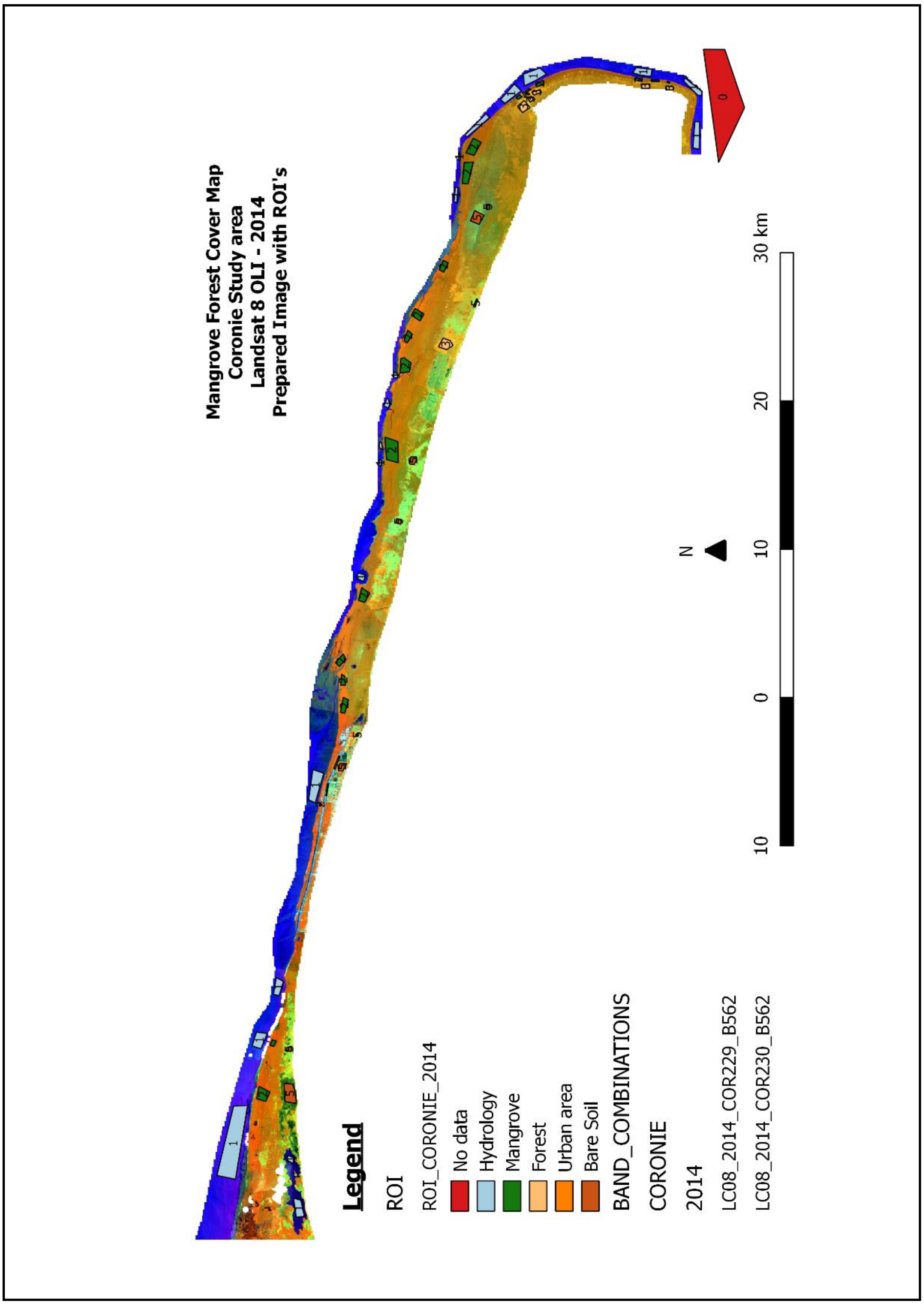

Figure X-4-2: Prepared image of Coronie in 2014 with drawn ROI's

The image underwent the SVM classifier which is illustrated figure X-4-3.

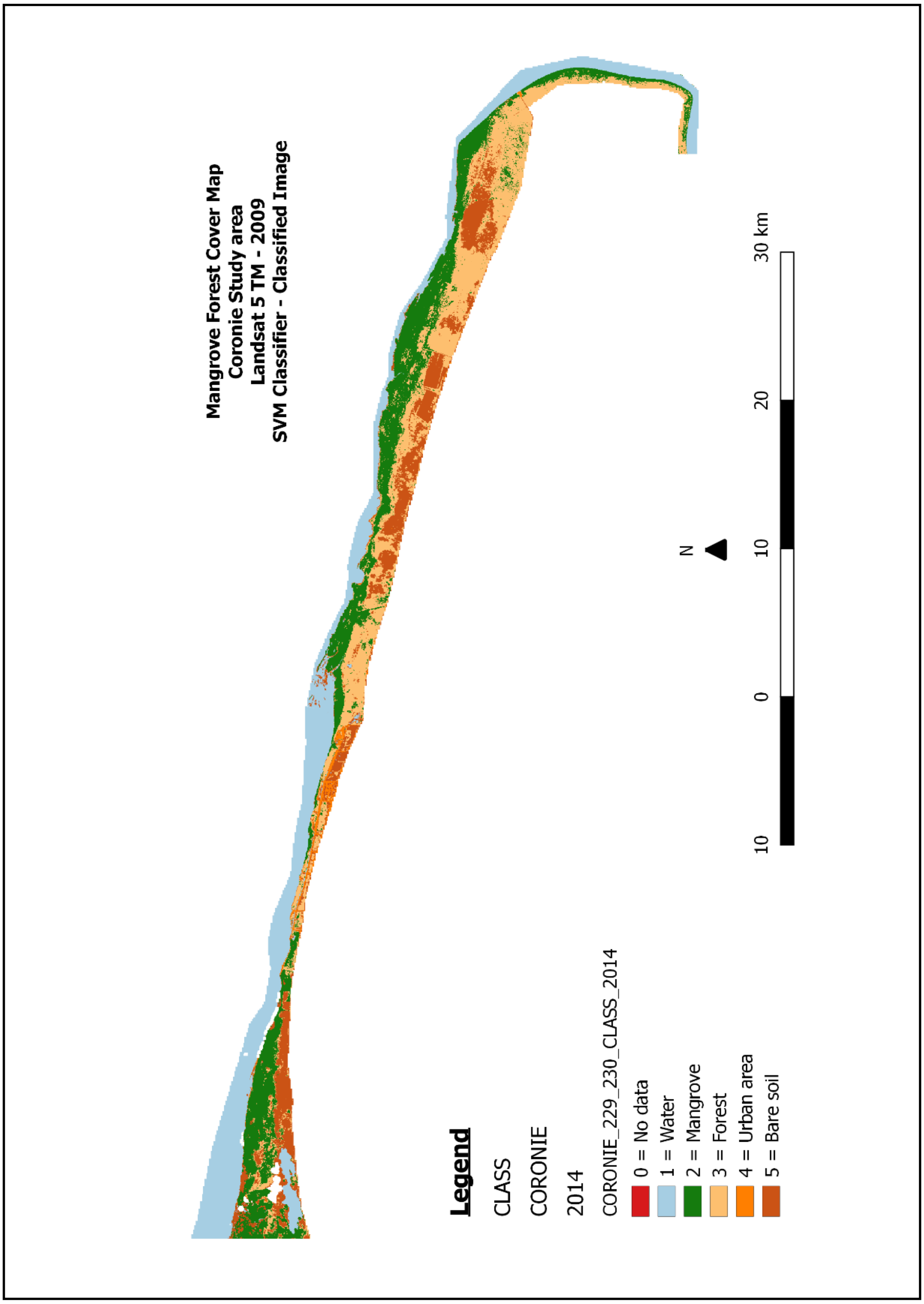

Figure X-4-3: The classified image of Coronie in 2014 as result of the SVM classifier

In the final process the classified image was filtered and manual adjusted. Figure X-4-4 gives an illustration of the adjusted image.

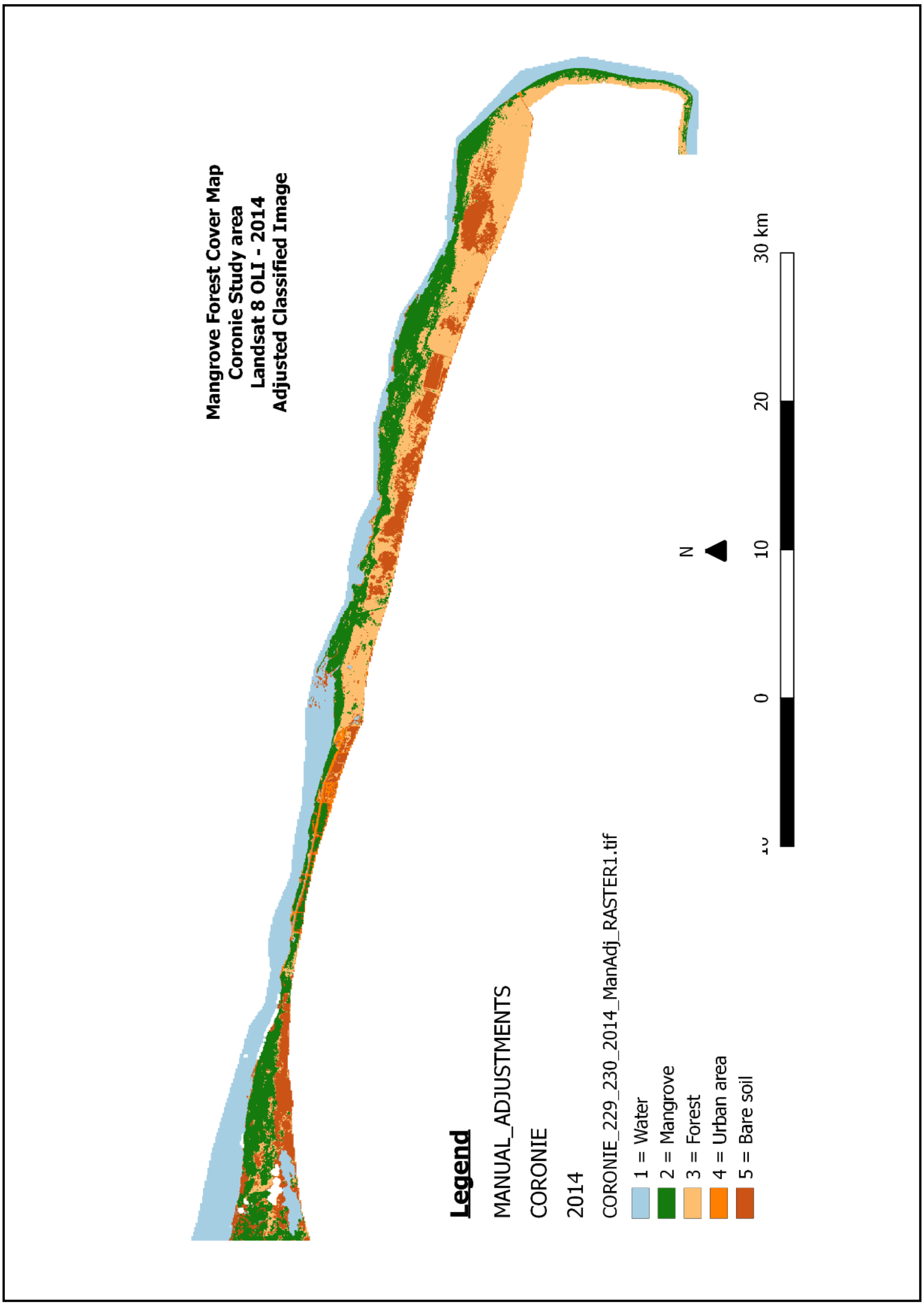

Figure X-4-4: Filtered and manual adjusted classified image of Coronie in 2014

Validating the classified image with reference data produced an error matrix in number of pixels for scene 229056 and 230056, which is demonstrated respectively in table X-4-1.

Table X-4-1: The produced error matrix of the classified Coronie map for 2014, scene 229056 and 230056 in pixels

CORONIE 2014		Reference						
		Hydrology	Mangrove	Forest	Urban area	Bare soil	Total	user Accuracy (%)
Classification	Hydrology	101739	0	0	0	0	101739	100
	Mangrove forest	0	84705	4569	0	0	89274	94,88204852
	Forest	0	1256	84823	0	0	86079	98,54087524
	Urban area	0	0	0	4649	0	4649	100
	Bare soil	0	0	0	0	51900	51900	100
	Total	101739	85961	89392	4649	51900	333641	
	Producer Accuracy (%)	100	98,5388723	94,8888044	100	100		
	Kappa hat Class (%)	97,6551331						
	Overall Accuracy (%)	98,2541115						

According to the error matrix of scene 229056 and 230056 between the remotely sensed classification and the reference data, the total number of correct pixels (diagonal) and the total number of pixels in the error matrix gave an overall accuracy of 98 %. Subsequently, the measured agreement between the two data gave a kappa hat of 98 %. Also, did the error matrix showed that 4569 pixels of the mangrove class in were misclassified into the forest class (Figure.X-4-5) and 1256 pixels of the forest class were misclassified into the mangrove class (Figure X-4-6). The misclassification occurred because of wrong color identification by the SVM classifier and due to cloud fill data, that had a darker color preview than the prepared image. After comparison of the remotely sensed classification and the reference data, the producer's accuracy of the mangrove class for Coronie was 99 % that indicates how well the area was classified. At the end, the user's accuracy was 95 % that gave the reliability and probability of the mangrove class on the map that represents the category on the ground.

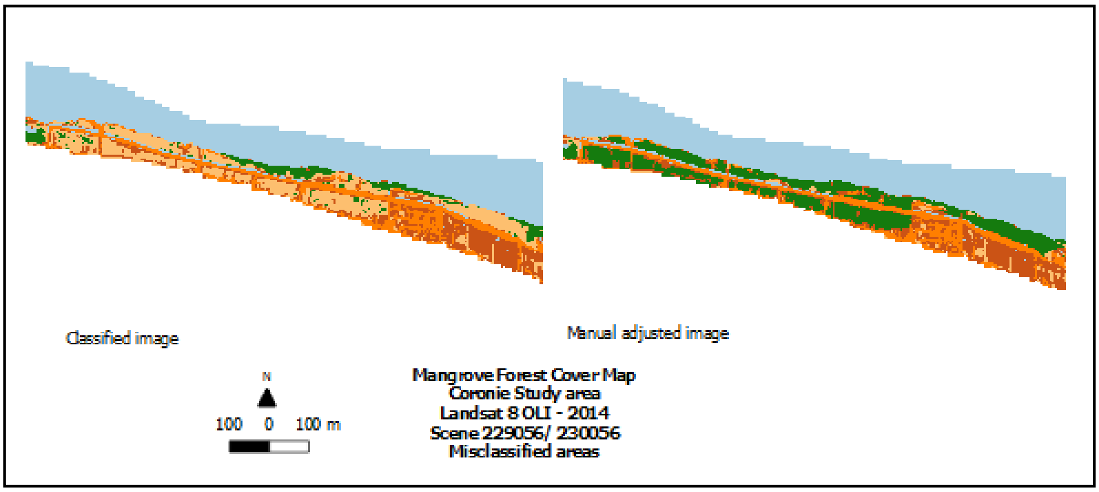

Figure X-4-5: Misclassification 1 - Coronie 2014

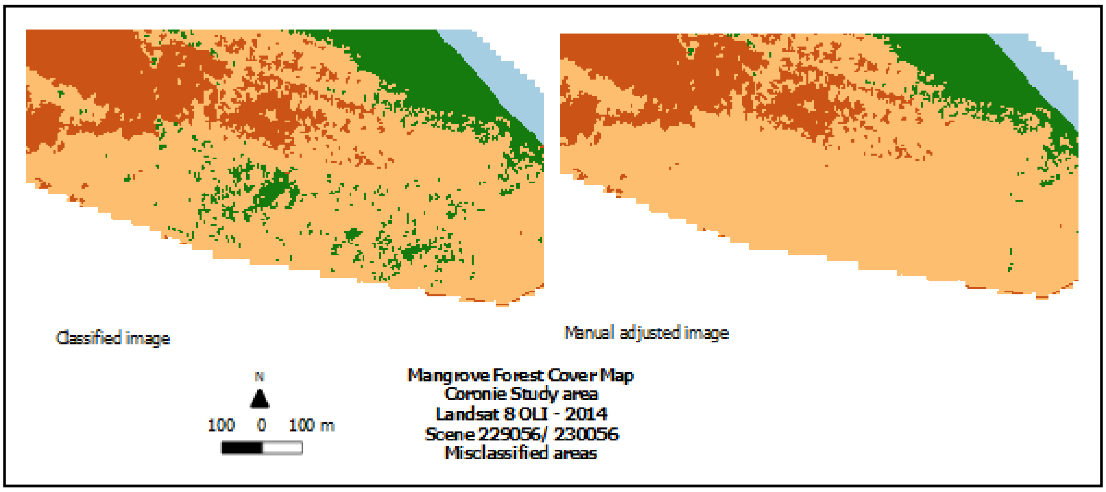

Figure X-4-6: Misclassification 2 - Coronie 2014

In the end, the mangrove class was extracted, which is shown in figure X-4-7 as the mangrove map of Coronie in 2014.

According to the results, the mangrove forest cover of Coronie in 2014 was extended over a total area of 8035 ha and was 7 % of the total mangrove forest cover of Suriname.

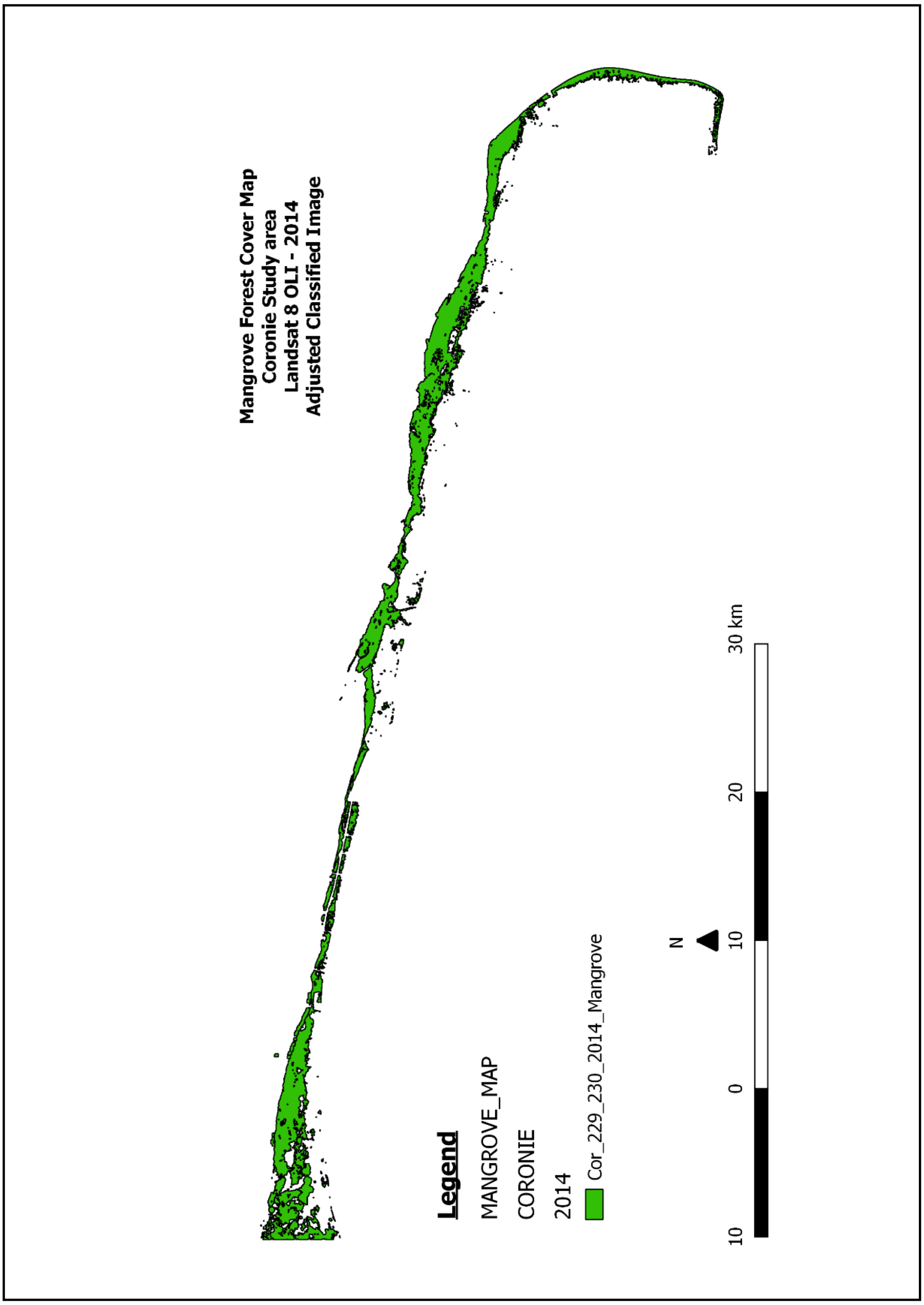

Figure X-4-7: The extracted mangrove map of Coronie in 2014

X.5 Mangrove Map of Coronie in 2017

Figure X-5-1 illustrates the result of the pre-processing of Coronie in 2017. The prepared image was derived from the Landsat 8 OLI image of September 2, 2017 (scene 229/56) and September 9, 2017 (scene 230/56) with cloud coverage of, respectively, 7.99 % and 5.64 %. The clouds were refilled with data of the image of October 4, 2017 for scene 229/56.

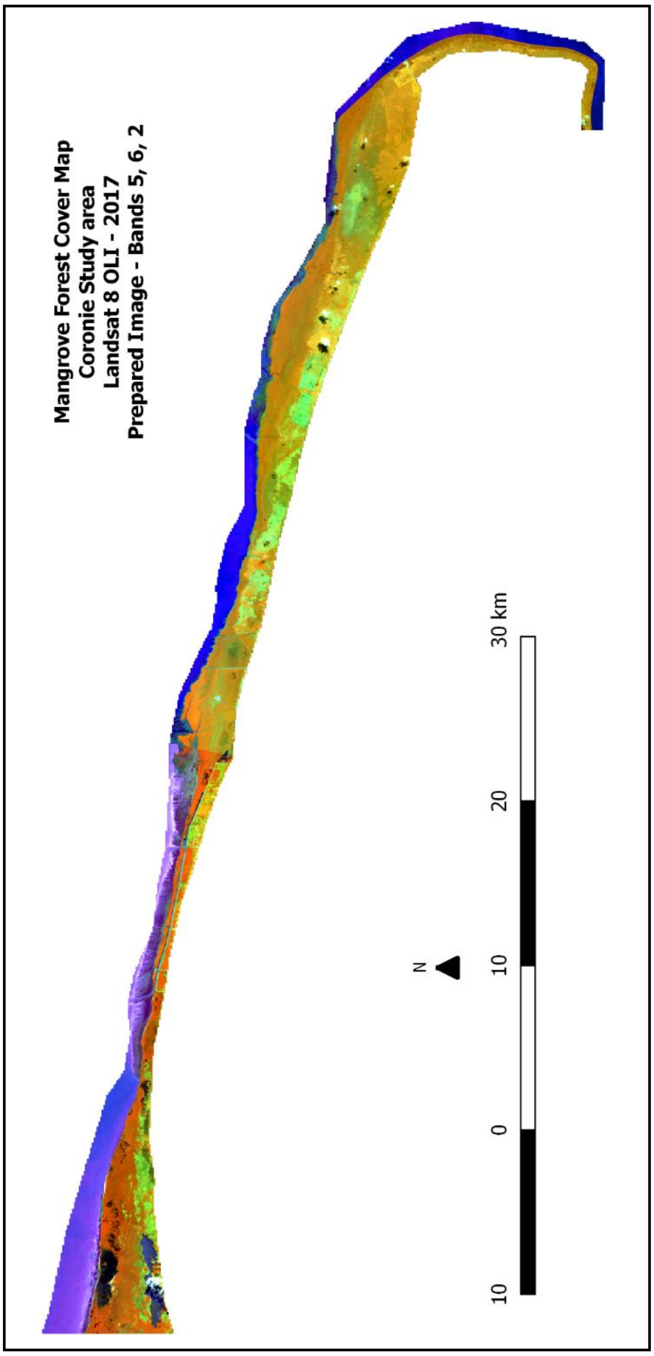

Figure X-5-1: Prepared image of Coronie derived from Landsat 8 OLI in 2017 with a band combination of 5, 6, 2

In the following step, Region of interest (ROI) were drawn, which has been illustrated in figure X-5-2.

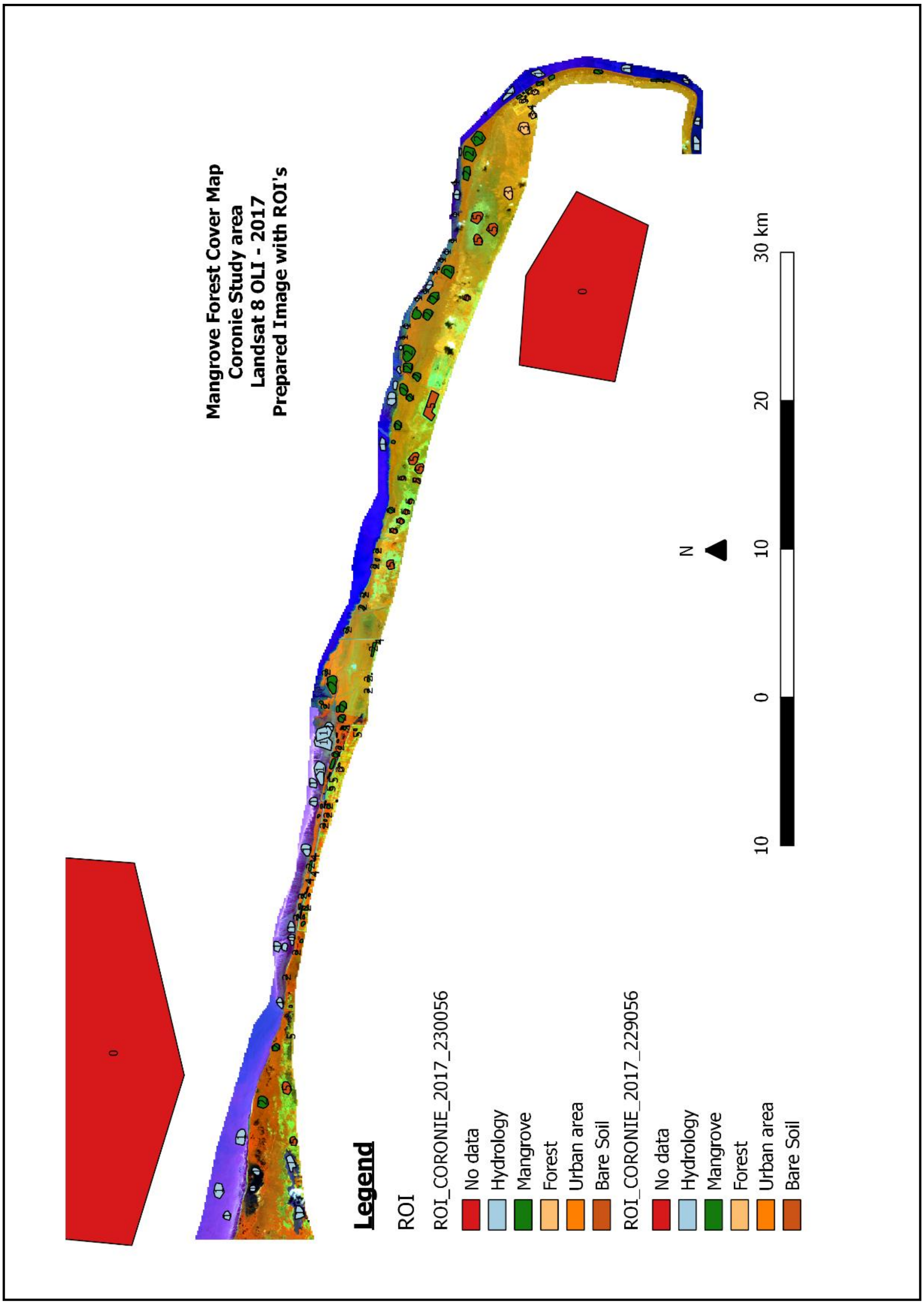

Figure X-5-2: Prepared image of Coronie in 2017 with drawn ROI's

The image underwent the SVM classifier which is illustrated figure X-5-3.

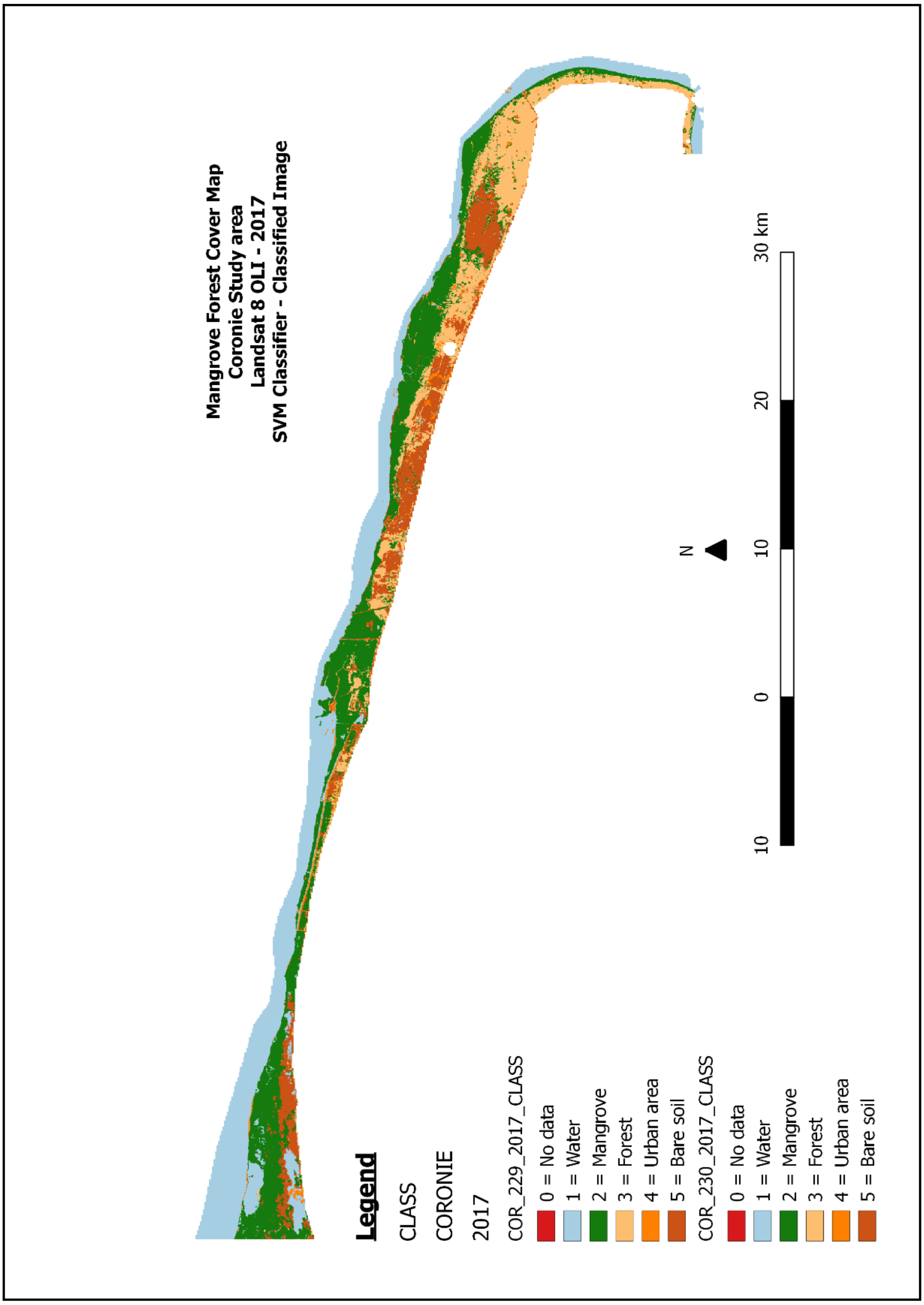

Figure X-5-3: The classified image of Coronie in 2017 as result of the SVM classifier

In the final process the classified image was filtered and manual adjusted. Figure X-5-4 gives an illustration of the adjusted image.

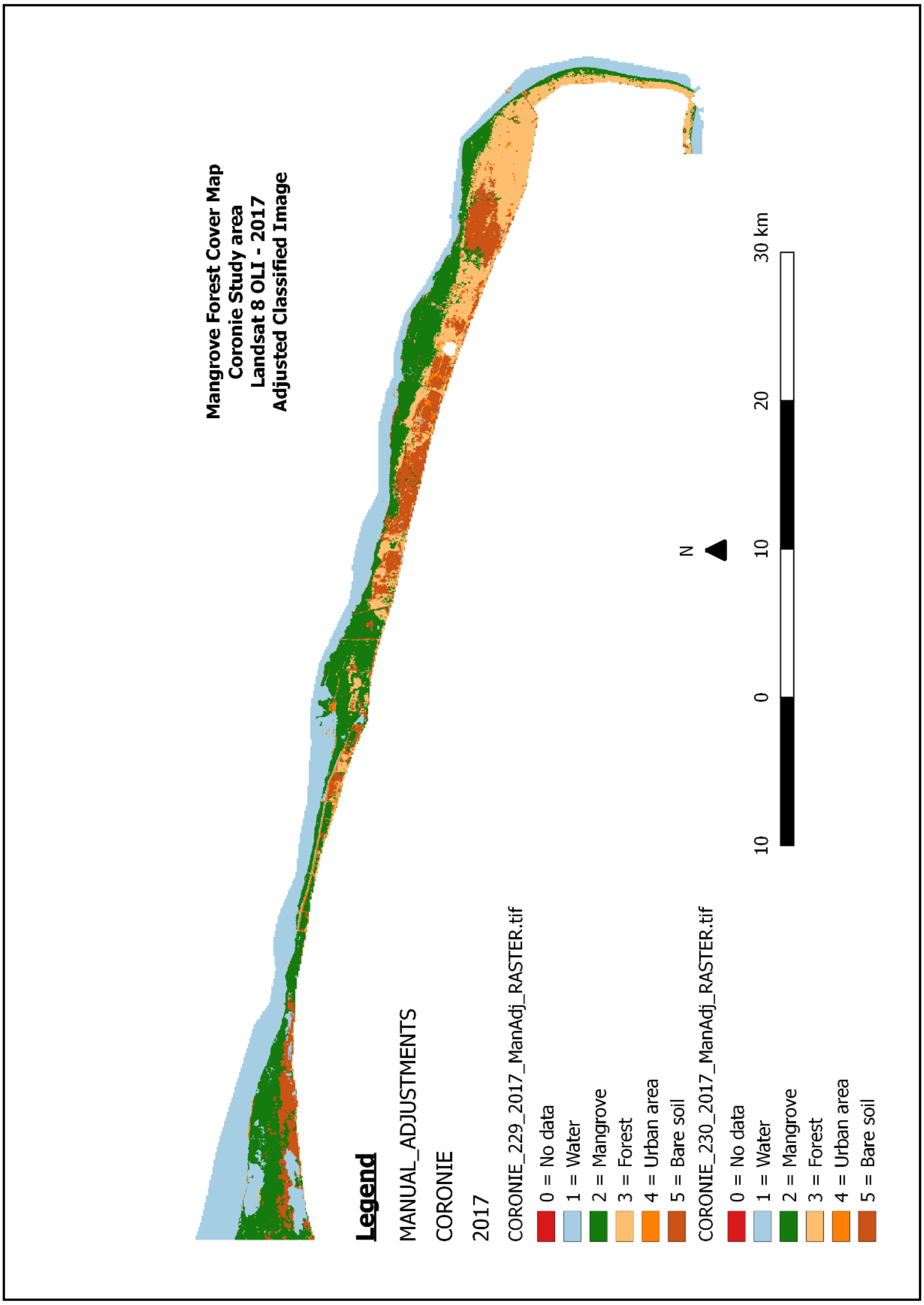

Figure X-5-4: Filtered and manual adjusted classified image of Coronie in 2017

Validating the classified image with reference data produced an error matrix in number of pixels for scene 229056 and 230056, which is demonstrated respectively in table X-5-1 and X-5-2.

Table X-5-1: The produced error matrix of the classified Coronie map for 2017, scene 229056 in pixels

CORONIE 2017 - 229056		Reference						
		Hydrology	Mangrove	Forest	Urban area	Bare soil	Total	user Accuracy (%)
Classification	Hydrology	47279	0	0	0	0	47279	100
	Mangrove forest	0	59363	0	0	0	59363	100
	Forest	0	2325	55171	0	0	57496	95,95624043
	Urban area	0	0	0	3178	0	3178	100
	Bare soil	0	0	0	0	34271	34271	100
	Total	47279	61688	55171	3178	34271	201587	
	Producer Accuracy (%)	100	96,2310336	100	100	100		
	Kappa hat Class (%)	98,4574108						
	Overall Accuracy (%)	98,8466518						

Table X-5-2: The produced error matrix of the classified Coronie map for 2017, scene 230056 in pixels

CORONIE 2017 - 230056		Reference						
		Hydrology	Mangrove	Forest	Urban area	Bare soil	Total	user Accuracy (%)
Classification	Hydrology	70311	0	0	498	0	70809	99,29669957
	Mangrove forest	0	42495	0	0	0	42495	100
	Forest	0	0	3062	0	0	3062	100
	Urban area	0	0	0	2303	0	2303	100
	Bare soil	0	0	0	0	14005	14005	100
	Total	70311	42495	3062	2801	14005	132674	
	Producer Accuracy (%)	100	100	100	82,2206355	100		
	Kappa hat Class (%)	99,377032						
	Overall Accuracy (%)	99,6246439						

According to the error matrix of scene 229056 and 230056 between the remotely sensed classification and the reference data, the total number of correct pixels (diagonal) and the total number of pixels in the error matrix gave an overall accuracy of 99 % for both scenes. Subsequently, the measured agreement between the two data gave a kappa hat of 99 %. Also, did the error matrix showed that 2325 pixels of the forest class in scene 229056 were misclassified into the mangrove forest class (Figure X-5-5) and 498 pixels of the hydrology class were misclassified into the urban class (Figure X-5-6). The misclassification occurred because of wrong color identification by the SVM classifier (scene 229056) and due to cloud fill data, that had a darker color preview than the prepared image (scene 230056). After comparison of the remotely sensed classification and the reference data, the producer's accuracy of the mangrove class for Coronie was 98 % that indicates how well the area was classified. At the end, the user's accuracy was 100 % that gave the reliability and probability of the mangrove class on the map that represents the category on the ground.

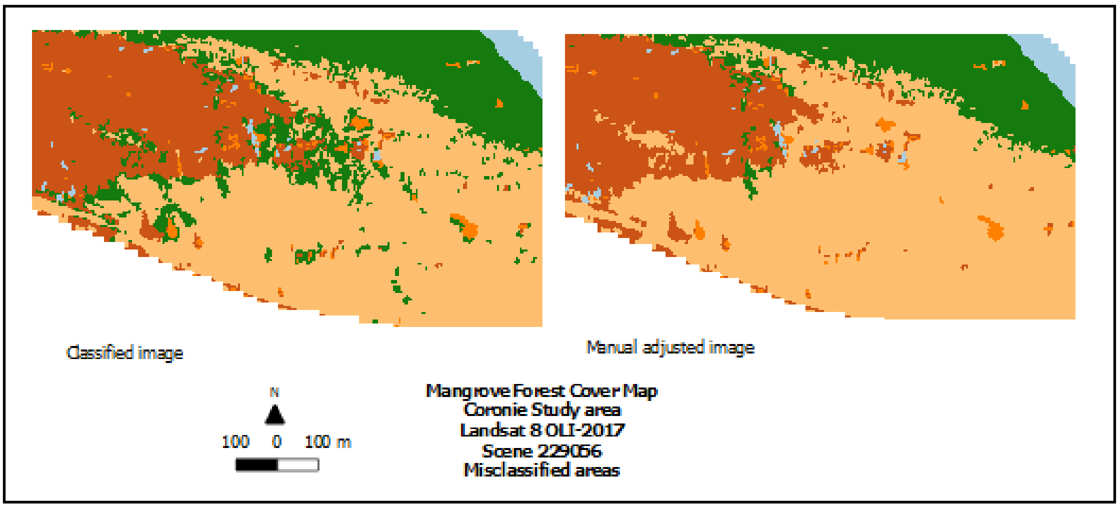

Figure X-5-5: Misclassification 1 - Coronie 2017, Scene 229056

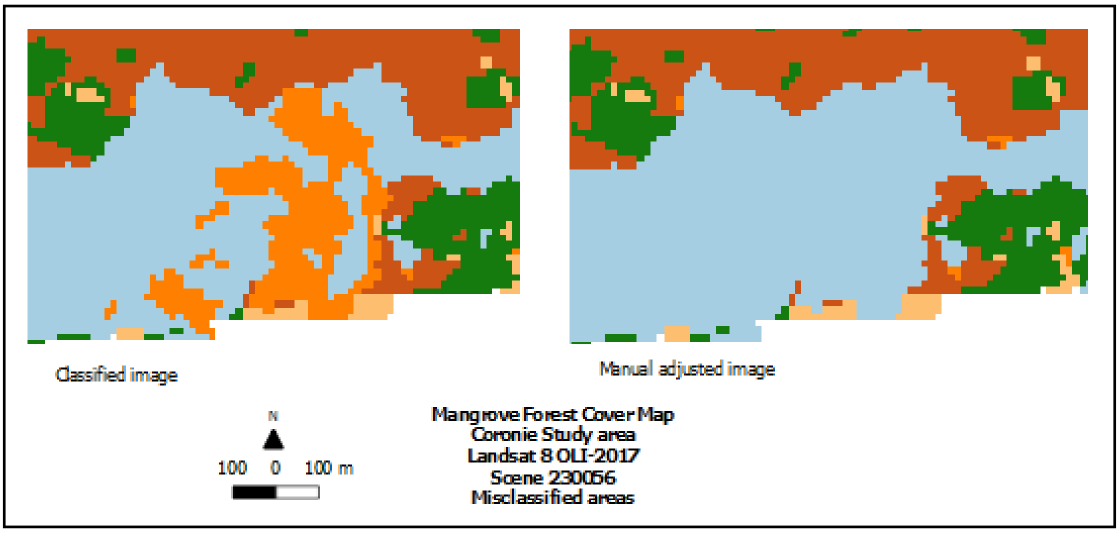

Figure X-5-6: Misclassification 2 - Coronie 2017, Scene 230056

In the end, the mangrove class was extracted, which is shown in figure X-5-7 as the mangrove map of Coronie in 2017.

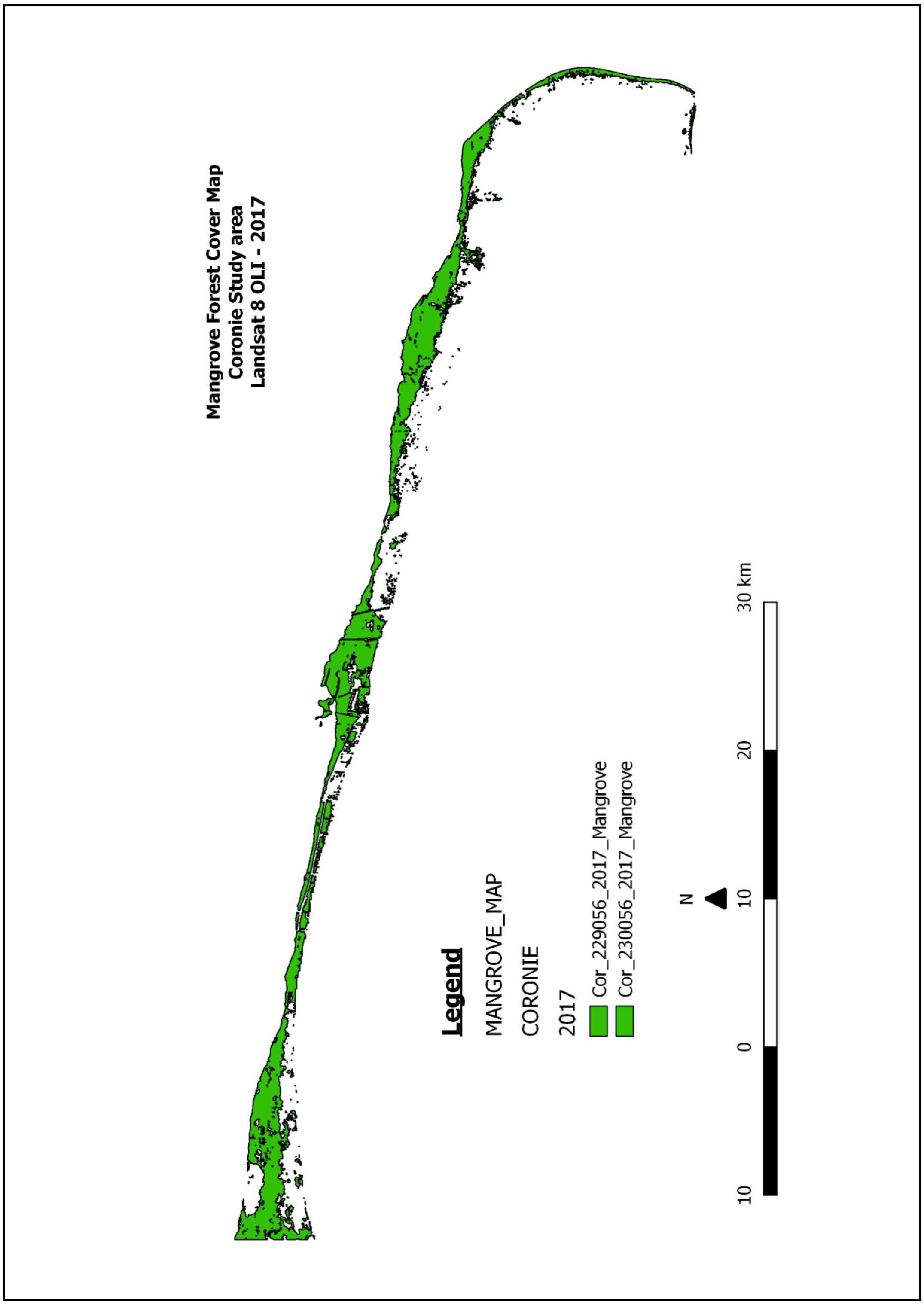

Figure X-5 7: The extracted mangrove map of Coronie in 2017

According to the results, the mangrove forest cover of Coronie in 2017 was extended over a total area of 9167.22 ha and was 7.97 % of the total mangrove forest cover of Suriname.

EEE

REFERENCES

Abadal, G, and et al. 2014. "Electromagnetic Radiation Energy Harvesting - The Rectenna Based Approach. Ch 1."

Canada, Natural Resources. 2015. *Fundamentals of Remote Sensing - Introduction.* November 19. Accessed Augustus 9, 2018. http://www.nrcan.gc.ca/node/9363.

FCMU, Forest Cover Monitoring Unit -. 2015. "Overview Mangrove Forest Area."

Humboldt State University, Geospatial Online. 2017. *GSP 216 Introduction to Remote Sensing.* Accessed July 24, 2018. http://gsp.humboldt.edu/OLM/Courses/GSP_216_Online/lesson2-1/surface.html.

Moe Soe Let, V. 2016. "Study on the dynamics of the coastline of Suriname and the relationship to mangrove using Remote Sensing."

Rene, Somopawiro, Matai Rewiechand, Crabbe Sarah, Djojodikromo Mark, Paloeng Consuela, and Svensson Sara. 2015. "Global Forest Resources Assessment ." Country report.

SBB. 2014. "Baseline Mangrove Forest Suriname."

UNDP. 2011. "Suriname Coastal Protected Area Management."

UNDP. 2011. "Suriname Coastal Protection Area Management."